

GASKELL: CROSSING SYMMETRIC MODELS WITH FINITE WIDTH RESONANCES

Dual, Crossing Symmetric Representations
with Finite Width Resonances

Robert W. Gaskell

A thesis submitted to the Faculty of Graduate Studies
and Research in partial fulfillment of requirements
for the degree of Doctor of Philosophy.

Department of Physics
McGill University
Montreal 110, Quebec

June 1972

Acknowledgements

I wish to express my appreciation to Professor A. P. Contogouris for many hours of helpful discussion. In addition, I would like to thank Professors D. Atkinson, R. Kreps and R. Roskies and Drs. Chan Hong-Mo, M. Milgram and D. Schiff for useful discussions and correspondence. Finally, I am grateful to the National Research Council of Canada for financial assistance.

Author's Statement

The original work contained in this thesis consists of the following:

- 1) The construction of the early distorted trajectory (DT) model discussed in chapter III and the determination of its properties;
- 2) The analysis of the right half plane asymptotic behavior of the CHKZ model;
- 3) The derivation of restrictions on general DT models (chapter IV);
- 4) The construction of the revised DT model discussed in chapter V and the determination of its properties;
- 5) Various physical applications of the revised DT model which appear in chapter VI.

Abstract

Dual, crossing symmetric representations with resonances having finite width are proposed and developed in detail. In particular, the asymptotic behavior over the whole complex energy plane is studied and it is shown that certain recently proposed scattering amplitudes lead to non-Regge contributions in most (or all) of the physically important regions of the kinematical variables. Conditions for Regge behavior are developed, a class of models satisfying these conditions (along with other physically important requirements) is presented and a simple model obeying them is studied in detail. A number of physical applications are also presented, including an explanation of the Dalitz plot distribution for $\bar{p}n \rightarrow 3\pi$, the behavior of the most important $\pi\pi$ phase shifts and a determination of the $\pi\pi$ S-wave scattering lengths.

Contents

<u>Chapter</u>	<u>Page</u>
I. Introduction	1
II. The Veneziano Model	6
1. The Form of the Amplitudes	6
2. Properties of the Amplitudes	8
3. Summary	24
III. Early Models	26
1. Models to be Examined	26
2. Properties of the Models	28
3. Summary and Discussion	40
IV. Restrictions on DT Models	42
1. Unitarity Cut	43
2. Double Spectral Region	45
3. Asymptotic Behavior, t fixed	46
4. Asymptotic Behavior, fixed angle	51
5. Threshold Behavior	53
6. Summary	54
V. A Simple Example	56
1. Properties of the Basic Model	58
2. Neutralizer Correction	75

<u>Chapter</u>	<u>Page</u>
3. Subtractive Corrections	77
4. The $\pi\pi\rightarrow\pi\pi$ Amplitude	84
VI. Physical Applications	89
1. Experimental Situation	89
2. The DT Model	94
3. Applications of the Veneziano and DT Models	102
VII. Conclusions, Prospects for Future Development	109
1. Applications to Two Body Reactions	110
2. Theoretical Problems in Two Body Reactions	114
3. Extensions, Applications in Production Processes	116
Appendix. Non-Leading Terms	120
References	127
Figure Captions	130
Figures	133

I. Introduction

Since the end of 1968 one of the most important developments in the theory of strong interactions of elementary particles has been the construction by Veneziano (1968)* of a simple model combining crossing symmetry and Regge asymptotic behavior together with the property of duality. The subsequent successful explanation by Lovelace (1968) of the Dalitz plot distribution for the process $\bar{p}n \rightarrow \pi^- \pi^- \pi^+$, the derivation of $\pi\pi$ scattering lengths and of a number of other Current Algebra results, the application of the representation to phenomenological calculations at high energy and its relatively simple extension to production reactions (N-point function) are several of the reasons responsible for the great interest in this model shown by particle theorists.

Soon after the Veneziano proposal, the problem of introducing the property of unitarity into the original scheme started attracting a considerable amount of effort. The attempts in this direction fall roughly into five categories:

i) The K-Matrix approach. This was suggested by Lovelace in order to study low energy $\pi\pi$, $K\pi$ and $K\bar{K}$ phase shifts (Lovelace 1969). As we shall discuss in chapter VI, this method destroys the crossing symmetry which was built into the Veneziano model. Since crossing symmetry is difficult to reintroduce while retaining unitarity, this approach is, in a sense, a step backwards.

* References will be indicated by the surname of the first author, the year of publication and, if the reference is a text, the relevant chapter.

ii) The perturbative approach. This approach was first suggested by Kikkawa, Sakita and Virasoro (Kikkawa 1969) and by Fubini and Veneziano (Fubini 1969a). It consists of treating the original Veneziano amplitude as a Born term and using the multiparticle Veneziano formula (see Alessandrini 1971) to obtain higher order terms. Although this method is made more systematic by the operator formalism of Fubini, Gordon and Veneziano (Fubini 1969b), it has not yet come close to providing a simple unitary amplitude.

iii) The Roskies approach. This procedure, which has been examined by Roskies (1968) and used by Lovelace (1968), consists of substituting trajectories which are complex above threshold into the original Veneziano form. The result is that, at a given mass, resonances of arbitrarily high spin ("ancestors") are introduced.

iv) The Martin approach. Martin (1969) smeared out the Veneziano amplitude by integrating it with an appropriate weighting factor. With this method it is possible to introduce Regge cuts but the resulting amplitudes have no Regge pole behavior. More recent work along these lines has been undertaken by Friedman, Nath and Srivastava (Friedman 1970).

v) Modified Beta function approach. These attempts, dating from the work of Suzuki (1969), substitute a modified Beta function for the one appearing in Veneziano's formula. The modifications consist of changing slightly the integrand of the usual integral form for the Beta function*. In a sense, these

* Properties of the Beta and Gamma functions and related functions can be found in Carrier (1965, ch.5) and in Gradshteyn (1965, ch.8).

models are like those of type iv) except that the smearing is done inside the Beta function integrand rather than outside.

The models of types i) and ii) clearly suffer significant drawbacks. The models of types iii) and iv) may prove worth studying, but they lack the simplicity necessary for practical application. We shall therefore concentrate on the models of type v).

In chapter II we shall examine the ordinary Veneziano model and, in particular, the properties most relevant to the developments of the subsequent chapters. We shall use methods which are directly applicable to the study of the basic problems of this work.

In chapter III we shall examine three early models of type v) and analyze some of their most important shortcomings. Particular emphasis will be given to the difficult problem of the asymptotic behavior of these models as $|s| \rightarrow \infty$ with t fixed and s in the right half of the complex s -plane.

Chapter IV will be concerned with restrictions arising from the requirements of Regge asymptotic behavior ($|s| \rightarrow \infty$, t fixed), Mandelstam analyticity, threshold behavior and asymptotic behavior for large s with u or θ_s fixed.

In chapter V we present an amplitude which satisfies the restrictions obtained in chapter IV. Again, particular care is devoted to the study of its asymptotic behavior for $|s| \rightarrow \infty$ with t fixed as well as to certain other properties.

Chapter VI presents a number of physical applications of this model including the behavior of the Dalitz plot distribution for the reaction $\bar{p}n \rightarrow \pi^- \pi^- \pi^+$, the determination of the physical

features of the most important $\pi\pi$ phase shifts and the comparison of the $\pi\pi$ scattering lengths with both experimental and Current Algebra results. The ρ - f^0 trajectory used is found to be in reasonable agreement with the (almost linear) one observed experimentally. The satisfaction of the elastic unitarity condition for the most important partial waves is also examined.

Finally, in chapter VII, we shall make suggestions for future work in this area.

The body of this work is followed by a short Appendix which examines in detail certain non-leading terms in the model of chapter V.

Throughout this work we shall use the Mandelstam variables s , t , and u . In figure I.1 these are defined in terms of the four-momenta of the particles being scattered. We shall also work with units such that

$$4m_{\pi}^2 = 1 \quad (m_{\pi} = \text{pion mass}) \quad (1)$$

so that for the process $\pi\pi \rightarrow \pi\pi$ the Mandelstam variables are constrained by

$$s + t + u = 1. \quad (2)$$

Regge trajectories which are complex above threshold will be written in terms of the once subtracted dispersion relation

$$\alpha(s) = \lambda s + b + \frac{s}{\pi} \int_1^{\infty} ds' \frac{\Psi(s')}{s'(s'-s)} \quad (3)$$

We use the function $\Psi(s')$ rather than the usual $\text{Im}\alpha(s')$ since in part of the work we shall be interested in examining the integrand for values of s' away from the real, positive s' axis.

Finally, we should mention some of the mathematical notation which we shall use. The symbol " \propto " will be used for proportionality. The symbol " \sim " stands for "asymptotic to" :

$$F(s) \sim G(s) \quad (s \rightarrow s_0) \text{ implies } \lim_{s \rightarrow s_0} \frac{F(s)}{G(s)} = 1 . \quad (4)$$

The symbol " \approx " will be used for approximate equality while the symbol " \sim " stands for asymptotic proportionality:

$$F(s) \sim G(s) \quad (s \rightarrow s_0) \text{ implies } \lim_{s \rightarrow s_0} \frac{F(s)}{G(s)} = \text{constant} . \quad (5)$$

II. The Veneziano Model

In this chapter we shall review some of the properties of the Veneziano model (Veneziano 1968)*. The usual procedure for discussing this model appeals to the well known properties of the Gamma function. We shall not use this procedure in most of this chapter. Instead, we shall use methods applicable to the models which will be discussed in later chapters.

II.1 The Form of the Amplitudes

According to the Veneziano model, invariant amplitudes for the process $1+2 \rightarrow 3+4$ can be written

$$A^I(s, t, u) = \sum_{\substack{\mu, \nu, \\ p, q, r}} \gamma_{\mu\nu I}^{st}(p, q, r) \frac{\Gamma(p - \alpha_\mu(s)) \Gamma(q - \alpha_\nu(t))}{\Gamma(r - \alpha_\mu(s) - \alpha_\nu(t))} \quad (1)$$

+ Permutations.

The first term in this equation corresponds to figure II.1a while the permutations refer to figures II.1b and II.1c. The indices μ and ν refer to trajectories which can be exchanged in the corresponding channels. The numbers p , q and r are limited to those which yield correct asymptotic behavior and poles in the proper positions and with correct residues. The $\gamma_{\mu\nu I}^{st}(p, q, r)$ are constants and I is included to indicate that there may be several invariant amplitudes. Finally, the trajectories are

* An extensive bibliography of work on the Veneziano model and on related models is found in a review article by Sivers and Yellin (Sivers 1971)

given by

$$\alpha_\mu(s) = \lambda s + b_\mu \quad (2)$$

where λ is a universal slope and b_μ is the intercept of the trajectory of type μ .

We shall now consider two examples of such amplitudes. Both are dominated by the degenerate ρ - f^0 trajectory. The first process is the reaction $\pi\pi \rightarrow \pi\omega$. The invariant amplitude is defined in terms of the T-matrix by (Veneziano 1968)

$$T = \epsilon_{\mu\nu\rho\sigma} e^\mu_{q_1} \nu_{q_2} \rho_{q_3} \sigma A(s,t,u) \quad (3)$$

where e^μ is the polarization four-vector of the ω and q_i are the four-momenta of the pions. The invariant amplitude is given by

$$A(s,t,u) = \beta[A(s,t) + A(s,u) + A(t,u)] \quad (4)$$

where β is a constant and

$$A(s,t) = \frac{\Gamma(1-\alpha(s))\Gamma(1-\alpha(t))}{\Gamma(2-\alpha(s)-\alpha(t))} \quad (5)$$

In terms of (1) we therefore have

$$\gamma_{\rho\rho}^{st}(1,1,2) = \gamma_{\rho\rho}^{su}(1,1,2) = \gamma_{\rho\rho}^{tu}(1,1,2) = \beta \quad (6)$$

Equation (1) still allows the addition of "satellite terms"

such as $(p,q,r) = (1,1,3)$ but these are usually ignored for simplicity.

The second process is $\pi\pi \rightarrow \pi\pi$. This has three invariant amplitudes corresponding to the three possible isospin states. The invariant amplitudes for the s-channel isospin decomposition are (Lovelace 1968)

$$\begin{aligned} A^0(s,t,u) &= \frac{3}{2}[C(s,t) + C(s,u)] - \frac{1}{2}C(t,u) \\ A^1(s,t,u) &= C(s,t) - C(s,u) \\ A^2(s,t,u) &= C(t,u) \end{aligned} \quad (7)$$

where

$$\begin{aligned} C(s,t) &= -\gamma \frac{\Gamma(1-\alpha(s))\Gamma(1-\alpha(t))}{\Gamma(1-\alpha(s)-\alpha(t))} \\ &+ \beta \frac{\Gamma(1-\alpha(s))\Gamma(1-\alpha(t))}{\Gamma(2-\alpha(s)-\alpha(t))} \end{aligned} \quad (8)$$

As with the previous amplitude we can easily identify the coefficients in equation (1). Notice that we now have a "leading" contribution $(p,q,r) = (1,1,1)$ and a "satellite" contribution $(p,q,r) = (1,1,2)$.

II.2 Properties of the Amplitudes

We notice first that the functions (5) and (8) can be written

$$A(s,t) = B(1-\alpha(s), 1-\alpha(t)) \quad (9)$$

and

$$C(s,t) = \gamma(\lambda s + \lambda t + c)A(s,t) \quad (10)$$

where $c = 2b-1+\beta/\gamma$ and B is the Beta function. It is therefore sufficient to examine the properties of the Beta function in order to find the properties of $A(s,t)$ and $C(s,t)$. With the integral representation for the Beta function we have

$$A(s,t) = \int_0^1 dz z^{-\alpha(s)} (1-z)^{-\alpha(t)} \quad (11)$$

for $\text{Re}\alpha(s) < 1$, $\text{Re}\alpha(t) < 1$.

We now examine the properties of the two amplitudes introduced above.

i) Crossing Symmetry. This requirement demands that the amplitudes for the processes

$$\begin{aligned} 1 + 2 &\rightarrow 3 + 4 \\ 1 + \bar{3} &\rightarrow \bar{2} + 4 \\ \text{and } 1 + \bar{4} &\rightarrow 3 + \bar{2} \end{aligned} \quad (12)$$

be related by analytic continuation in the variables s , t and u . Consider first the reactions $\omega + \pi_1 \rightarrow \pi_2 + \pi_3$ and $\omega + \bar{\pi}_2 \rightarrow \bar{\pi}_1 + \pi_3$. In the first process the s -channel is physical while in the second the t -channel is physical (see figure II.2). The T -matrix elements for these reactions, including isospin terms, are

$$T(\omega\pi_1 \rightarrow \pi_2\pi_3) = \epsilon_{\mu\nu\rho\sigma} e^\mu q_1^\nu q_2^\rho q_3^\sigma \epsilon_{pqr} \pi_1^p \pi_2^{-q} \pi_3^{-r} A(s, t, u) \quad (13)$$

and

$$T(\omega\bar{\pi}_2 \rightarrow \bar{\pi}_1\pi_3) = \epsilon_{\mu\nu\rho\sigma} e^\mu q_2^\nu q_1^\rho q_3^\sigma \epsilon_{pqr} \bar{\pi}_2^p \pi_1^q \pi_3^{-r} A(t, s, u) \quad (14)$$

where $\vec{\pi}_i$ are the isospin vectors of the pions. If we make the changes $\nu \leftrightarrow \rho$, $p \leftrightarrow q$ and use the fact that $\epsilon_{\mu\nu\rho\sigma} \epsilon_{pqr} = \epsilon_{\mu\rho\nu\sigma} \epsilon_{qpr}$ then we see that (13) and (14) are the same function provided that $A(s, t, u) = A(t, s, u)$. The latter condition is satisfied provided that

$$A(s, t) = A(t, s) \quad . \quad (15)$$

We can show that (15) is satisfied by making the substitution $s \leftrightarrow t$ and the change of variables $z \leftrightarrow 1-z$ in (11). Thus the Veneziano representation for $\pi\pi \rightarrow \pi\omega$ is crossing symmetric.

We next consider the reactions $\pi_1 + \pi_2 \rightarrow \pi_3 + \pi_4$ and $\pi_1 + \bar{\pi}_3 \rightarrow \bar{\pi}_2 + \pi_4$. These processes are shown in figure II.3. Using (7) and the isospin projection operators for $\pi\pi \rightarrow \pi\pi$, we can construct the T-matrix for the first process. We find

$$\begin{aligned} T(\pi_1\pi_2 \rightarrow \pi_3\pi_4) &= \frac{1}{2} \pi_1^p \pi_2^p \pi_3^{-q} \pi_4^{-q} [C(s, t) + C(s, u) - C(t, u)] \\ &+ \frac{1}{2} \pi_1^p \pi_3^{-p} \pi_2^q \pi_4^{-q} [C(s, t) + C(t, u) - C(s, u)] \\ &+ \frac{1}{2} \pi_1^p \pi_4^{-p} \pi_2^q \pi_3^{-q} [C(s, u) + C(t, u) - C(s, t)] . \end{aligned} \quad (16)$$

Comparing figures II.3a and II.3b we find that the T-matrix

for the second process is

$$\begin{aligned}
T(\pi_1 \bar{\pi}_3 \rightarrow \bar{\pi}_2 \pi_4) &= \frac{1}{2} \pi_1^P \bar{\pi}_3^P \pi_2^Q \bar{\pi}_4^Q [C(t,s) + C(t,u) - C(s,u)] \\
&+ \frac{1}{2} \pi_1^P \bar{\pi}_3^P \bar{\pi}_2^Q \pi_4^Q [C(t,s) + C(s,u) - C(t,u)] \quad (17) \\
&+ \frac{1}{2} \pi_1^P \bar{\pi}_3^P \bar{\pi}_2^Q \pi_4^Q [C(t,u) + C(s,u) - C(t,s)] .
\end{aligned}$$

Again, we see that the two T-matrices are the same provided that (15) is satisfied. The Veneziano representation for $\pi\pi \rightarrow \pi\pi$ is therefore crossing symmetric.

It should not be surprising that the amplitudes described above are crossing symmetric since they were constructed that way. What we have seen here is that crossing symmetry follows from the symmetry in s and t of A(s,t). If A(s,t) is generalized to the form

$$A(s,t) = \int_0^1 dz F(s,z) F(t,1-z) \quad , \quad (18)$$

then the amplitudes will retain their crossing symmetry.

ii) Singularity Structure. The representation (11) for A(s,t) converges for $\text{Re}\alpha(s) < 1$, $\text{Re}\alpha(t) < 1$. In order to examine the properties of (9) and (10) outside of this region, we shall need to find an analytic continuation of (11). In order to do this for finite s and $\text{Re}\alpha(t) < 1$, we first write

$$\begin{aligned}
A(s,t) &\equiv I_{0\nu}(s,t) + I_{\nu 1}(s,t) = \\
&= \int_0^\nu dz z^{-\alpha(s)} (1-z)^{-\alpha(t)} + \int_\nu^1 dz z^{-\alpha(s)} (1-z)^{-\alpha(t)} \quad . \quad (19)
\end{aligned}$$

The first integral converges for $\text{Re}\alpha(s) < 1$ while the second converges for $\text{Re}\alpha(t) < 1$. We can rewrite $I_{0\nu}$ by expanding the $(1-z)$ term in powers of z . We have

$$I_{0\nu}(s, t) = \sum_{k=0}^{\infty} \frac{\Gamma(k+\alpha(t))}{k! \Gamma(\alpha(t))} \int_0^1 dz z^{k-\alpha(s)} \quad . \quad (20)$$

The integration in (20) can be performed for $\text{Re}\alpha(s) < 1$ with the result

$$I_{0\nu}(s, t) = \sum_{k=0}^{\infty} \frac{\Gamma(k+\alpha(t)) \nu^{k+1-\alpha(s)}}{k! \Gamma(\alpha(t)) (k+1-\alpha(t))} \quad . \quad (21)$$

The representation (21) provides an analytic continuation of $I_{0\nu}$ into the region $\text{Re}\alpha(s) > 1$. With (21) it is easily seen that $A(s, t)$ has poles at

$$\alpha(s) = k + 1 \quad (k = 0, 1, 2, \dots) \quad (22)$$

whose residues are polynomials of degree k in $\alpha(t)$. Since $\alpha(t)$ is a linear function of t these residues are also polynomials of degree k in t .

We shall now examine the consequences of the above expansion for the process $\pi\pi \rightarrow \pi\pi$. From (10) and (21) we see that $C(s, t)$ has poles at $\alpha(s) = j$ ($j = 1, 2, \dots$) whose residues are polynomials of degree j in t . The extra power of t comes from the factor $\gamma(\lambda s + \lambda t + c)$ in (10). The variable t is related to the angle of scattering in the s -channel center of mass system (see figure II.4) by

$$t = \frac{1}{2}(1-s)(1-\cos\theta_s) \quad . \quad (23)$$

Thus the pole of $C(s,t)$ at $\alpha(s) = j$ has a residue which is a polynomial of degree j in $\cos\theta_s$. In terms of the usual partial wave decomposition of $C(s,t)$

$$C(s,t) = \sum_{j=0}^{\infty} (2j+1)C_j(s)P_j(\cos\theta_s) \quad (24)$$

it is clear that the pole at $\alpha(s) = j$ will contribute to $C_j(s)$, $C_{j-1}(s), \dots, C_0(s)$. The pole at $\alpha(s) = 1$, for example, is just the ρ resonance.

We can now examine the singularity structure of the invariant amplitudes (7). Notice first that if the s -channel is physical we have $t < 0$ and $u < 0$. Since $b = \frac{1}{2} < 1$ for the ρ - f^0 trajectory we have $\text{Re}\alpha(t) < 1$ and $\text{Re}\alpha(u) < 1$. In this region the representation (11) for $A(t,u)$ converges and is analytic. Therefore $C(t,u)$ has no singularities in the physical s -channel. From the third equation in (7) we immediately see that the process $\pi\pi \rightarrow \pi\pi$ has no $I=2$ resonances.

The procedures used in the discussion of $C(s,t)$ can be used for $C(s,u)$ as well. The only difference is that

$$u = \frac{1}{2}(1-s)(1+\cos\theta_s) \quad (25)$$

so that

$$C(s,u) = \sum_{j=0}^{\infty} (2j+1)C_j(s)P_j(-\cos\theta_s) \quad . \quad (26)$$

Since $P_j(x) = (-1)^j P_j(-x)$ we find that the $I=0$ resonances have even j while the $I=1$ resonances have odd j .

A plot of the "resonances" occurring in (7) according to their $(\text{mass})^2$ and angular momentum is shown in figure II.5. The set of parameters $\beta=0$, $\lambda=.90 \text{ GeV}^{-2}$, $b=.48$ is used while the elastic partial widths are normalized to $\Gamma_\rho=112 \text{ MeV}$. It is easily seen that the resonances lie on a series of parallel, unit spaced Regge trajectories.

As was the case with crossing symmetry, it should not be surprising that the above results were obtained since the invariant amplitudes (7) were constructed that way. Similar methods can be used for the process $\pi\pi \rightarrow \pi\omega$ although the partial wave decomposition is not so simple. The important result here is the method by which the singularities of $A(s,t)$ were determined. Notice in particular that the s -channel singularities arose from the divergence of the integrand of (11) near $z=0$.

iii) Regge Asymptotics. We now wish to examine (11) as $|s| \rightarrow \infty$ for t fixed. For s in the left half plane the representation (11) converges. For $\text{Re}\alpha(s) > 1$, however, we shall need an analytic continuation.

To begin the discussion we make the change of variables (Suzuki 1969) $z=e^{-x}$ in (11) to obtain

$$A(s,t) = \int_0^\infty dx e^{-x(1-\alpha(s))} (1-e^{-x})^{-\alpha(t)} . \quad (27)$$

This integral is convergent in the region $-\frac{1}{2}\pi < \phi_s \equiv \arg(1-\alpha(s)) < \frac{1}{2}\pi$, $\text{Re}\alpha(t) < 1$. As $|s| \rightarrow \infty$ in this region we expect that the major

contribution to the integral will come from the region of integration near $x=0$. In order to show this explicitly we write (27) as

$$\begin{aligned}
 A(s,t) &= I_1 + I_2 + I_3 = \\
 &= \int_0^{\nu e^{-i\phi s}} + \int_{\nu e^{-i\phi s}}^{\nu} + \int_{\nu}^{\infty} dx e^{-x(1-\alpha(s))} (1-e^{-x})^{-\alpha(t)} \quad (28)
 \end{aligned}$$

where ν is a real constant. Notice that since the t term of the integrand has a singularity at $x=0$ it is not immediately obvious that the contour deformation (27) \rightarrow (28) (see figure II.6) can be performed. In order to validate the rotation near $x=0$ we must show that

$$\lim_{r \rightarrow 0} \int_r^{re^{-i\phi s}} dx e^{-x(1-\alpha(s))} (1-e^{-x})^{-\alpha(t)} = 0. \quad (29)$$

This condition is satisfied for $\text{Re}\alpha(t) < 1$.

We now examine the asymptotic behavior of the three integrals in (28). An upper bound on $|I_3|$ is given by

$$\begin{aligned}
 |I_3| &< \int_{\nu}^{\infty} dx e^{-x(1-\text{Re}\alpha(s))} (1-e^{-x})^{-\text{Re}\alpha(t)} \\
 &< e^{\nu \text{Re}\alpha(s)} \int_{\nu}^{\infty} dx e^{-x} (1-e^{-x})^{-\text{Re}\alpha(t)} \quad (30) \\
 &\rightarrow e^{-\nu \lambda |s| \cos \phi s} \frac{1-\nu^{1-\text{Re}\alpha(t)}}{1-\text{Re}\alpha(t)}
 \end{aligned}$$

as $|s| \rightarrow \infty$. The final term in (30) vanishes faster than any

inverse power of s provided that $-\frac{1}{2}\pi < \phi_s < \frac{1}{2}\pi$. Thus I_3 does not contribute to the asymptotic expansion of $A(s,t)$. The same situation prevails for I_2 since the integrand vanishes faster than any power of s^{-1} as $|s| \rightarrow \infty$ for $|\phi_s| < \frac{1}{2}\pi$. The asymptotic expansion of (28) is therefore given by the asymptotic expansion of I_1 . With the change of variables $y=x(1-\alpha(s))$ and some algebra we have

$$I_1 = (1-\alpha(s))^{\alpha(t)-1} \int_0^{v|1-\alpha(s)|} dy e^{-y} y^{-\alpha(t)} H(y,s,\alpha(t)) \quad (31)$$

where

$$H(y,s,\alpha(t)) = \left[\frac{1-\exp\{-y/(1-\alpha(s))\}}{y/(1-\alpha(s))} \right]^{-\alpha(t)}. \quad (32)$$

The following conditions are satisfied for the integral in (31): A) The integral exists; B) For an arbitrarily small ϵ independent of y we can choose an s_δ such that $|H(y,s,\alpha(t))| < \epsilon$ for all $|s| > s_\delta$ and for all y in some interval $(0, |s|^{\gamma_1})$ with $\gamma_1 > 0$; C) For an arbitrarily small ϵ independent of y we can find an s_δ such that $|H(y,s,\alpha(t))e^{-\gamma_2 y}| < \epsilon$ for all $|s| > s_\delta$ and for all y in $(|s|^{\gamma_1}, v|1-\alpha(s)|)$ with $\gamma_2 < 1$. Under these conditions we can take the limit $|s| \rightarrow \infty$ of the integral in (31) with the result

$$\begin{aligned} A(s,t) &\sim I_1 \sim (1-\alpha(s))^{\alpha(t)-1} \int_0^\infty dy e^{-y} y^{-\alpha(t)} \\ &\sim (-\lambda s)^{\alpha(t)-1} \Gamma(1-\alpha(t)) \end{aligned} \quad (33)$$

as $|s| \rightarrow \infty$ for $|\phi_s| < \frac{1}{2}\pi$. The non-leading terms can be found

by expanding the function $H(y,s,\alpha(t))$ in powers of $y/(1-\alpha(s))$.

We now turn to the problem of finding an analytic continuation of (27) into the right half s -plane. We begin by taking s and t in the region $\text{Im}\alpha(s) > 0$, $\text{Re}\alpha(s) < 1$, $\text{Re}\alpha(t) < 1$. We are free to rotate the path of integration of (27) counter-clockwise through some angle $\frac{1}{2}\pi - \phi$ to obtain (see figure II.7)

$$A(s,t) = \int_0^{\infty} dx e^{-x(1-\alpha(s))} (1-e^{-x})^{-\alpha(t)} e^{i(\frac{1}{2}\pi - \phi)x} \quad (34)$$

There are three points which must be checked here. First, that the analogue of (29) is still valid. This is the case since $\text{Re}\alpha(t) < 1$. Second, that the contour at infinity can be neglected:

$$\lim_{R \rightarrow \infty} \int_R^{\text{Re}^{-1}(\frac{1}{2}\pi - \phi)} dx e^{-x(1-\alpha(s))} (1-e^{-x})^{-\alpha(t)} = 0 \quad (35)$$

This is satisfied provided that $\text{Re}\alpha(s) < 1$, $\text{Im}\alpha(s) > 0$ and $\phi \geq 0$. Finally, we must make sure that no singularities are encountered during the deformation. There are, in fact, singularities at $x = \pm 2n\pi i$ ($n=0,1,2,\dots$) coming from the t term in the integrand. It is precisely this set of singularities which prevents our taking $\phi < 0$.

The representation (34) converges for $\phi - \pi < \phi_s < \phi$. We can therefore use it to determine the asymptotic behavior of $A(s,t)$ in that region. We change (34) to

$$A(s,t) = \int_{C_1 + C_2 + C_3} dx e^{-x(1-\alpha(s))} (1-e^{-x})^{-\alpha(t)} \equiv I_1 + I_2 + I_3 \quad (36)$$

where the paths of integration C_1 , C_2 and C_3 are shown in

figure II.8. In order to avoid the singularity at $x=2\pi i$ we must take $\nu < 2\pi$ where ν is the radius of the arc C_2 . The final two integrals of (36) have integrands which vanish faster than any power of s^{-1} as $|s| \rightarrow \infty$ for $-\pi+\phi+\epsilon < \phi_s < \phi-\epsilon$ where ϵ is small and positive. The first integral of (36) is identical to I_1 of (28). Therefore the asymptotic behaviors of $A(s,t)$ in the regions $-\pi+\phi+\epsilon < \phi_s < \phi-\epsilon$ and $|\phi_s| < \frac{1}{2}\pi$ are identical.

Using the same method but rotating the contour of (27) clockwise we find that the asymptotic expansion remains the same in the region $\epsilon-\phi < \phi_s < \pi-\phi-\epsilon$. Since $\phi \geq 0$ we therefore have the result

$$A(s,t) \sim (-\lambda s)^{\alpha(t)-1} \Gamma(1-\alpha(t)) \quad (37)$$

for $\text{Re}\alpha(t) < 1$, $-\pi+\epsilon < \phi_s < \pi-\epsilon$. Substituting this result into the Veneziano formulae for $\pi\pi \rightarrow \pi\pi$ and $\pi\pi \rightarrow \pi\omega$ we find that the asymptotic behavior is characteristic of processes dominated by exchange of the degenerate ρ - f^0 trajectory.

As an example we consider the $I=1$ amplitude of (7) as $|t| \rightarrow \infty$. Substituting the form (37) for $A(t,s)$ and $A(u,s)$ and using the fact that $s+t+u=1$ we obtain

$$\begin{aligned} A^1(s,t,u) &\sim \gamma \Gamma(1-\alpha(s)) \{ (-\lambda t)^{\alpha(s)} - (\lambda t)^{\alpha(s)} \} \\ &= -\gamma \Gamma(1-\alpha(s)) (\lambda t)^{\alpha(s)} \{ 1 - e^{-i\pi\alpha(s)} \}. \end{aligned} \quad (38)$$

Notice that a signature factor arises from the combination of the two terms.

There are several points to be mentioned before proceeding further. First, the result (37) can be shown to hold even for $\text{Re}\alpha(t) > 1$. In order to do this we integrate (27) by parts until the resulting integral converges in the desired region of the t -plane. We then proceed with the same analysis as above. Second, the Veneziano model does not give Regge behavior for $|s| \rightarrow \infty$, $\arg(s) = 0$. The reason for this is that $A(s, t)$ has an infinite series of poles on the real, positive s -axis. If the trajectory functions are given an imaginary part above threshold then the poles can be shifted onto the second sheet of the s -plane and Regge behavior can be obtained for $\arg(s) = 0$ (Roskies 1968).

iv) Duality. This property, while not firmly established, has been built into the Veneziano model. In contrast to interference models, in which the amplitudes are built from direct channel resonances plus crossed channel Regge pole contributions, dual models are built either from resonances or from Regge poles. The simplest quantitative statement of duality is found in terms of finite energy sum rules (FESR) (see Jackson 1970 for a review). If resonances are used to saturate the left hand side of an FESR then the right hand side should show characteristic Regge pole behavior.

As an example for the Veneziano model, we saturate the FESR

$$\frac{1}{N} \int_0^N ds \text{Im}C(s, t) = \frac{\pi \gamma \alpha(t) (\lambda N)^{\alpha(t)}}{(\alpha(t)+1) \Gamma(\alpha(t)+1)} \quad (39)$$

with the zero width "resonances" of $C(s, t)$. We define $C(s, t)$

by choosing $\beta=0$ in (8). The left hand side of (39) can be integrated explicitly to give

$$\frac{1}{N} \int_0^N ds \operatorname{Im} C(s,t) = \frac{\pi \gamma \alpha(t)}{\lambda N} \frac{\Gamma(M+\alpha(t)+2)}{\Gamma(\alpha(t)+2)\Gamma(M+1)} \quad (40)$$

M is the largest integer such that $\lambda N + b - 1 > M$. The right hand sides of (39) and (40) are compared in figure II.9 with $b=.5$, $\gamma=1.0$ and $\lambda=1 \text{ GeV}^{-2}$ for $\lambda N=2$ and $\lambda N=4$.

v) Asymptotic Behavior, $\theta_s = \pi$. The fact that $C(s,t)$ and $C(s,u)$ exhibit Regge behavior as $|t| \rightarrow \infty$ with s fixed is not sufficient to guarantee that the $I=0$ amplitude of (7) is Regge behaved. We must still make sure that the $C(t,u)$ term does not cause any difficulty in this limit. To keep the discussion consistent with our earlier examination of Regge behavior we shall examine the function $A(s,t)$ in the limit $|s| \rightarrow \infty$, u fixed. In terms of figure II.1a this corresponds to $|s| \rightarrow \infty$, $\theta_s \rightarrow \pi$.

We begin by making the change of variables $e^{-x} = z(1-z)^{-1}$ (Suzuki 1969) in (11) to obtain

$$A(s,t) = \int_{-\infty}^{\infty} dx e^{-x(1-\alpha(s))} (1+e^{-x})^{2b-2-\lambda(u-1)} \quad (41)$$

This representation converges for $2b-1+\lambda(1-\operatorname{Re}u) < \operatorname{Re}\alpha(s) < 1$. If we take $\operatorname{Im}\alpha(s) > 0$ then we can rotate the integration contour of (41) in the manner shown in figure II.10. The rotation is hindered only by the fact that the second term in (41) has singularities at $x = \pm(2n+1)\pi i$ ($n = 0, 1, \dots$). There are no singularities in the right half x -plane. The new representation

converges for $\phi - \pi < \phi_S \leq -\frac{1}{2}\pi$, $2b - 1 + \lambda(1 - \text{Re}u) < \text{Re}\alpha(s)$. It is easily seen that for $\phi - \pi < \phi_S < -\frac{1}{2}\pi - \delta$ the integrand of (41) vanishes faster than any power of s^{-1} as we move away from the point $x = i(\pi - \epsilon)$ along either C_1 or C_2 . The leading behavior of (41) is thus

$$A(s, t) \sim O(e^{-(\pi - \epsilon)|\text{Im}\alpha(s)|}) \quad (42)$$

as $|s| \rightarrow \infty$, u fixed, $-\pi < \phi - \pi < \phi_S < -\frac{1}{2}\pi - \delta$. This result can also be shown for $\frac{1}{2}\pi + \delta < \phi_S < \pi - \phi < \pi$ by rotating the contour in the opposite direction.

Notice that the real s -axis is excluded as it was in the case of Regge behavior. If we set $|\phi_S| = \pi$ then we no longer obtain the exponentially decreasing behavior (42). It is hoped that when trajectories which are complex above threshold are introduced the decreasing behavior will persist even on the real s -axis. This problem has been studied in the context of the Veneziano model by Roskies (1968)

Finally, we should point out that the region $|s| \rightarrow \infty$, u fixed, $\phi < |\phi_S| < \frac{1}{2}\pi$ can be studied by examining the behavior of $A(s, t)$ for $|t| \rightarrow \infty$, u fixed, $\frac{1}{2}\pi < |\phi_t| < \pi - \phi$. The same exponentially damped behavior as in (42) will naturally persist.

Because of the exponentially decreasing behavior just off the real axis, the $C(t, u)$ terms in (7) are usually ignored asymptotically ($|t| \rightarrow \infty$, s fixed).

vi) Asymptotic Behavior, fixed angle. For completeness, we examine the behavior of $A(s, t)$ as $|s| \rightarrow \infty$ with θ_S fixed.

In order to simplify the discussion we define the quantity

$$\chi_s = \frac{1}{2}(1 - \cos\theta_s) \quad (43)$$

so that (23) gives $t = (1-s)\chi_s$ for $\pi\pi$ elastic scattering. With the change of variables $e^{-x} = z(1-z)^{-\chi_s}$ (11) becomes

$$A(s, t) = \int_{-\infty}^{\infty} dx \frac{e^{-x(1-\lambda s)} z^{-b} (1-z)^{\chi_s(1-\lambda)+1-b}}{1-(1-\chi_s)z} \quad (44)$$

where $z = z(x)$. Notice that for $\chi_s = 0(1)$ the change of variables above reduces to that used for the fixed $t(u)$ case. The representation (44) converges for $1 > \text{Re}\alpha(s) > \lambda + b + (b-1)/\chi_s$. If we also take $\text{Im}\alpha(s) > 0$ then we can perform the path rotation of figure II.11. It is easily seen that the first singularity which interferes with the deformation is a pole coming from the $(1-z+z\chi_s)^{-1}$ term of (44) at

$$x = P = (1-\chi_s)\ln(1-\chi_s) + \chi_s\ln(\chi_s) + i\pi\chi_s \quad (45)$$

where χ_s is real. The new representation converges for $\phi - \pi < \phi_s < -\frac{1}{2}\pi$, $\text{Re}\alpha(s) > \lambda + b + (b-1)/\chi_s$. The major contribution to the integrand will come from near the point P of figure II.11. Since similar arguments can be used for $\frac{1}{2}\pi < \phi_s < \pi - \phi$ we finally obtain

$$A(s, t) \sim O(\exp(\text{Re}P \times \text{Re}\alpha(s) - \pi\chi_s |\text{Im}\alpha(s)|)) \quad (46)$$

as $|s| \rightarrow \infty$, $\frac{1}{2}\pi < |\phi_s| < \pi - \phi < \pi$, θ_s fixed. Since $0 < \chi_s < 1$, the factor

multiplying $\text{Re}\alpha(s)$ is negative. Thus (46) vanishes exponentially with s as $|s| \rightarrow \infty$ in the above region. As usual, we must take ϕ non-negative. Notice, however, that if we set $\phi=0$, $|\phi_s|=\pi$ we will receive contributions from near all of the poles in figure II.11. Because these poles are in the left half x -plane, $A(s,t)$ will still be exponentially decreasing.

vii) Zeros of the Amplitudes. The poles which were found in part ii) of this section should be observed experimentally as "bumps" in the scattering cross sections. These bumps represent only half of the structure of the Veneziano model. We should also expect to find "holes" where the amplitudes have zeros. In order to find these zeros we use the representation (5) for $A(s,t)$. Using the well known properties of the Gamma function we find that $A(s,t)$ has zeros when

$$\alpha(s) + \alpha(t) = n + 2 \quad (n = 0, 1, 2, \dots) \quad (47)$$

unless $\alpha(s)$ or $\alpha(t)$ is a positive integer.

In addition to the zeros (47), the function $C(s,t)$ has a zero at

$$s + t = -c/\lambda = (1-2b-\beta/\gamma)/\lambda \quad (48)$$

If $\beta=0$ then (48) is a member of the set (47) with $n=-1$.

II.3 Summary

We have seen that the Veneziano model has an infinite number of poles lying on parallel, unit spaced Regge trajectories. The most leading of these poles can be chosen to correspond to observed resonances in both mass and angular momentum content. The behavior of the term $C(s,t)$ is satisfactory as $|s| \rightarrow \infty$ for t fixed, u fixed or for fixed angle provided that we stay away from the real, positive s -axis. The properties of duality and crossing symmetry are built into the model.

Many of the difficulties of the Veneziano model can be traced to one fact: The trajectories have no imaginary part above threshold. For example, the model cannot be unitary. Near the ρ pole the $j=1$ partial wave projection has an imaginary part

$$\text{Im}A_{j=1}(s) \propto \delta(s-M_\rho^2) \quad . \quad (49)$$

The elastic unitarity relation,

$$\text{Im}A_j(s) \propto |A_j(s)|^2 \quad , \quad (50)$$

therefore has a factor $\delta(s-M_\rho^2)$ on the left and a factor $\delta^2(s-M_\rho^2)$ on the right. This difficulty would be avoided if the ρ resonance had a nonzero width. Notice also that if the trajectories had an imaginary part with the proper behavior at infinity then the asymptotic behavior discussed above could be extended to the real axis (Roskies 1968). Finally, we should

mention that for many physical applications of the Veneziano model it is necessary to use trajectories which are complex above threshold in order to have a smooth behavior. Certain applications of the Veneziano model will be discussed in chapter VI.

The introduction of complex trajectories into the Veneziano model is not simple. In the models of Lovelace (1968) and Roskies (1968) there are resonances with the same masses as those lying on the leading trajectory but with higher spin. The remainder of this thesis will be concerned with models which avoid these "ancestors" while introducing complex trajectories into a Veneziano-like form.

III. Early Models

In this chapter we shall examine three models which introduce finite-width resonances into a Veneziano-like form while avoiding the problem of ancestors. All of these models have double spectral functions which are non-vanishing in reasonable regions. Two of the models (Cohen-Tannoudji 1971, Gaskell 1972) can be adjusted to provide the correct threshold behavior for both the real and imaginary parts of all partial waves. These properties are not shared by the Veneziano model. However, each of the models has serious difficulties (Atkinson 1972, Gaskell 1972). These will be discussed below in detail.*

III.1 Models to be Examined

All of the models of this and succeeding chapters will redefine $A(s,t)$ by replacing the Beta function integral representation (II.11) with the representation

$$A(s,t) = \int_0^1 dz z^{-\alpha(s,z)} (1-z)^{-\alpha(t,1-z)} \quad . \quad (1)$$

The three models which we now describe differ only in their definitions of $\alpha(s,z)$ and $\alpha(t,1-z)$.

i) The Suzuki Model (Suzuki 1969). In this model the trajectory function is defined by

* Other models which have been proposed along these lines are those of (Bugrij 1971), (Ramachandran 1971), (Mestres 1971) and (Schmidt 1971). All of these suffer from the difficulties mentioned in this chapter.

$$\alpha(s, z) = \alpha(s) - \gamma(z)\Delta\alpha(s) \quad (2)$$

where

$$\alpha(s) = \lambda s + b + \Delta\alpha(s) \quad (3)$$

and

$$\Delta\alpha(s) = \frac{s}{\pi} \int_1^{\infty} ds' \frac{\Psi(s')}{s'(s'-s)} \quad (4)$$

The function $\gamma(z)$ is a Van der Corput neutralizer, defined such that

$$\gamma(0) = \gamma(1) - 1 = 0 \quad (5)$$

and

$$\left. \frac{d^m \gamma(z)}{dz^m} \right|_{z=0} = \left. \frac{d^m \gamma(1-z)}{dz^m} \right|_{z=0} = 0 \quad (m=1, 2, \dots). \quad (6)$$

The function chosen by Suzuki to satisfy these requirements is

$$\gamma(z) = \frac{1}{c} \int_0^z dx (-\ln x)^{\ln x} (-\ln(1-x))^{\ln(1-x)} \quad (7a)$$

where

$$c = \int_0^1 dx (-\ln x)^{\ln x} (-\ln(1-x))^{\ln(1-x)} \quad (7b)$$

ii) The Distorted Trajectory (DT) Model (Gaskell 1972).

In this model we define the trajectory function by

$$\alpha(s, z) = \alpha(s) - \frac{s}{\pi} \int_1^{\infty} ds' \frac{\Psi(s')}{s'(s'-s)} \quad (8)$$

where $\alpha(s)$ is given by (3) with (4). The use of $\Psi(s')$ rather than $\text{Im}\alpha(s')$ in the dispersion relation now becomes important

since $1/(1-z)$ is not necessarily on the line $s' = (1, \infty)$.

iii) The CHKZ Model (Cohen-Tannoudji 1971). This model uses the trajectory function

$$\alpha(s, z) = \alpha(s(1-z)) + f(s(1-z))/(\ln z) \quad . \quad (9)$$

In the original work the functions

$$\alpha(y) = \lambda y + b + \eta(1-y)^{\frac{1}{2}} \quad (10)$$

and

$$f(y) = \beta(1-y)^{\frac{1}{4}} \quad (11)$$

are used where β and η are constants.

III.2 Properties of the Models

We shall now examine the above models in detail, comparing the results with those found in chapter II for the Veneziano model.

i) Narrow Resonance Limit. If we take $\Psi(s') \equiv 0$ then both the Suzuki and DT models reduce to the Veneziano form (II.11). This property is not shared by the CHKZ model.

ii) Crossing Symmetry. Since (1) is in the form (II.18), the amplitudes constructed from these models will be crossing symmetric.

iii) Singularity Structure. The integral (1) converges only for $\text{Re}\alpha(s) < 1$, $\text{Re}\alpha(t) < 1$ in all the models under consideration. In order to examine the singularities in $\text{Re}\alpha(s) > 1$ we shall need an analytic continuation. As with the Veneziano model, the singularities of $A(s,t)$ in the s-channel come from the $z=0$ region of integration in (1). We therefore need only examine this region.

In the region $\text{Re}\alpha(s) < 1$, $\text{Re}\alpha(t) < 1$ the Suzuki form of (1) can be written

$$\begin{aligned}
 A(s,t) &= \int_{\nu}^1 dz z^{-\alpha(s,z)} (1-z)^{-\alpha(t,1-z)} \\
 &+ \sum_{j,k=0}^{\infty} \frac{1}{j!k!} \int_0^{\nu} dz \{ z^{-\alpha(s)} (1-z)^{-\lambda t-b} [\gamma(z) \ln z \Delta\alpha(s)]^j \\
 &\quad \times [(\gamma(1-z)-1) \ln(1-z) \Delta\alpha(t)]^k \} .
 \end{aligned} \tag{12}$$

The first integral in (12) converges as long as $\text{Re}\alpha(t) < 1$. Since $\gamma(z)$ and $\gamma(1-z)-1$ vanish faster than any power of z as $z \rightarrow 0$, only the $j=k=0$ term of the sum in (12) diverges as we move into the region $\text{Re}\alpha(s) > 1$. The $j=k=0$ integral can be performed. Writing the convergent terms mentioned above as a remainder we have

$$A(s,t) = B_{\nu}(1-\alpha(s), 1-\lambda t-b) + R_{\nu}(s,t) \tag{13}$$

for $\text{Re}\alpha(t) < 1$. B_{ν} is the incomplete Beta function. Thus $A(s,t)$ in the Suzuki model has a series of poles at $\alpha(s) = n + 1$ ($n=0,1,2,\dots$) with residues which are polynomials of degree n in t . This is precisely the same as the singularity structure of the Veneziano model except that if $\Psi(s') > 0$ for $1 < s' < \infty$ the

poles are shifted onto the second sheet of the s -plane becoming resonances with finite positive width. Notice that $\alpha(s)$ has a branch point at $s=1$ so that $A(s,t)$ has a cut starting there. This branch point and the poles mentioned above are the only s -channel singularities in Suzuki's model.

The leading singularities of the other two models can be determined with the above method. In the DT model the trajectory functions have the $z \rightarrow 0$ limits

$$\begin{aligned}\alpha(s, z) &\rightarrow \alpha(s) \\ \alpha(t, 1-z) &\rightarrow \lambda t + b\end{aligned}\quad (14)$$

Thus the leading singularities of the DT model are given by

$$\begin{aligned}A(s, t) &\approx \int_0^v dz z^{-\alpha(s)} (1-z)^{-\lambda t - b} \\ &\equiv B_v(1-\alpha(s), 1-\lambda t - b)\end{aligned}\quad (15)$$

This is the first term in an expansion similar to (12). The singularity structure of (15) is the same as that obtained from the Suzuki model. Similarly, the expansion of the CHKZ model has the first term

$$A(s, t) \approx e^{-f(s)} \int_0^v dz z^{-\alpha(s)} (1-z)^{-\alpha(0)} e^{-f(tz)} \quad (16)$$

Since $f(y)$ is analytic near $y=0$ the final term in the integrand of (16) can be expanded in powers of tz . We find that the CHKZ model also has poles at $\alpha(s) = n + 1$ ($n=0, 1, 2, \dots$) with

polynomial residues of degree n in t .

Variations of the Suzuki model can be found which possess additional singularities such as cuts. The CHKZ and DT models, however, must have additional singularities coming from non-leading terms in the expansions analogous to (12). In the CHKZ model these additional singularities are multiple poles lying on non-leading trajectories. The extra singularities in the DT model may be non-leading simple poles, multiple poles or cuts depending upon the precise form of $\Psi(s')$. It is possible to choose $\Psi(s')$ so that no multiple poles appear in the DT model.

Finally, notice that the functions $A(s,t)$ in both the DT and CHKZ models have branch points at $s=1$. These arise because in both models $\alpha(s,z)$ has a singularity at $z=1-s^{-1}$. As $s \rightarrow 1$, this singularity encounters the lower endpoint of the integration (1) giving a singularity at $s=1$.

None of the models has singularities on the physical sheet of the s -plane except for the cut along the real, positive s -axis starting at $s=1$.

iv) Double Spectral Region. This region is defined as the part of the real s - real t plane in which

$$\text{Disc}_t \{ \text{Disc}_s A(s,t) \} \equiv -4\rho(s,t) \neq 0 \quad . \quad (17)$$

The function $\rho(s,t)$ is called the double spectral function.

The trajectory functions of the Suzuki representation are cut in the following regions:

$$\begin{aligned} \text{Disc}_s \alpha(s, z) &\neq 0 \quad \text{in } s > 1, \\ \text{Disc}_t \alpha(t, 1-z) &\neq 0 \quad \text{in } t > 1. \end{aligned} \quad (18)$$

Therefore, the double spectral function of the Suzuki model is nonzero in $s > 1, t > 1$. This region is shown in figure III.1.

The trajectory functions of both the DT and CHKZ models are cut as follows:

$$\begin{aligned} \text{Disc}_s \alpha(s, z) &\neq 0 \quad \text{in } z < 1-s^{-1}, \\ \text{Disc}_t \alpha(t, 1-z) &\neq 0 \quad \text{in } z > t^{-1}. \end{aligned} \quad (19)$$

With (1) we see that these models have the double spectral region

$$s > 1, t > 1, s^{-1} + t^{-1} < 1. \quad (20)$$

This region is shown in figure III.1 along with the exact region for scattering of scalar bosons in a ϕ^3 -interaction Lagrangian:

$$s > 1, t > 1, (s-1)(t-1) > \frac{1}{4}. \quad (21)$$

We should mention in passing that both the DT and CHKZ models can be altered slightly so that they have the ϕ^3 double spectral region (21). In the DT model this is done by using $(1-\frac{1}{2}z)/(1-z)$ as the upper endpoint of integration in (8).

v) Threshold Behavior. For amplitudes satisfying the Mandelstam representation there exists a simple relationship between the boundary of the double spectral region and the

threshold behavior (see, for example Frautschi 1963, ch. 4). Since we do not know whether the three models under discussion can be expressed in the form of the Mandelstam representation with a finite number of subtractions, we shall use a variation of the method.

The behavior of $A(s,t)$ near $s=1$ can be examined by expanding this function in powers of t :

$$A(s,t) = \sum_{k=0}^{\infty} v_k(s) t^k \quad . \quad (22)$$

If the $v_k(s)$ are known then the behavior of the partial waves near $s=1$ can be found.

We shall examine the amplitude for the process $\pi^+ \pi^- \rightarrow \pi^+ \pi^-$. With (II.7) and (II.10) we find the amplitude for this process to be

$$A^{+-}(s,t,u) = \gamma(\lambda s + \lambda t + c) A(s,t) \quad (23)$$

where $A(s,t)$ is now given by (1). With (22) and (23) we have

$$A^{+-}(s,t,u) = \gamma(\lambda s + c) v_0(s) + \gamma \sum_{k=1}^{\infty} [(\lambda s + c) v_k(s) + \lambda v_{k-1}(s)] t^k \quad . \quad (24)$$

With (II.23) we see that each power of t introduces a power of $\cos \theta_s$. As long as the $v_k(s)$ increase slower than $(s-1)^{-k}$ as k increases then the leading behaviors of (24) as $s \rightarrow 1$ are given by

$$A_0^{+-}(s) \sim \gamma(\lambda+c)v_0(s) \quad (25a)$$

and

$$A_j^{+-}(s) \sim \gamma[(\lambda+c)v_j(s) + \lambda v_{j-1}(s)] \frac{(j!)^2 (s-1)^j}{(2j+1)!} \quad (25b)$$

where $j \neq 0$ in (25b).

The functions $v_j(s)$ appearing in (25) could be determined from the relation

$$v_j(s) = \frac{1}{j!} \left(\frac{d^j}{dt^j} A(s,t) \right) \Big|_{t=0} \quad (26)$$

Instead of using (26), we shall estimate the $v_j(s)$ by using the relation

$$v_j(s) = \frac{1}{2\pi i} \oint_C dt' A(s,t') t'^{-j-1} \quad (27)$$

where the circular path C is chosen to be small enough to avoid the nearest singularity in t' .

In all of the models under discussion, $A(s,t)$ is a real analytic function for $s, t < 1$ and real. Using the Schwartz reflection principle, we therefore see that for $s > 1$, real and $t < 1$, real, $A(s,t)$ has the real and imaginary parts

$$\text{Re}A(s,t) = \frac{1}{2} \text{Sum}_s A(s,t) \equiv \frac{1}{2} [A(s+i\epsilon,t) + A(s-i\epsilon,t)] \quad (28a)$$

$$\text{Im}A(s,t) = -\frac{1}{2} i \text{Disc}_s A(s,t) \quad (28b)$$

In all three models, $\text{Sum}_s A(s,t)$ has a singularity at $t=1$. Using the path of integration of figure III.2 and equation

(27) we therefore have

$$\text{Re}v_j(s) = \frac{(1-\epsilon)^{-j}}{4\pi} \int_0^{2\pi} d\eta e^{-i\eta j} \text{Sum}_s A(s, (1-\epsilon)e^{i\eta}) \quad (29)$$

where ϵ is a small positive number. In all of the models $\text{Sum}_s A(s, (1-\epsilon)e^{i\eta}) \rightarrow F(e^{i\eta})$ independent of s as $s \rightarrow 1$. Therefore, as $s \rightarrow 1$, $\text{Re}v_j(s) \rightarrow \text{Re}v_j(1)$ finite. Thus we find, with (25),

$$\text{Re}A_j^{+-}(s) \sim (s-1)^j \quad \text{as } s \rightarrow 1. \quad (30)$$

In the model of Suzuki, the function $\text{Disc}_s A(s, t)$ also has a singularity at $t=1$. With a treatment similar to that above we find

$$\text{Im}A_j^{+-}(s) \sim (s-1)^j \quad \text{as } s \rightarrow 1. \quad (31)$$

As we shall see shortly, this behavior is inconsistent with elastic unitarity near threshold.

With (20) and the definition (17), we see that $\text{Disc}_s A(s, t)$ in the DT and CHKZ models has a singularity at

$$t = f(s) \equiv s/(s-1) \quad . \quad (32)$$

With the path of integration shown in figure III.3 and with equation (27) we have

$$\text{Im}v_j(s) = \frac{(1-\epsilon)^{-j}}{4\pi i} \left(\frac{s-1}{s} \right)^j \int_0^{2\pi} d\eta e^{-i\eta j} \text{Disc}_s A(s, (1-\epsilon)f(s)e^{i\eta}) \quad (33)$$

where ϵ is small and positive. The trajectory functions in both models can be chosen so that*

$$\text{Disc}_s A(s, (1-\epsilon)f(s)e^{i\eta}) \sim (s-1)^{3/2} F(e^{i'}) \quad (34)$$

as $s \rightarrow 1$. The function $F(x)$ cannot be a polynomial of finite degree in x . If this were the case then (36b) below would follow only up to $j=n+1$ with n the degree of $F(x)$. With (33) and (34), we have

$$\text{Im}v_j(s) \sim (s-1)^{j+3/2} \quad (35)$$

as $s \rightarrow 1$ and finally, with (25),

$$\text{Im}A_0^{+-}(s) \sim (s-1)^{3/2} \quad (36a)$$

$$\text{Im}A_j^{+-}(s) \sim (s-1)^{2j+1/2} \quad (j \neq 0) \quad (36b)$$

The elastic unitarity relation for $\pi^+\pi^- \rightarrow \pi^+\pi^-$ can be written

$$\text{Im}A_j^{+-}(s) = \left(\frac{s-1}{s}\right)^{1/2} |A_j^{+-}(s)|^2 + R_j(s) \quad (37)$$

$R_j(s)$ contains contributions from the $\pi^-\pi^+$ and $\pi^0\pi^0$ intermediate states and can be ignored without effecting the following arguments. If we substitute (30) and (36) into (37), we find

* The function which accomplishes this in the CHKZ model is very complicated. See footnote 2 of (Cohen-Tannoudji 1971).

that the power dependence on $(s-1)$ is the same on both sides of (37) for all partial waves except $j=0$. As we shall demonstrate in connection with the model of chapter V, the $j=0$ threshold behavior can be corrected by adding a satellite term. Notice that the result (36) depends upon the boundary of the double spectral region through (32) and upon the behavior of $\text{Disc}_s A(s, (1-\epsilon)f(s)e^{i\eta})$ as $s \rightarrow 1$.

We shall now examine the restrictions on the trajectory functions which lead to the behavior (34) in the DT model. With (1) and (8) we have

$$\begin{aligned} \text{Disc}_s A(s, (1-\epsilon)f(s)e^{i\eta}) &= -2i \int_0^{\frac{s-1}{s}} dz \{ z^{-\text{Re}\alpha(s,z)} \\ &\times (1-z)^{-\alpha((1-\epsilon)e^{i\eta}s/(s-1), 1-z)} \sin(\text{Im}\alpha(s)\ln z) \} . \end{aligned} \quad (38)$$

If $\text{Im}\alpha(s)$ vanishes faster than $1/(\ln(s-1))$ as $s \rightarrow 1$ then we find that

$$\begin{aligned} \text{Disc}_s A(s, (1-\epsilon)f(s)e^{i\eta}) &\sim -2i \left(\frac{s-1}{s} \right)^{1-\alpha(1)} \text{Im}\alpha(s) \\ &\times \ln \left(\frac{s-1}{s} \right) \int_0^1 dq q^{-\alpha(1)} e^{\lambda q(1-\epsilon)} e^{i\eta} \end{aligned} \quad (39)$$

as $s \rightarrow 1$. Therefore (34) is satisfied provided that

$$\Psi(s) \equiv \text{Im}\alpha(s) \sim - \frac{(s-1)^{\alpha(1)+\frac{1}{2}}}{\ln(s-1)} \quad (s \rightarrow 1). \quad (40)$$

It is interesting to notice that with this choice for $\Psi(s)$ no multiple poles appear in the DT model.

vi) Asymptotic Behavior, t fixed. We shall now use the methods of chapter II to examine the behavior of $A(s,t)$ as $|s| \rightarrow \infty$ with t fixed.

This Suzuki model can be treated in precisely the same way as was the Veneziano model (Suzuki 1969). All of the contour deformations are valid so that we find

$$A(s,t) \sim (-\lambda s)^{\alpha(t)-1} \Gamma(1-\alpha(t)) \quad (41)$$

as $|s| \rightarrow \infty$, $-\pi+\epsilon < \arg(-s) < \pi-\epsilon$. There is, however, one major difficulty with this model. Despite the fact that $\alpha(s)$ is now complex above threshold, we still cannot extend the Regge behavior to the real, positive s -axis. This problem stems from the fact that $\gamma(e^{-x})$ defined in (7) diverges exponentially as $|x| \rightarrow \infty$, $|\arg x| \rightarrow \frac{1}{2}\pi$. Thus the contour rotation of figure II.7 can only be performed through angles $\frac{1}{2}\pi-\phi$ with $\phi > 0$.

There is nothing in the behavior of the DT model at $x=0$ and $x=\infty$ to prohibit the contour rotations of figures II.6 - II.8. Applying the contour rotation of figure II.6 to the integral representation

$$A(s,t) = \int_0^{\infty} dx e^{-x(1-\alpha(s, e^{-x}))} (1-e^{-x})^{-\alpha(t, 1-e^{-x})} \quad (42)$$

we find that the leading behavior of $A(s,t)$ is just (41) as $|s| \rightarrow \infty$ for $|\arg(-s)| < \frac{1}{2}\pi$. With (8) we see that $\alpha(s, e^{-x})$ has a series of singularities at

$$x = -\ln(1-s^{-1}) \pm 2n\pi i \quad (n = 0, 1, 2, \dots) \quad (43)$$

Although these singularities can lie in the right half x -plane, they do not interfere with the contour deformations. The function $\alpha(t, 1-e^{-x})$, however, does present a problem. It has singularities at

$$x = \ln t \pm 2n\pi i \quad (n = 0, 1, 2, \dots) \quad (44)$$

For $|t| < 1$ these singularities lie in the left half x -plane. We can therefore perform all of the contour deformations of chapter II with the result that $A(s, t)$ has the asymptotic behavior (41) for $|\arg(-s)| < \pi - \epsilon$ and $|t| < 1$. For $|t| > 1$ the singularities (44) lie in the right half x -plane and can destroy the Regge behavior. For example, the integral around C_t of figure III.4 gives a contribution with a factor $t^{\alpha(s)}$ as $|s| \rightarrow \infty$, t fixed. This term clearly dominates the Regge behavior (Atkinson 1972, Gaskell 1972).

Even more problems arise with the CHKZ model. This model can be shown to have Regge behavior as $|s| \rightarrow \infty$ in the left half s -plane (Cohen-Tannoudji 1971). We now make the change of variables $y = -(1-z)\ln z$ in (1), substituting the CHKZ definition of $\alpha(s, z)$. We have

$$A(s, t) = \int_0^{\infty} dy \left[\frac{z}{(1-z) - z \ln z} \right] e^{\lambda s y} z^{-\sigma(s(1-z))} \times (1-z)^{-\alpha(tz)} e^{-f(s(1-z))} e^{-f(tz)} \quad (45)$$

where $z = z(y)$ and where we have written $\alpha(s) = \lambda s + \sigma(s)$.

In order to determine the asymptotic behavior of $A(s, t)$ in the

right half s -plane, we must perform the same rotations in the y -plane as we did in the x -plane for the Veneziano, Suzuki and DT models. The functions $\alpha(tz)$ and $f(tz)$ yield singularities in the y -plane at

$$y = (1-t^{-1})(\ln t \pm 2n\pi i) \quad (n = 0, 1, 2, \dots) \quad (46)$$

These singularities imply non-Regge contributions similar to those of the DT model (Atkinson 1972, Gaskell 1972). In addition, the term in brackets in the integrand of (45) yields a series of singularities in the approximate positions

$$y = 1 + \ln((2n+1)\pi/2) \pm (2n+1)i\pi/2 \quad (n = 0, 1, 2, \dots) \quad (47)$$

The exact positions of the first few singularities are $y_1 = 2.56 \pm 4.4i$, $y_3 = 3.42 \pm 10.8i$, $y_5 = 3.86 \pm 17.14i$. As is seen in figure III.5, the contour rotation can only be made through an angle of $\frac{1}{2}\pi - 30.5^\circ$ before the singularity at $y=y_1$ interferes. Thus, even if there is no interference from the singularities (46), the CHKZ model cannot have Regge behavior as $|s| \rightarrow \infty$ for any t if $|\arg s| < 30.5^\circ$ (Atkinson 1972).

III.3 Summary and Discussion

We have examined three models which have finite width resonances and a Veneziano-like form. The amplitudes constructed from these models are ancestor-free and crossing symmetric. The leading singularities are resonances lying on the ρ - f^0

trajectory. Non-leading singularities can be simple poles, multiple poles or cuts depending on the model used. We have shown that if the boundary of the double spectral region is given by $t \sim (s-1)^{-1}$ as $s \rightarrow 1$ then, provided that (34) is satisfied, the partial wave projections of the amplitudes can have the correct threshold behavior. The Suzuki model does not have the proper type of double spectral boundary but the DT and CHKZ models do. The most important results arise from the study of asymptotic behavior. For some t the DT model is Regge behaved for all s on the physical sheet of the s -plane* as $|s| \rightarrow \infty$. For other values of t , however, this model has non-Regge behavior for some $\arg(s)$. The CHKZ model is non-Regge for all values of t as $|s| \rightarrow \infty$ with $|\arg s| < 30.5^\circ$. In addition, for some values of t it lacks Regge behavior for an even larger portion of the s -plane. The Suzuki model is non-Regge as $|s| \rightarrow \infty$ for $\arg(s) = 0, 2\pi$.

The prospects for extending the Regge behavior of the Suzuki and CHKZ models to the real, positive s -axis are not good. The most promising approach therefore appears to be a search for a new model in the spirit of the DT form.

* The proof of Regge behavior along the real, positive s -axis is somewhat lengthy. It follows along the lines of a similar proof given in Chapter V.

IV. Restrictions on DT Models

We shall now examine a generalized form of the DT model. The definition (III.1) for $A(s,t)$ will be retained. We define $\alpha(s,z)$ and two useful related functions, $f(s,z)$ and $g(s,z)$, by

$$\alpha(s,z) = \lambda s + b + \frac{s}{\pi} \int_{\phi(z)}^{\infty} ds' \frac{\Psi(s')}{s'(s'-s)} \quad (1)$$

$$\equiv \lambda s + b + g(s,z) \equiv \alpha(s) - f(s,z)$$

where $\alpha(s)$ is defined by (III.3) with (III.4). The function $\phi(z)$ is a real, increasing function of z for $0 < z < 1$ such that

$$\phi(0) = 1, \quad \phi(1) = \infty \quad . \quad (2)$$

We therefore have

$$\alpha(s,0) = \alpha(s), \quad \alpha(s,1) = \lambda s + b \quad . \quad (3)$$

Since the integral defining $\alpha(s)$ is required to be convergent we demand that

$$s^{-1} \Psi(s) \rightarrow 0 \quad \text{as} \quad s \rightarrow \infty \quad . \quad (4)$$

We shall also require that $\Psi(s)$ be such that

$$\alpha(s,z) \sim \lambda s \quad \text{as} \quad |s| \rightarrow \infty \quad . \quad (5)$$

The amplitudes constructed from this model are clearly crossing symmetric since (III.1) is in the form (II.18). We shall now obtain some of the other properties of these models in order to restrict the functions $\phi(z)$ and $\Psi(s')$.

IV.1 Unitarity Cut

If $\Psi(s')$ is a real analytic function of s' for $s' > 1$ and real then $A(s,t)$ is a real analytic function of s and t for $s, t < 1$ and real. If we increase s so that $s > 1$ and slightly above the real axis then $\alpha(s,z)$ will have an imaginary part

$$\text{Im}\alpha(s,z) = -\frac{1}{2}i \text{Disc}_s \alpha(s,z) = \Psi(s)\theta(s-\phi(z)) \quad . \quad (6)$$

In order for $\alpha(s)$ to have a positive imaginary part for $s > 1$ and real, we must have

$$\Psi(s) > 0 \quad (1 < s < \infty, \text{ real}) \quad . \quad (7)$$

Substituting (6) into (III.1) we find

$$\begin{aligned} \text{Im}A(s,t) = & - \int_0^{\phi^{-1}(s)} dz \{ z^{-\text{Re}\alpha(s,z)} (1-z)^{-\alpha(t,1-z)} \\ & \times \sin[\text{Im}\alpha(s)\ln z] \} \end{aligned} \quad (8)$$

for $s > 1$, real and $t < 1$, real. We have used the fact that $\Psi(s) = \text{Im}\alpha(s)$ for $s > 1$ and real and we have written the inverse function of $\phi(z)$ as $\phi^{-1}(s)$, i.e.

$$\phi(\phi^{-1}(s)) = s \quad . \quad (9)$$

The function (8) must be an analytic function of s . We therefore require that $\phi^{-1}(s)$ be an analytic function of s and that the integral in (8) converge. The first requirement is satisfied provided that $\phi(z)$ is analytic in $0 < z < 1$ and

$$\frac{d}{dz}\phi(z) \neq 0 \quad (0 < z < 1) \quad . \quad (10)$$

If $\text{Re}\alpha(s) < 1$ then the integral (8) converges near the lower endpoint. Notice, however, that

$$f(s, \phi^{-1}(s)) = \frac{s}{\pi} \int_1^s ds' \frac{\Psi(s')}{s'(s'-s)} \quad (11)$$

diverges logarithmically. The function $f(s, z)$ is defined in (1). If we integrate $f(s, z)$ by parts then we can write the first term in the integrand of (8) as

$$z^{-\text{Re}\alpha(s, z)} = \left[z^{-\text{Re}\alpha(s) - \frac{s}{\pi}} \int_1^{\phi(z)} ds' \ln(s-s') \frac{d}{ds'} \left(\frac{\Psi(s')}{s'} \right) \right] \quad (12)$$

$$\times [s - \phi(z)]^{\frac{s}{\pi}} \Psi(\phi(z)) [\phi(z)]^{-1} \ln z$$

In deriving (12) we have required that $\text{Im}\alpha(s)$ vanish at threshold

$$\Psi(1) = 0 \quad . \quad (13)$$

This is necessary if $\text{Re}\alpha(s)$ is to be well behaved at $s=1$. With (12) we find that there is no divergence of (8) at the upper

endpoint of integration provided that

$$\left. \frac{s}{\pi} \Psi(\phi(z)) [\phi(z)]^{-1} \ln z \right|_{z=\phi^{-1}(s)} = \frac{\Psi(s)}{\pi} \ln(\phi^{-1}(s)) > -1 \quad (14)$$

for $s > 1$ and real.

IV.2 Double Spectral Region

We can now increase t above threshold while keeping $s > 1$ and real. The function $\alpha(t, 1-z)$ is cut for $z > 1 - \phi^{-1}(t)$. Using the definition (III.17) and the arguments of section IV.1 we find

$$\begin{aligned} \rho(s, t) = & \int_0^1 dz \{ z^{-\text{Re}\alpha(s, z)} (1-z)^{-\text{Re}\alpha(t, 1-z)} \Theta(\phi^{-1}(s) - z) \\ & \times \Theta(\phi^{-1}(t) + z - 1) \sin[\text{Im}\alpha(t) \ln(1-z)] \sin[\text{Im}\alpha(s) \ln z] \} . \end{aligned} \quad (15)$$

The double spectral function is nonzero in the region

$$s > 1, t > 1, \phi^{-1}(s) + \phi^{-1}(t) \geq 1 . \quad (16)$$

The boundary of this region is given by the equality in (16).

One of the requirements we used in order to obtain the correct threshold behavior for the DT model of the last chapter was that the double spectral boundary have the asymptotic behavior (see III.32)

$$t(s-1) \sim \text{constant} \quad (17)$$

as $s \rightarrow 1$ from above. If (17) is to be satisfied then we have, with (16),

$$[\phi(1-z)][\phi(z)-1] \sim \text{constant} \quad (18)$$

as $z \rightarrow 0$.

IV.3 Asymptotic Behavior, t fixed

As in the Veneziano, Suzuki and earlier DT models, we make the change of variables $z=e^{-x}$ to write (III.1) in the form (III.42):

$$A(s,t) = \int_0^{\infty} dx e^{-x(1-\alpha(s,e^{-x}))} (1-e^{-x})^{-\alpha(t,1-e^{-x})} \quad (19)$$

where the trajectory functions are now defined by (1). As with the early DT model, it is a simple matter to show that the asymptotic behavior of (19) is

$$A(s,t) \sim \nu e^{-i\phi s} \int_0^{\infty} dx e^{-x(1-\alpha(s,e^{-x}))} (1-e^{-x})^{-\alpha(t,1-e^{-x})} \quad (20)$$

as $|s| \rightarrow \infty$ with $-\frac{1}{2}\pi < \phi_s = \arg(1-\alpha(s)) < \frac{1}{2}\pi$ and $\text{Re}\alpha(t) < 1$ where ν is a constant. With the methods of chapter II we can show that the asymptotic behavior of (20) is the usual Regge behavior (II.37) or (III.41).

In order to continue (19) into the region $\text{Re}\alpha(t) < 1$, $\phi - \pi < \arg(1-\alpha(s)) < \phi$, we perform the contour rotations of chapter II. The rotation of figure II.7 accomplishes the continuation.

The additional deformation of figure II.8 enables us to derive the asymptotic relation (20) for $|s| \rightarrow \infty$, $\phi - \pi < \phi_s = \arg(1 - \alpha(s)) < \phi$ and finally to show that $A(s, t)$ is Regge behaved. The rotations are performed while $\alpha(s)$ is fixed in the initial region $-\pi < \arg(1 - \alpha(s)) < -\frac{1}{2}\pi$. We should emphasize at this point that ϕ_s is the final value of $\arg(1 - \alpha(s))$, i.e. the direction in the $(1 - \alpha(s))$ -plane in which we will eventually study the asymptotic behavior.

While $\alpha(s)$ is in the initial region, we must verify three points in order to validate the rotations:

i) We must show that singularities at $x=0$ do not hinder the rotation. This condition is

$$\lim_{r \rightarrow 0} \int_r^{re^{-i\phi_s}} dx e^{-x(1-\alpha(s, e^{-x}))} (1-e^{-x})^{-\alpha(t, 1-e^{-x})} = 0. \quad (21)$$

ii) We must show that the arc at infinity may be neglected:

$$\lim_{R \rightarrow \infty} \int_R^{Re^{i(\frac{1}{2}\pi - \phi)}} dx e^{-x(1-\alpha(s, e^{-x}))} (1-e^{-x})^{-\alpha(t, 1-e^{-x})} = 0. \quad (22)$$

iii) We must show that no singularities occur in the integrand of (19) which interfere with the rotation.

We shall postpone an examination of conditions (21) and (22) and the derivation of (20) until a specific choice has been made for the function $\phi(z)$ (chapter V). Here we shall examine some very strong restrictions on the function (1) which can be obtained from condition iii) above. We begin the discussion by noticing that $\alpha(t, 1-e^{-x})$ has singularities when

$$t = \phi(1-e^{-x}) \quad (23)$$

coming from the lower endpoint of integration in (1). Suppose we demand that when t is in some sector about the real, negative t -axis, $|\arg(-t)| < \pi - \theta$, the singularities in x implied by (23) do not occur in the right half x -plane. This demand can be written

$$|\arg(\phi(1-e^{-x}))| < \theta \quad \text{for } \text{Re} x > 0 \quad . \quad (24)$$

Condition (24) is sufficient to guarantee that t -dependent non-Regge behavior similar to that observed in the CHKZ and DT models of chapter III does not occur for $A(s,t)$ as $|s| \rightarrow \infty$ with t fixed in the sector $|\arg(-t)| < \pi - \theta$.

If we now define the new function

$$\check{\phi}(y) \equiv i[\phi(1-e^{-i/y})]^{\pi/2\theta} \quad (25)$$

then condition (24) becomes

$$\text{Im} \check{\phi}(y) > 0 \quad \text{for } \text{Im} y > 0 \quad . \quad (26)$$

We next notice that $\alpha(t, 1-e^{-x})$ will have singularities wherever $\phi(1-e^{-x})$ is singular. In order to prevent non-Regge behavior coming from this source it is sufficient to require

$$\phi(1-e^{-x}) \text{ analytic in } \text{Re} x > 0 \quad . \quad (27)$$

In terms of the function (25), condition (27) becomes

$$\check{\phi}(y) \text{ analytic in } \text{Im}y > 0 \quad . \quad (28)$$

Finally, we notice that (2) implies

$$\check{\phi}(\infty) = 1, \quad |\check{\phi}(0)| = \infty \quad . \quad (29)$$

Properties (26) and (27) imply that $\check{\phi}(y)$ is a Herglotz function and therefore has the representation (Eden 1967, ch. 6)

$$\check{\phi}(y) = A + By + \frac{1}{\pi} \int_{-\infty}^{\infty} dx \frac{\text{Im}\check{\phi}(x)(1+xy)}{(1+x^2)(x-y)} \quad . \quad (30)$$

The integrals

$$\int_{-\infty}^{\infty} dx \frac{\text{Im}\check{\phi}(x)}{1+x^2} \quad \text{and} \quad \int_{-\infty}^{\infty} dx \frac{\text{Im}\check{\phi}(x)}{|\check{\phi}(x)|^2(1+x^2)} \quad (31)$$

must be convergent. With (29) we see that $\check{\phi}(y)$ is singular at $y=0$. In order to examine this singularity we substitute

$$\text{Im}\check{\phi}(x) \approx \omega\delta(x) \quad (x \approx 0) \quad (32)$$

into (30). Any singularity stronger than this would cause the first integral in (31) to diverge. We find

$$\check{\phi}(y) \approx -\omega/\pi y \quad (y \approx 0) \quad (33)$$

which gives, with (25),

$$\phi(1-z) \approx \left[-\frac{\omega}{\pi} \ln z\right]^{2\theta/\pi} \quad (z \approx 0) \quad . \quad (34)$$

We can reach the same conclusion by examining the Herglotz function

$$\bar{\phi}(\bar{y}) \equiv i[\phi(1-e^{i\bar{y}})]^{\pi/2\theta} \quad (35)$$

for large values of \bar{y} .

We shall now examine the implications of the behavior (34) for the function $\alpha(s, e^{-x})$. This function has singularities when $s = \phi(e^{-x})$. For large $|s|$ these s-dependent singular points will occur near singular points of the function $\phi(e^{-x})$ itself since only near these points does $\phi(e^{-x})$ become unbounded. In order to satisfy condition iii) we demand that $\phi(e^{-x})$ be analytic in the right half x-plane. With (34) we see that $\phi(e^{-x})$ is singular at $x=0$. Thus if any s-dependent singularity violates condition iii) for large $|s|$ it will occur near $x=0$ at a position defined by the relation

$$s = \phi(e^{-x}) \approx \phi(1-x) \approx \left[-\frac{\omega}{\pi} \ln x\right]^{2\theta/\pi} . \quad (36)$$

When examining the asymptotic behavior of $A(s, t)$ for $\text{Im}s > 0$, we make all contour rotations into the upper half x-plane as in figure II.8. If (2) is to be satisfied we must take ω to be real and positive. It is easily seen that for $\pi > \arg x > 0$ and $|x|$ small, (36) has no solution for $\text{Im}s > 0$. Therefore, no s-dependent singularities occur which violate condition iii) for continuation into the region $\text{Im}s > 0$, $|s|$ large. Similarly, the only s-dependent singularities near $x=0$ for $\text{Im}s < 0$, $|s|$ large on the first sheet of the x-plane occur in $\pi > \arg x > 0$. Since the contour

deformations in this case are into $-\pi < \arg x < 0$, condition iii) is again satisfied.

Finally, we notice that if the function $s^{-1}\psi(s)$ has singularities at a series of points $s=s_i$ then $\alpha(s, e^{-x})$ and $\alpha(t, 1-e^{-x})$ can have singularities in x at values of x such that

$$s_i = \phi(e^{-x}) \quad \text{and} \quad s_i = \phi(1-e^{-x}) \quad (37)$$

respectively. In order to satisfy condition iii) we require that these values of x not be in the right half x -plane.

Condition iii), then, implies that $\phi(e^{-x})$, $\phi(1-e^{-x})$, $[\phi(e^{-x})]^{-1}\psi(\phi(e^{-x}))$ and $[\phi(1-e^{-x})]^{-1}\psi(\phi(1-e^{-x}))$ must be analytic functions of x in $|\arg x| < \frac{1}{2}\pi$. Singularities at $x=\infty$ are allowed if (22) is satisfied. (24) is sufficient to guarantee that no t -dependent singularities violate condition iii) for t in the sector $|\arg(-t)| < \pi - \theta$. In order to satisfy (24) the relation

$$\phi(1-z)(-\ln z)^{-2\theta/\pi} \leq \text{constant} \quad (38)$$

must be satisfied as $z \rightarrow 0$. If the equality in (38) is satisfied then the s -dependent singularities in x of $\alpha(s, e^{-x})$ do not violate condition iii).

IV.4 Asymptotic Behavior, fixed angle

For $\pi\pi$ elastic scattering, t is related to the s -channel center of mass scattering angle θ_s by (II.23, II.43)

$$t = \frac{1}{2}(1-s)(1-\cos\theta_s) \equiv (1-s)\chi_s \quad (39)$$

As we did in deriving (II.44) for the Veneziano model, we make the change of variables $e^{-x} = z(1-z)^{-\chi_s}$. Then (III.1) becomes

$$A(s,t) = \int_{-\infty}^{\infty} dx \frac{e^{-x(1-\lambda s)}}{1-(1-\chi_s)z} [z^{-b-g(s,z)} \cdot (1-z)^{\chi_s(1-\lambda)-b+1-g((1-s)\chi_s,1-z)}] \quad (40)$$

where $z=z(x)$ and the functions g are defined in (1). In order to examine the behavior of $A(s,t)$ as $|s| \rightarrow \infty$ in the right half s -plane we must perform the rotation shown in figure II.11. If $g(s,z)$ or $g((1-s)\chi_s,1-z)$ has singularities in $|\arg x| < \frac{1}{2}\pi$ then $A(s,t)$ will have an exponentially increasing behavior as $s \rightarrow \infty$, χ_s fixed. This behavior is unacceptable. In order to avoid having these singularities we must require that $\phi(z(x))$, $\phi(1-z(x))$, $[\phi(z(x))]^{-1}\Psi(\phi(z(x)))$ and $[\phi(1-z(x))]^{-1}\Psi(\phi(1-z(x)))$ be analytic in $\text{Re } x > 0$ with the possible exception of $x = \infty$. Since x is related to z by

$$x = -\ln z + \chi_s \ln(1-z) \quad , \quad (41)$$

the functions $\phi(z)$ and $[\phi(z)]^{-1}\Psi(\phi(z))$ must be analytic for all z in the regions

$$-\ln|z| + \chi_s \ln|1-z| > 0, \quad -\ln|1-z| + \chi_s \ln|z| > 0 \quad . \quad (42)$$

These regions are shown in figure IV.1 for several values of χ_s . As χ_s increases from 0 to 1 the region (42) expands to fill

the entire z -plane except for the points

$$z = \frac{1}{2} + iy \quad \text{and} \quad z = \infty \quad (43)$$

where $y^2 > 3/4$. The functions $\phi(z)$ and $[\phi(z)]^{-1}\psi(\phi(z))$ are also allowed to have singularities at the points

$$z = 0 \quad \text{and} \quad z = 1 \quad (44)$$

provided that the analogue of (22) for the rotation of figure II.11 is satisfied. The positions (43) and (44) are the only ones at which the above functions can have singularities in z if $A(s,t)$ is to have acceptable behavior as $|s| \rightarrow \infty$ with χ_s fixed and between 0 and 1 (θ_s physical).

IV.5 Threshold Behavior

In this section we shall examine the threshold behavior of a model satisfying the constraints of this chapter and whose double spectral boundary has the asymptotic form (17)

$$t = \phi(1-\phi^{-1}(s)) \equiv f(s) \approx c(s-1)^{-1} \quad (45)$$

for $s \approx 1$. We have used (16) to express the dependence of $f(s)$ on the function ϕ . In a manner analogous to the derivation of (III.33) we find

$$\text{Im}v_j(s) = \frac{(1-\epsilon)^{-j}}{4\pi i} \left(\frac{s-1}{c}\right)^j \int_0^{2\pi} d\eta e^{-i\eta j} \text{Disc}_s A(s, (1-\epsilon)f(s)e^{i\eta}) \quad (46)$$

where the $v_j(s)$ are defined in (III.22). With (38) we have

$$\phi(1-\phi^{-1}(s)) \leq \frac{1}{d}[-\ln(\phi^{-1}(s))]^{2\theta/\pi} \quad (47)$$

for $s \rightarrow 1$ ($\phi^{-1}(s) \approx 0$) and where d is a constant. With (45) and (47) we have

$$\phi^{-1}(s) \leq \exp\left\{-\left(\frac{cd}{s-1}\right)^{\pi/2\theta}\right\} \quad (48)$$

as $s \rightarrow 1$ from above. Using (8) and the fact that (48) is very small in this limit, we find

$$\begin{aligned} \text{Disc}_s A(s, (1-\varepsilon)f(s)e^{i\eta}) &\approx \\ &\approx \frac{-2i[\phi^{-1}(s)]^{1-\alpha(1)} \sin[\Psi(s)\ln(\phi^{-1}(s))]}{1-\alpha(1)} \end{aligned} \quad (49)$$

as $s \rightarrow 1$ from above. Since $\alpha(1) \approx \frac{1}{2}$ for the ρ - f^0 trajectory, (49) vanishes faster than any power of $(s-1)$ as $s \rightarrow 1$ from above. Thus (III.34) cannot be satisfied.

IV.6 Summary

The original DT model of chapter III possessed a number of desirable properties including a curved double spectral boundary, the elastic unitarity cut, reasonable threshold behavior and resonances with finite positive widths. For some values of t and $\arg s$, however, the amplitudes constructed from the model were not Regge behaved for large $|s|$. For large positive s ,

for example, the model was Regge behaved only for $|t| < 1$. Since the asymptotic region for $\pi\pi$ elastic scattering is s large and positive, $(1-s) < t < 0$, the above result is unacceptable.

In this chapter we have devised a class of models which may still possess the non-Regge behavior mentioned above, but not in the physical region for $\pi\pi$ elastic scattering. In addition, we have eliminated the possibility of exponentially increasing fixed angle asymptotic behavior. The models still have the elastic unitarity cut and a curved double spectral boundary. However, we were not able to satisfy the requirements of chapter III for threshold behavior. If the double spectral boundary is chosen to have the correct asymptotic form (17), for example, then the imaginary parts of the partial wave amplitudes will vanish faster than any power of $(s-1)$ near threshold.

V. A Simple Example

It is not difficult to construct a $\phi(z)$ for equation (IV.1) such that $A(s,t)$ will have the correct ϕ^3 double spectral boundary. Once this is done, we can add background terms to provide the correct threshold behavior. Functions satisfying all of the restrictions set down in the preceding chapter, however, are rather complicated. The simplest obtained so far is

$$\phi(z) = \frac{1}{2} \left(\frac{4 \ln z + 2 \ln(1-z) - 3\Lambda}{2 \ln z - \Lambda} \right) \quad (1)$$

with $\Lambda > \ln 4$ and real. In this chapter we shall examine a model in which $\phi(z)$ has a simpler form than (1) but which has neither the correct double spectral boundary nor the proper threshold behavior. We shall then introduce a background term which simultaneously corrects both of these. For completeness, we shall discuss a neutralizer method which also enables us to obtain the correct threshold behavior.

The model we shall examine has the standard form of (III.1)

$$A(s,t) = \int_0^1 dz z^{-\alpha(s,z)} (1-z)^{-\alpha(t,1-z)} \quad (2)$$

while the trajectory function is defined by

$$\alpha(s,z) = \lambda s + b + \frac{s}{\pi} \int_0^{\infty} ds' \frac{\Psi(s')}{s'(s'-s)} \cdot \quad (3)$$

$$1 - \eta \ln(1-z)$$

The functions $f(s,z)$ and $g(s,z)$ are defined, with (IV.1), by

$$f(s, z) = \frac{1-\eta \ln(1-z)}{\pi} \int_1^s ds' \frac{\Psi(s')}{s'(s'-s)} \quad (4)$$

and

$$g(s, z) = \frac{\int_1^{\infty} ds' \frac{\Psi(s')}{s'(s'-s)}}{1-\eta \ln(1-z)} \quad (5)$$

The parameter η appearing in (3) - (5) is adjustable.

$\Psi(s)$ is restricted by the arguments of chapter IV to those functions satisfying

$$s^{-1}\Psi(s) \rightarrow 0 \quad \text{as } s \rightarrow \infty \quad (6)$$

$$\Psi(s) \rightarrow 0 \quad \text{as } s \rightarrow 1 \quad (7)$$

$$0 < \Psi(s) < -\pi \{ \ln(1 - \exp[(1-s)/\eta]) \}^{-1} \quad (1 < s < \infty) \quad (8)$$

and with $s^{-1}\Psi(s)$ having possible singularities at the points

$$s = \{ \infty, 1 \pm 2n\pi i \eta, 1 - \eta \ln(\frac{1}{2} + iy) \pm 2n\pi i \eta \} \quad (9)$$

where $n=0,1,2,\dots$ and $y^2 > 3/4$. We shall also suppose that $\Psi(s)$ is bounded for large $|s|$ as follows:

$$c_1 |s| (\ln |s|)^{-\rho_1 - 1} > |\Psi(s)| > c_2 |s|^{\rho_2} \quad (10)$$

for all s such that $|s| > W$ where W is a (large) constant.

The constants ρ_1 and ρ_2 are real and positive. The upper bound

is a sufficient condition for (IV.5) while the lower bound is one of the sufficient conditions for the proof that Regge behavior applies along the real, positive s -axis.

V.1 Properties of the Basic Model

We shall restrict our discussion to the process $\pi\pi\rightarrow\pi\pi$. The invariant amplitudes for this process are given by (II.7) with

$$C(s,t) = \gamma(\lambda s + \lambda t + c)A(s,t) \quad . \quad (11)$$

An analysis similar to the one we shall use can also be applied to the amplitude for $\pi\pi\rightarrow\pi\omega$ (II.4).

i) Crossing Symmetry. Since (2) is in the form (II.18), the amplitudes constructed from this model are crossing symmetric.

ii) Unitarity Cut. As we discussed in chapter IV, the function $\alpha(s,z)$ has an imaginary part given by

$$\text{Im}\alpha(s,z) = \Psi(s)\theta(s-1+\eta\ln(1-z)) \quad (12)$$

for s real and $0 < z < 1$. We therefore find that $A(s,t)$ is cut along the real, positive s -axis starting at $s=1$. The discontinuity across this cut is

$$\text{Disc}_s A(s,t) = -2i \int_0^{1-\exp\{(1-s)/\eta\}} dz \{ z^{-\text{Re}\alpha(s,z)} (1-z)^{-\alpha(t,1-z)} \times \sin[\text{Im}\alpha(s)\ln z] \} \quad . \quad (13)$$

iii) Double Spectral Region. From section IV.2 we see that $A(s,t)$ has a double spectral function

$$\rho(s,t) = \int_0^1 dz \{ z^{-\text{Re}\alpha(s,z)} (1-z)^{-\text{Re}\alpha(t,1-z)} \\ \times \sin[\text{Im}\alpha(s)\ln z] \sin[\text{Im}\alpha(t)\ln(1-z)] \theta(s-1+\eta\ln(1-z)) \\ \times \theta(t-1+\eta\ln z) \} \quad (14)$$

This function is nonzero in the region

$$s > 1, t > 1, e^{(1-s)/\eta} + e^{(1-t)/\eta} \leq 1 \quad (15)$$

The boundary of the region is shown in figure V.1 along with the ϕ^3 boundary for the scattering of scalar bosons. We make the choice $\eta = (2\ln 2)^{-1} \approx .72$ so that the boundaries coincide for $s=t=1.5$.

iv) Asymptotic Behavior, t fixed. We shall now prove in detail that the asymptotic behavior of $A(s,t)$ as $|s| \rightarrow \infty$ with t fixed and $\text{Re}t < 1$ is given by the asymptotic behavior of (IV.20) for $|\arg(-s)| \leq \pi$, i.e. in all directions on the first sheet of the s -plane including the real, positive s -axis. The derivation of (IV.20) for $|\arg(1-\alpha(s))| < \frac{1}{2}\pi$ and $\text{Re}t < 1$ is straightforward. We shall therefore be concerned with the behavior of $A(s,t)$ in the right half s -plane.

We begin by making the usual change of variables $z=e^{-x}$ so that the representation (2) becomes

$$A(s,t) = \int_0^{\infty} dx e^{-x(1-\alpha(s,e^{-x}))} (1-e^{-x})^{-\alpha(t,1-e^{-x})} . \quad (16)$$

In order to continue $A(s,t)$ into the right half s -plane with $\text{Im}\alpha(s) > 0$, we perform the contour rotation shown in figure V.2.

With (5) and (6) it is easily shown that

$$\lim_{x \rightarrow 0} g(s, e^{-x}) = 0 \quad (17)$$

while, with (4) and (7), we have

$$\lim_{x \rightarrow 0} f(t, 1-e^{-x}) = 0 . \quad (18)$$

With these limits we can show that (IV.21) is satisfied provided that $\text{Re}\alpha(t) < 1$.

For the deformation of figure V.2, condition (IV.22) becomes

$$\lim_{R \rightarrow \infty} \int_R^{iR+\epsilon} dx e^{-x(1-\alpha(s,e^{-x}))} (1-e^{-x})^{-\alpha(t,1-e^{-x})} = 0 . \quad (19)$$

The bounds (10), with (5), give the result

$$\lim_{|x| \rightarrow \infty} g(t, 1-e^{-x}) = 0 . \quad (20)$$

Thus for large R we replace the $\alpha(t, 1-e^{-x})$ in (19) by $\lambda t + b$.

If we restrict t to be real for simplicity it is easily seen that the second term in the integrand of (19) is bounded by

$$|(1-e^{-x})^{-\alpha(t,1-e^{-x})}| < (1 \pm \epsilon)^{-\lambda t - b} \quad (21)$$

where the $+(-)$ sign applies when $\lambda t + b <(>) 0$.

We now notice that, for fixed x and $|s| \gg |1 - \eta \ln(1 - e^{-x})|$, we can approximate $f(s, e^{-x})$ by

$$f(s, e^{-x}) = -\frac{1}{\pi} \int_1^{1-\eta \ln(1-e^{-x})} ds' s'^{-1} \Psi(s') + O(|s|^{-1}) \quad (22)$$

Since $s^{-1} \Psi(s)$ has singularities only at the positions (9), the right hand side of (22) is bounded for x on the path of integration of (19). Thus for

$$|s| \gg |1 - \eta \ln(1 - e^{-x}) + i\pi| > \max |1 - \eta \ln(1 - e^{-x})| \quad (23)$$

we can write

$$|f(s, e^{-x})| < c(\epsilon) \quad (24)$$

We have not, as yet, specified the value of ϵ . Let us make ϵ s -dependent according to

$$\epsilon \equiv d |s|^{-\kappa} \quad (\kappa > 0) \quad (25)$$

for large $|s|$. The right hand sides of (23) and (24) can be shown to increase logarithmically with $|s|$ for large $|s|$. Since $|1 - \alpha(s)|$ increases linearly with $|s|$ for large $|s|$, we can choose a constant s_0 large enough so that (23), (24) and the inequality

$$|1 - \alpha(s)| \cos(\frac{1}{2}\pi - \delta) > c(\epsilon) \quad (26)$$

are satisfied for $|s| > s_0$. The constant δ in (26) is small and positive.

If we perform the deformation of figure V.2 while s is fixed in the region $\delta - \frac{1}{2}\pi < \arg(1-\alpha(s)) < -\delta$, $|s| > s_0$, then with (24) we see that the first term in the integrand of (19) is bounded by

$$\begin{aligned} |e^{-x(1-\alpha(s, e^{-x}))}| &< \\ &< \exp\{-R[|1-\alpha(s)|\cos(\arg(1-\alpha(s))+\phi)-c(\epsilon)]\} \end{aligned} \quad (27)$$

where $0 < \phi < \frac{1}{2}\pi$.

With (26) it is clear that (27) vanishes faster than any inverse power of R as $R \rightarrow \infty$. The contribution (21) has no R dependence. Finally, the path length of the integration (19) increases linearly with R . Multiplying these contributions we see that the limit (19) is satisfied.

Since $s^{-1}\Psi(s)$ has singularities only at the positions (9), the integrand of (16) has no s - or t -independent singularities in the right half x -plane. The function $\alpha(t, 1-e^{-x})$ is singular at

$$x = (t-1)/\eta \quad . \quad (28)$$

If we fix t in the region $\text{Re}t < 1$ then the singularity (28) is in the left half x -plane. Finally, the function $\alpha(s, e^{-x})$ is singular at the points

$$x = -\ln(1-e^{(1-s)/\eta}) \pm 2n\pi i \quad (29)$$

where $n=0,1,2,\dots$. For $|s|>s_0$ and $\delta-\frac{1}{2}\pi<\arg(1-\alpha(s))<-\delta$, these singularities are in the left half of the x -plane. Therefore, provided that we take ν sufficiently small:

$$\nu < \min\{ |(t-1)/\eta|, \pi/3 \}, \quad (30)$$

the path of integration of (16) encounters no singularities during its deformation.

As we have now demonstrated, conditions i) - iii) of section IV.3 are satisfied. Therefore the representation

$$A(s,t) = \int_{C_1+C_2+C_3} dx e^{-x(1-\alpha(s,e^{-x}))} (1-e^{-x})^{-\alpha(t,1-e^{-x})} \quad (31)$$

is a valid one for $|s|>s_0$, $\delta-\frac{1}{2}\pi<\arg(1-\alpha(s))<-\delta$, $\text{Ret}<1$. The paths C_1 , C_2 and C_3 are those of figure V.2 while ϵ is given by (25).

The representation (31) provides the desired continuation of $A(s,t)$ into the right half s -plane. Condition (23), which is satisfied for $|s|>s_0$, also guarantees that no s -dependent singularity will encounter the path C_3 during the continuation. Furthermore, as we discussed in chapter IV, the $n=0$ member of the set (29) will not encounter the path C_1 during the continuation. Thus (31) is a valid representation in (at least) the region $|s|>s_0$, $\text{Ret}<1$, $-\pi\leq\arg(1-\alpha(s))<-\delta$. The lower limit on the last inequality is determined by the inequality $\text{Im}\alpha(s)>0$. For the purposes of our discussion we shall choose the lower limit to correspond to $\text{Im}s=0$ so that for large $|s|$ the region of interest is

$$-\pi + \frac{\Psi(|s|)}{\lambda|s|} \leq \arg(1-\alpha(s)) < -\delta \quad . \quad (32)$$

We shall now examine the contribution of the integral along the path C_2 to (31) as $|s| \rightarrow \infty$ in the region (32). The function $\alpha(t, 1-e^{-x})$ is analytic along this path so that the second factor in the integrand of (31) is bounded by a constant. The function $f(s, e^{-x})$ is also bounded by a constant so that (24) is certainly satisfied for x on C_2 and $|s|$ large. Thus the first factor in the integrand of (31) is bounded by

$$|e^{-x(1-\alpha(s, e^{-x}))}| < e^{-\nu|1-\alpha(s)|\cos(\phi_s+\phi)+\nu c(\epsilon)} \quad (33)$$

for large $|s|$, where we have written $\phi_s \equiv \arg(1-\alpha(s))$ and $\phi \equiv \arg x$. With (10), (25), (32) and figure V.2 we see that, for large $|s|$,

$$\begin{aligned} |\phi_s + \phi| &< \left| -\pi + \frac{\Psi(|s|)}{\lambda|s|} + \frac{1}{2}\pi - \epsilon/\nu \right| \\ &< \left| \frac{1}{2}\pi + \frac{d|s|^{-\kappa}}{\nu} - \frac{c_2|s|^{\rho_2-1}}{\lambda} \right| \end{aligned} \quad (34)$$

If we choose κ so that

$$\kappa > 1-\rho_2 \quad , \quad (35)$$

then for large $|s|$ we clearly have

$$\cos(\phi_s + \phi) > \frac{c_2|s|^{\rho_2-1}}{\lambda} \quad . \quad (36)$$

The inequality (33), then, becomes

$$|e^{-x(1-\alpha(s, e^{-x}))}| < \exp\{-\nu c_2 \frac{|1-\alpha(s)|}{\lambda|s|} |s|^{\rho_2 + \nu c(\epsilon)}\}. \quad (37)$$

Since $(\lambda|s|)^{-1}|1-\alpha(s)| \rightarrow 1$ and $c(\epsilon) \lesssim \ln|s|$ as $|s| \rightarrow \infty$ and since $\rho_2 > 0$, it is clear that (37) vanishes faster than an inverse power of s as $|s| \rightarrow \infty$. This is sufficient to eliminate the contribution of C_2 to (31) from the asymptotic expansion.

The function $f(s, e^{-x})$ can be shown to satisfy (24) for $|s| > s_0$ and x on C_3 . Using arguments similar to those above we can show that the first factor in the integrand of (31) is bounded by

$$|e^{-x(1-\alpha(s, e^{-x}))}| < e^{-|x|c_2|s|^{\rho_2} + |x|c(\epsilon)} \quad (38)$$

for large $|s|$ and for x on C_3 . We must be careful in handling the function $\alpha(t, 1-e^{-x})$ for x on C_3 . With (3) we see that this function can have singularities on the imaginary x -axis at $x = \pm 2n\pi i$. These singularities arise from the singularities of $s^{-1}\Psi(s)$ at (see (9))

$$s = 1 \pm 2n\pi i \eta \equiv s_n^{\pm} \quad (39)$$

Suppose that the strongest of the singularities (39) is at $s = s_m$ and has the behavior $(s-s_m)^{-\zeta}$. Then we can show that $\alpha(t, 1-e^{-x})$ has the bound

$$|\alpha(t, 1-e^{-x})| < A(t) + B(t)|s|^{K(\zeta-1)} \quad (40)$$

for large $|s|$ and x on C_3 . We therefore find

$$|(1-e^{-x})^{-\alpha(t, 1-e^{-x})}| < e^{\kappa \ln |s| A(t) + \kappa \ln |s| B(t)} |s|^{\kappa(\zeta-1)} \quad (41)$$

for large $|s|$ and x on C_3 . With (38) and (41) it can be shown that the contribution of C_3 to (31) vanishes faster than any inverse power of s as $|s| \rightarrow \infty$ provided that $\rho_2 > \kappa(\zeta-1)$. The last condition gives, with (35),

$$\zeta < 1/(1-\rho_2) \quad (42)$$

so that we have obtained an upper bound to the strength of the singularities (39).

Since the contributions of C_2 and C_3 to (31) vanish faster than any inverse power of s we are left with the C_1 contribution

$$A(s, t) \sim \int_0^{\nu e^{-i\phi} s} dx e^{-x(1-\alpha(s, e^{-x}))} (1-e^{-x})^{-\alpha(t, 1-e^{-x})} \quad (43)$$

as $|s| \rightarrow \infty$ with t fixed and $\text{Ret} < 1$. By rotating the path of integration of (16) clockwise as well, we can show that (43) is a valid asymptotic representation for $|\arg(-s)| \leq \pi$.

The leading asymptotic behavior of (43) can be found by making the change of variables $y = (1-\alpha(s))x \equiv |1-\alpha(s)|x e^{i\phi}$ to obtain

$$A(s, t) \sim (1-\alpha(s))^{\alpha(t)-1} \int_0^{\nu |1-\alpha(s)|} dy e^{-y} y^{-\alpha(t)} H(y, s, \alpha(t)) \quad (44)$$

where, with $x \equiv y/(1-\alpha(s))$,

$$H(y, s, \alpha(t)) = e^{-xf(s, e^{-x})} (1-e^{-x})^{-\alpha(t)} \left(\frac{1-e^{-x}}{x} \right)^{-\alpha(t)}. \quad (45)$$

The integral (44) can be shown to satisfy the conditions A) - C) following equation (II.32). Thus the leading asymptotic behavior of (43) is determined by taking the $|s| \rightarrow \infty$ limit of the integral in (44)

$$\begin{aligned}
 A(s,t) &\sim (1-\alpha(s))^{\alpha(t)-1} \int_0^{\infty} dy e^{-y} y^{-\alpha(t)} \\
 &\sim (-\lambda s)^{\alpha(t)-1} \Gamma(1-\alpha(t)) \quad .
 \end{aligned}
 \tag{46}$$

This is the same as the leading behavior (II.37) for the Veneziano definition of $A(s,t)$. Therefore, all amplitudes constructed from this model will have the same leading asymptotic behavior as those constructed from the Veneziano model. The $I=1$ invariant amplitude for $\pi\pi$ scattering, for example, still has the leading asymptotic behavior (II.38) as $|t| \rightarrow \infty$ with s fixed.

There are three important differences between the asymptotic behavior of this model and that of the Veneziano model. First, the Veneziano model does not exhibit Regge behavior as $|s| \rightarrow \infty$ on the real positive s -axis while this model does. Second, the asymptotic behavior of $A(s,t)$ in the Veneziano model is given by (II.37) for all fixed t while (46) has only been proven for $\text{Re}t < 1$. Finally, non-leading terms in the asymptotic expansion of the Veneziano model correspond to exchanges of non-leading Regge pole trajectories in the crossed channel. These non-leading Regge pole contributions occur for the model of this chapter as well. There are, however, additional non-leading contributions

which are not necessarily characteristic of Regge pole exchange. The non-leading terms in the asymptotic expansion of $A(s,t)$ will be discussed in the Appendix.

v) Direct Channel Singularities. With (3) - (7) it is clear that the trajectory functions of this model have the same $z \rightarrow 0$ limit as those of the early DT model (III.14):

$$\alpha(s,z) \rightarrow \alpha(s); \quad \alpha(t,1-z) \rightarrow \lambda t + b \quad . \quad (47)$$

As we have seen in sections II.2.ii and II.2.iii, the s-channel singularities arise from the divergence of the integral (2) at the lower endpoint. With the limits (47) we therefore find, as in (III.15), that $A(s,t)$ has a series of poles at

$$\alpha(s) = n + 1 \quad (n = 0, 1, 2, \dots) \quad (48)$$

with residues which are polynomials of degree n in t . This structure is the same as that observed in the Veneziano, Suzuki and early DT models. Because of condition (IV.7), the poles (48) occur on the second sheet of the s-plane and therefore represent resonances with finite positive width. The model of this chapter has additional s-channel singularities as does the early DT model. These will be discussed in the Appendix.

vi) Threshold Behavior. In order to examine the partial wave amplitudes for the process $\pi\pi \rightarrow \pi\pi$ near threshold, we use the methods of section II.2.v. We write

$$A(s, t) = \sum_{k=0}^{\infty} v_k(s) t^k \quad . \quad (49)$$

The real parts of the $v_k(s)$ remain finite as $s \rightarrow 1$. We can determine them explicitly by expanding $A(s, t)$ in a Taylor series about $t=0$. The $\text{Im}v_k(s)$ could also be found in this way but the best method for exhibiting their behavior as $s \rightarrow 1$ from above is to use (III.27) with the integration path shown in figure V.3. We find

$$\begin{aligned} \text{Im}v_k(s) &\equiv \text{Im}v_k'(s) + \text{Im}\bar{v}_k(s) = \\ &= -\frac{1}{4\pi} \int_{f(s)}^{g(s)} dt' \text{Disc}_s \text{Disc}_t A(s, t') t'^{-k-1} \\ &+ \frac{1}{4\pi i} [g(s)]^{-k} \int_0^{2\pi} d\zeta \text{Disc}_s A(s, g(s)e^{i\zeta}) e^{-ik\zeta} \end{aligned} \quad (50)$$

where

$$f(s) = 1 - \eta \ln(1 - e^{(1-s)/\eta}) \quad (51)$$

and

$$g(s) = 1 + \frac{1}{4(s-1)} \quad . \quad (52)$$

The function $f(s)$ is the position of the branch point in t of the function $\text{Disc}_s A(s, t)$ in this model while $g(s)$ is the position of this branch point in a model with the correct ϕ^3 double spectral boundary.

We shall first examine the threshold behavior of the second term in (50). If we substitute $g(s)e^{i\zeta}$ for t in (10) and make the change of variable $z=(s-1)x/\eta$, we can take the limit of the

resulting integral as $s \rightarrow 1$ from above to obtain

$$\begin{aligned} \text{Disc}_s A(s, g(s) e^{i\zeta}) &\sim \\ &\sim -2i \text{Im} \alpha(s) \ln \left(\frac{s-1}{\eta} \right) \left(\frac{s-1}{\eta} \right)^{1-\alpha(1)} \int_0^1 dx x^{-\alpha(1)} \exp \left(\frac{\lambda x e^{i\zeta}}{4\eta} \right) . \end{aligned} \quad (53)$$

Substituting (53) into (50) we find

$$\text{Im} \bar{v}_k(s) \sim (s-1)^{k+1-\alpha(1)} \ln(s-1) \text{Im} \alpha(s) \quad (54)$$

as $s \rightarrow 1$ from above. If this were the only contribution to $\text{Im} v_k(s)$ then the imaginary parts of the partial wave amplitudes for $\pi\pi$ elastic scattering could have the correct threshold behavior for $j \geq 1$ provided that $\Psi(s)$ behaved like (III.40) near $s=1$. Notice, however, that the first term in (50) behaves like

$$\text{Im} v'_k(s) \sim [-\ln(s-1)]^{1-k} (s-1)^{2-\alpha(1)} \text{Im} \alpha(s) \text{Im} \alpha(f(s)) \quad (55)$$

as $s \rightarrow 1$ from above. This behavior is inconsistent with (III.35). The possibility of obtaining the correct threshold behavior for all partial waves is therefore destroyed.

vii) Asymptotic Behavior, fixed angle. The study of the behavior of $A(s, t)$ as $|s| \rightarrow \infty$ with $\chi_s \equiv \frac{1}{2}(1 - \cos \theta_s)$ fixed follows the discussions of sections IV.4 and II.2.vi. As usual, we make the change of variable $e^{-x} = z(1-z)^{-\chi_s}$ so that (2) is given by (IV.40). In order to examine $A(s, t)$ in the region $|s| \rightarrow \infty$, $-\frac{1}{2}\pi > \arg(-s) > -\pi + \epsilon$, we deform the path of integration

of (IV.40) as is shown in figure V.4. The leading behavior as $|s| \rightarrow \infty$ will come from the region of integration near the right-most singularity of the integrand, the point P of figure V.4. Other singularities, such as P', will not enter into the discussion. With (IV.40) we therefore have

$$A(s,t) \sim e^{\lambda s P} R(s, \chi_s) \quad (s \rightarrow \infty, \chi_s \text{ fixed}) \quad . \quad (56)$$

The function R in (56) does not alter the dominant exponential behavior.

We now recall that the integrand of (2) can have singularities at the points

$$z = \{0, 1, \infty, 1 - e^{(1-s)/\eta}, e^{(1-t)/\eta}, \frac{1}{2} \pm iy\} \quad (57)$$

where $y^2 > 3/4$. The point $z=0$ is mapped into $x=\infty$. We can show, however, that this singularity does not hinder the contour deformation of figure V.4. In fact, we can use the same arguments as in section V.1.iv to establish the rotation. The points $z=1, \infty$ map into $x=-\infty$ so that we may ignore those singularities. Finally, for large positive s ($\text{Re}s \rightarrow \infty$) the points $z=1 - e^{(1-s)/\eta}$ and $z=e^{[1-(1-s)\chi_s]/\eta}$ occur far to the left in the x -plane and therefore need not concern us. The only remaining singularities are those at $z=\frac{1}{2} \pm iy$ ($y^2 > 3/4$) and a singularity of the integrand of (IV.40) at $z=(1-\chi_s)^{-1}$. Both of these singularities have images lying in the left half x -plane so that the dominant behavior of (56) is exponentially decreasing. The value of P coming from the singularity at $z=\frac{1}{2} - iy$ ($y > \sqrt{3}/2$) is

$$P = -\frac{1}{2}(1-\chi_s)\ln(\frac{1}{4}+y^2) - i(1+\chi_s)\tan^{-1}(2y) \quad (58)$$

while the singularities at $z=(1-\chi_s)^{-1}$ gives

$$P = \chi_s \ln \chi_s + (1-\chi_s)\ln(1-\chi_s) + i\pi\chi_s \quad (59)$$

The latter value of P is the one which occurs in connection with the Veneziano model (see figure II.11 and equation II.45).

Since $\text{Re}P < 0$, the above method can be used to show that $A(s,t)$ vanishes exponentially with s for χ_s fixed and s on the real, positive s -axis. An interesting situation arises if we allow the possibility $y^2=3/4$. In this case we have $\text{Re}P=0$ so that we must keep non-leading terms in $\alpha(s)$ in order to discuss the $|s| \rightarrow \infty$ $\arg(-s)=\pi$ limit. The integral (IV.40) is again dominated by the region of integration near the singularity so that we have

$$A(s,t) \sim e^{i(\pi/3)(\alpha(s)-\alpha([1-s]\chi_s))} R(s,t) \quad (60)$$

If s is on the real, positive s -axis, then the real parts of $\alpha(s)$ and $\alpha([1-s]\chi_s)$ will provide rapid oscillations. The magnitude of $A(s,t)$ is thus determined by the $\text{Im}\alpha(s)$ contribution:

$$|A(s,t)| \sim e^{-\pi \text{Im}\alpha(s)/3} |R(s,t)| \quad (61)$$

as $s \rightarrow \infty$ ($\arg s=0$) with χ_s fixed. Notice that if $\Psi(s)$ grows less rapidly than $s^{\frac{1}{2}}$ as $s \rightarrow \infty$ then the fixed angle asymptotic behavior of the amplitudes will obey the Martin lower bound (Eden 1967, ch. 6)

$$|A(s,t)| > Ce^{-Ds^{\frac{1}{2}}} \quad (62)$$

as $s \rightarrow \infty$ with χ_s fixed.

viii) Asymptotic Behavior, fixed u . We shall now examine the behavior of $A(s,t)$ as $s \rightarrow \infty$ with $u = \Sigma - s - t$ fixed. For the process $\pi\pi \rightarrow \pi\pi$ we have $\Sigma = 4m_{\pi}^2 = 1$. As in section II.2.v, we make the change of variables $z = (1 + e^{-x})^{-1}$ which transforms (2) into

$$A(s,t) = \int_{-\infty}^{\infty} dx [(e^x + 1)^{\alpha(s, (e^x + 1)^{-1}) - 1} \cdot (e^{-x} + 1)^{\alpha(1-s-u, (e^{-x} + 1)^{-1}) - 1}] \quad (63)$$

for $\pi\pi$ elastic scattering. In order to examine the behavior of $A(s,t)$ as $|s| \rightarrow \infty$ with u fixed and $-\frac{1}{2}\pi > \arg(-s) > -\pi$, we deform the integration contour of (63) as shown in figure II.10. If $y^2 > 3/4$, then the right-most singularities in the integrand of (63) occur at $x = \pm(2n+1)\pi i$ and at $x = \ln(1 - e^{-(s+u)/\eta}) \pm (2n+1)\pi i$ where $n=0,1,2,\dots$. For large positive $\text{Re}s$, the points in the latter set approach those in the former. We can therefore determine the nature of the asymptotic behavior by examining the integrand of (63) near the point $x = \pi i + \delta$. We have

$$|A(s,t)| \sim \exp\{-\pi \text{Im}\alpha(s) - [\text{Re}\alpha(s) + \text{Re}\alpha(1-s-u)] \ln(1/\delta) + \pi \text{Im}f(s, -1/\delta) + [\text{Re}f(s, -1/\delta) + \text{Re}f(1-s-u, 1/\delta) + 2] \ln(1/\delta)\}. \quad (64)$$

The functions $f(s, -1/\delta)$ and $f(1-s-u, 1/\delta)$ behave like constants

as $|s| \rightarrow \infty$ while the function $-\text{Re}\alpha(s) + \text{Re}\alpha(1-s-u)$ grows less rapidly than linearly with s . Since $\text{Im}\alpha(s)$ grows linearly with s in the region under consideration we have

$$A(s,t) \sim e^{-\text{Im}\alpha(s)} R(s,t) \quad (65)$$

as $|s| \rightarrow \infty$ with u fixed and $-\frac{1}{2}\pi > \arg(-s) > -\pi + \epsilon$. A similar procedure may be used to examine the region $\frac{1}{2}\pi < \arg(-s) < \pi - \epsilon$ with the same exponentially decreasing result.

The behavior of $A(s,t)$ in the limit $s \rightarrow \infty$, u fixed $|\arg(-s)| = \pi$ is not easily determined. The above arguments no longer apply because $\text{Im}\alpha(s)$ does not increase linearly with s in this limit. We can gain some understanding of the situation if we recall that the f functions in (64) do not increase with s . We therefore do not expect them to enter crucially into the asymptotic behavior in this limit. If we ignore these functions then $A(s,t)$ becomes simply

$$A(s,t) \approx B(1-\alpha(s), 1-\alpha(t)) \quad (66)$$

The properties of this function in the limit $s \rightarrow \infty$, $|\arg(-s)| = \pi$, u fixed have been studied by Roskies (1968). He has found that if $s^{\mu-1} \text{Im}\alpha(s) \rightarrow 0$ for some $\mu > 0$, then (66) will grow faster than any power of s in the above limit. If, however, $\text{Im}\alpha(s)$ behaves like

$$\Psi(s) \equiv \text{Im}\alpha(s) \sim c s (\ln s)^{-\rho_1 - 1} \quad (67)$$

as $s \rightarrow +\infty$ where $\rho_1 > 0$, then (66) will vanish faster than any

inverse power of s in the large s , fixed u limit.

V.2 Neutralizer Correction

Suppose that we write, instead of (3),

$$\alpha(s, z) = \lambda s + b + \frac{s}{\pi}(1-\gamma(z)) \int_{1-\eta \ln(1-z)}^{\infty} ds' \frac{\Psi(s')}{s'(s'-s)} \quad (68)$$

$$\equiv \alpha(s) - f'(s, z) \equiv \lambda s + b + g'(s, z) \quad .$$

The function $\gamma(z)$ is the neutralizer defined in (III.5)-(III.7). In terms of the functions $f(s, z)$ and $g(s, z)$ defined in (4) and (5), we have

$$g'(s, z) = (1-\gamma(z))g(s, z) \quad (69)$$

and

$$f'(s, z) = f(s, z) + \gamma(z)g(s, z) \quad . \quad (70)$$

The model constructed by using (2) with (68) has properties similar to those of the basic model of section V.1. First, the amplitudes constructed from the model of this section will again be crossing symmetric. Second, the singularities discussed in section V.1.v will also be present in this model. Some of the additional singularities of the basic model will not occur in this model (see Appendix). Third, the leading asymptotic behavior of $A(s, t)$ for large $|s|$ and with t, u or θ_s fixed is the same in this model as in the basic model. The major disadvantage of the use of neutralizers is that we cannot obtain

this asymptotic behavior in any of the above regions for $|\arg(-s)| = \pi$. Similar difficulties occur with the Suzuki model discussed in chapter III. There are some differences between the non-leading Regge contributions of the basic model and the neutralized form. These differences are mentioned in the Appendix. Fourth, the model of this section again has a unitarity cut (see section V.1.ii) starting at $s=1$. The discontinuity across the cut is

$$\text{Disc}_s A(s, t) = -2i \int_0^{1-e^{(1-s)/\eta}} dz \{ z^{-\text{Re}\alpha(s, z)} (1-z)^{-\alpha(t, 1-z)} \times \sin[(1-\gamma(z)) \text{Im}\alpha(s) \ln z] \} . \quad (71)$$

Finally, the double spectral region is again given by (15). The double spectral function, however, is now

$$\begin{aligned} \rho(s, t) &= -\frac{1}{4} \text{Disc}_s \text{Disc}_t A(s, t) = \\ &= \int_0^1 dz \{ z^{-\text{Re}\alpha(s, z)} (1-z)^{-\text{Re}\alpha(t, 1-z)} \Theta_{(s-1+\eta \ln(1-z))} \\ &\quad \times \Theta_{(t-1+\eta \ln z)} \sin[(1-\gamma(z)) \text{Im}\alpha(s) \ln z] \\ &\quad \times \sin[(1-\gamma(1-z)) \text{Im}\alpha(t) \ln(1-z)] \} . \end{aligned} \quad (72)$$

The major difference between this model and the basic model of section V.1 lies in the threshold behavior of the partial wave projections. In terms of the expansion (49), we again find that the $\text{Re}v_k(s)$ approach finite constants as $s \rightarrow 1$. The $\text{Im}\bar{v}_k(s)$

defined in (50) have the same threshold behavior, (54), as those of the basic model. The $\text{Im}v'_k(s)$, however, are now altered. The double spectral function (72) has the upper endpoint of integration $z_{\text{max}} \approx (s-1)/\eta$ as $s \rightarrow 1$ from above. Since the integrand of (72) contains a factor $\sin[(1-\gamma(1-z))\text{Im}\alpha(t)\ln(1-z)]$ which vanishes faster than any power of z as $z \rightarrow 0$, $\rho(s,t)$ and $\text{Disc}_s \text{Disc}_t A(s,t)$ vanish faster than any power of $(s-1)$ as $s \rightarrow 1$. Therefore, with (50), we see that the $\text{Im}v'_k(s)$ vanish faster than any power of $(s-1)$ as we approach threshold. Thus the threshold behavior of the $\text{Im}v_k(s)$ is given by that of the $\text{Im}\bar{v}_k(s)$. Suppose that we take

$$\text{Im}\alpha(s) \equiv \Psi(s) \sim (s-1)^{\alpha(1)+\frac{1}{2}} [\ln(s-1)]^{-1} \quad (73)$$

as $s \rightarrow 1$. Then (54) gives

$$\text{Im}v_k(s) \sim \text{Im}\bar{v}_k(s) \sim (s-1)^{k+3/2} \quad (74)$$

This is just the behavior which is needed to satisfy the elastic unitarity relation (III.37) for all partial waves except $j=0$ (see section III.2.v).

V.3 Subtractive Corrections

In the last section we were able to obtain the correct threshold behavior for the partial wave projections of the $\pi\pi \rightarrow \pi\pi$ amplitude. The $\text{Im}v'_k(s)$ of (50), which ruined the threshold behavior in the basic model, were shown to vanish faster than any

power of $(s-1)$ near threshold in the neutralized model.

There are two difficulties with the model of section V.2. First, the boundary of the double spectral region remains incorrect. Second, in order to obtain the proper threshold behavior we have had to pay a price: we have destroyed the fixed t , u and θ_s asymptotic behavior of $A(s,t)$ as $s \rightarrow \infty$ on the real, positive s -axis.

In this section we shall discuss an alternate method for adjusting the threshold behavior. The model of section V.1 has given us a specific double spectral function (14). We can alter both the threshold behavior and the double spectral region by subtracting certain integrals containing $\rho(s,t)$ from the basic function $A(s,t)$ of section V.1. The method of this section does not alter the properties of $A(s,t)$. Thus, in this case, we can study the limit $|s| \rightarrow \infty$ with s on the real, positive s -axis.

i) The Basic Subtraction. Suppose that we define the new function

$$\begin{aligned} \bar{A}(s,t) &= A(s,t) - \frac{1}{\pi^2} \int_1^\infty ds' \int_1^{g(s')} dt' \frac{\rho(s',t')}{(s'-s)(t'-t)} \\ &\equiv A(s,t) - R(s,t) \end{aligned} \quad (75)$$

$A(s,t)$ is defined by (2) with (3), $\rho(s,t)$ is given by (14) while $f(s)$ and $g(s)$ are defined in (51) and (52). We have simply subtracted the double spectral integral over the region between the Φ^3 boundary (III.21) and the boundary (15). Thus the double spectral boundary for $\bar{A}(s,t)$ is the Φ^3 boundary (figure V.1).

We now use (49) to write

$$\begin{aligned}
 \text{Im}\bar{A}(s,t) &\equiv \text{Im}A(s,t) - \text{Im}R(s,t) \\
 &= \sum_{k=0}^{\infty} t^k \text{Im}v_k(s) - \frac{1}{\pi} \int_{f(s)}^{g(s)} dt' \frac{\rho(s,t')}{t'-t} \\
 &= \sum_{k=0}^{\infty} t^k \left\{ \text{Im}v_k(s) + \frac{1}{4\pi} \int_{f(s)}^{g(s)} dt' \text{Disc}_s \text{Disc}_t A(s,t') t'^{-k-1} \right\}
 \end{aligned} \tag{76}$$

for $t < 1 < s$, s and t real. Notice that the final term in the brackets of (76) is just $-\text{Im}v'_k(s)$ defined in (50). We therefore have

$$\text{Im}\bar{A}(s,t) = \sum_{k=0}^{\infty} t^k \text{Im}\bar{v}_k(s) \tag{77}$$

If we choose the behavior (73) for $\text{Im}\alpha(s)$ then the $j \geq 1$ $\pi \rightarrow \pi$ partial wave amplitudes will have the correct power dependence on $(s-1)$ near threshold.

The function $R(s,t)$ is symmetric under the interchange of s and t . This follows from the symmetry in s' and t' of the region of integration in (75). Thus the amplitudes constructed from $\bar{A}(s,t)$ will be crossing symmetric. The amplitudes for $\pi \rightarrow \pi$ elastic scattering are defined by (II.7) with \bar{A} replacing A in (11).

With (14), (51), (52) and (75) we can show that

$$\text{Disc}_s R(s,t) \sim O[\text{Im}\alpha(s) \text{Im}\alpha(1+\frac{1}{4}s^{-1}) s^{\alpha(1)-3} \ln s] \tag{78}$$

as $s \rightarrow \infty$. Since $\text{Im}\alpha(s)$ grows less rapidly than s as $s \rightarrow \infty$ and since $\text{Im}\alpha(1)=0$, the integration in (75), which can be written

$$R(s,t) = \frac{1}{2\pi i} \int_1^{\infty} ds' \frac{\text{Disc}_{s'} R(s',t)}{s'-s}, \quad (79)$$

certainly converges. Notice that as $|s| \rightarrow \infty$, the contribution of $R(s,t)$ to the function $C(s,t)$ is

$$-\gamma(\lambda s + \lambda t + c)R(s,t) \sim -\frac{\gamma\lambda}{\pi^2} \int_1^{\infty} ds' \int dt' \frac{g(s')}{f(s')} \frac{\rho(s',t')}{t'-t}. \quad (80)$$

For t fixed this term is $O(1)$. The fixed angle and fixed u subtractive corrections have $O(1/s)$ behavior for large s .

Instead of using (75), we could have worked directly with the $\pi\pi$ elastic scattering amplitude and written

$$C(s,t) = \gamma(\lambda s + \lambda t + c)A(s,t) - \frac{\gamma}{\pi^2} \int_1^{\infty} ds' \int dt' \frac{g(s')}{f(s')} \frac{\rho(s',t')(\lambda s' + \lambda t' + c)}{(s'-s)(t'-t)}. \quad (81)$$

With the alteration (81) we again obtain the correct double spectral region and the correct ($j \geq 1$) threshold behavior. The fixed t asymptotic behavior of the correction is now $O(1/s)$ while the fixed u and fixed angle behavior is $O(1/s^2)$. Notice, however, that (81) only describes $\pi\pi$ elastic scattering while the $\bar{A}(s,t)$ of (75) can be used to construct a variety of amplitudes.

ii) Further Corrections. We can make additional adjustments in the basic model by subtracting integrals over all or part of the new double spectral region. As an example, we shall consider

a correction to the double spectral function near the boundary of the double spectral region

$$(s-1)(t-1) = \frac{1}{4} \quad . \quad (82)$$

Notice that the double spectral function of $\bar{A}(s,t)$ vanishes abruptly at the boundary. In order to smooth this behavior we first notice, with (14), that

$$|\rho(s,t)| \leq c \exp(\lambda(s-1)(t-1)/\eta) \quad (83)$$

for large s and/or t . Thus the integral

$$R'(s,t) = \frac{1}{\pi^2} \int_1^\infty ds' \int_1^\infty dt' \frac{\rho(s',t') e^{-[(s'-1)(t'-1)-\frac{1}{4}]^\beta}}{(s'-s)(t'-t)} \quad (84)$$

is convergent for $\beta > 1$. If we redefine $\bar{A}(s,t)$ to be

$$\bar{A}(s,t) = A(s,t) - R(s,t) - R'(s,t) \quad , \quad (85)$$

then we can again construct crossing symmetric amplitudes with suitable threshold behavior and the correct Φ^3 double spectral region. The double spectral function is given by

$$\bar{\rho}(s,t) = \rho(s,t) \{1 - e^{-[(s-1)(t-1)-\frac{1}{4}]^\beta}\} \quad (86)$$

which vanishes like $[(s-1)(t-1)-\frac{1}{4}]^\beta$ near the boundary (82) of the double spectral region.

iii) Corrections for Pseudoscalar Bosons. In all of the discussions to this point, we have been satisfied with constructing models having double spectral boundaries close to the ϕ^3 boundary. Pions do not interact via a ϕ^3 interaction Lagrangian but according to ϕ^4 theory (a 3π vertex is forbidden by angular momentum and parity conservation). The ϕ^4 double spectral function can be nonzero in the regions $\tilde{R}(s,t)$ and $\tilde{R}(t,s)$ where the boundary of $\tilde{R}(x,y)$ is

$$(x-1)(y-4) = 4 \quad . \quad (87)$$

These regions are shown in figure V.5 along with the boundary (15) for the model of section V.1.

In order to obtain the correct threshold behavior for the $\pi\pi$ partial wave projections ($j \geq 1$) and the correct ϕ^4 double spectral boundary, we subtract the function

$$R(s,t) = \frac{1}{\pi^2} \iint ds' dt' \frac{\rho(s',t')}{(s'-s)(t'-t) R(s',t')} \quad (88)$$

from $A(s,t)$. $R(s,t)$ is the region between the ϕ^4 boundary and the boundary (15). The double spectral function for $A(s,t) - R(s,t)$ can be written

$$\rho''(s,t) = \rho'(s,t) + \rho'(t,s) \quad (89)$$

where

$$\rho'(x,y) \equiv \rho(x,y) \theta[(x-1)(y-4)-4] \{1 - \frac{1}{2} \theta[(x-4)(y-1)-4]\} \quad (90)$$

is nonzero in the region $\tilde{R}(x,y)$. The double spectral function

above has discontinuous behavior due to the Theta functions.

Suppose that we define

$$\bar{A}(s,t) = A(s,t) - R(s,t) - \tilde{R}(s,t) - \tilde{R}(t,s) \quad (91)$$

where

$$\begin{aligned} \tilde{R}(x,y) = \frac{1}{\pi^2} \iint dx' dy' \frac{\rho(x',y')}{(x'-x)(y'-y)} & (e^{-K_1(x',y')} - \\ & \tilde{R}(x',y') \\ & - \frac{1}{2} \theta[(x'-4)(y'-1)-4] e^{-K_2(x',y')}). \end{aligned} \quad (92)$$

The functions K_1 and K_2 are chosen to grow more rapidly than $\lambda(x'-1)(y'-1)/\eta$ for large x' and/or y' so that the integration (92) converges. The double spectral function for (91) is

$$\bar{\rho}(s,t) = \bar{\rho}'(s,t) + \bar{\rho}'(t,s) \quad (93)$$

where

$$\begin{aligned} \bar{\rho}'(x,y) \equiv \rho(x,y) \theta[(x-1)(y-4)-4] \{ & [1 - e^{-K_1(x,y)}] - \\ & - \frac{1}{2} \theta[(x-4)(y-1)-4] [1 - e^{-K_2(x,y)}] \} \end{aligned} \quad (94)$$

is nonzero in $\tilde{R}(x,y)$. If $K_1(x,y)$ vanishes for $(x-1)(y-4)=4$ and if $K_2(x,y)$ vanishes for $(x-1)(y-4)=4$ and for $(x-4)(y-1)=4$, then the double spectral function (94) will be smooth.

V.4 The $\pi\pi\rightarrow\pi\pi$ Amplitude

In the previous section we defined a function $\bar{A}(s,t)$ which has a reasonable, although not polynomially bounded, double spectral function. It is easy to check that if $\bar{A}(s,t)$ is substituted into (II.4) and if the function $\Psi(s)$ is suitably chosen, then the invariant amplitude for the process $\pi\pi\rightarrow\pi\omega$ will have the following properties:

- a) Crossing symmetry;
- b) Elastic unitarity cut;
- c) Correct ϕ^4 double spectral region;
- d) Correct power dependence on $(s-1)$ near the s-channel 2π threshold for all partial waves;
- e) Resonances with finite positive total widths;
- f) Regge asymptotic behavior in the physical region for the scattering process;
- g) Reasonable asymptotic behavior at fixed angle.

The last two properties are valid even for real values of the asymptotic variable.

The amplitudes for the process $\pi\pi\rightarrow\pi\pi$, obtained by substituting $\bar{A}(s,t)$ into (11) and the resulting $C(s,t)$ into (II.7), have all of the above properties except that d) is satisfied only for $j \geq 1$. In this section we shall introduce a satellite function which enables us to satisfy d) for $j=0$. We shall also review the restrictions on $\Psi(s)$ which are necessary for a)-g) to be obtained.

i) The Satellite Term. An amplitude which satisfies a)-g) may be written

$$C(s,t) = \gamma(\lambda s + \lambda t + c)\bar{A}(s,t) + \gamma d\bar{A}_1(s,t) \quad (95)$$

The function $\bar{A}_1(s,t)$ is determined from the basic function

$$A_1(s,t) = \int_0^1 dz z^{-\alpha_1(s,z)-1} (1-z)^{-\alpha_1(t,1-z)-1} \quad (96)$$

with

$$\alpha_1(s,z) = \lambda s + b_1 + \frac{s}{\pi} \int ds' \frac{\Psi_1(s')}{s'(s'-s)} \cdot \quad (97)$$

$$1 - \eta \ln(1-z)$$

We shall take the trajectory $\alpha_1(s)$ to be approximately one unit of angular momentum below the leading (ρ - f^0) trajectory so that $b_1 \approx b-1$. The function $\bar{A}_1(s,t)$ is defined by

$$\bar{A}_1(s,t) = A_1(s,t) - R_1(s,t) - \tilde{R}_1(s,t) - \tilde{R}_1(t,s) \quad (98)$$

where R_1 and \tilde{R}_1 are given by (88) and (92) with

$$\rho_1(s,t) = -\frac{1}{2} \text{Disc}_s \text{Disc}_t A_1(s,t) \quad (99)$$

replacing $\rho(s,t)$ in these relations.

If we now perform expansions similar to (III.22) for $\bar{A}(s,t)$ and $\bar{A}_1(s,t)$,

$$\bar{A}(s,t) = \sum_{k=0}^{\infty} t^k \bar{v}_k(s) \quad (100)$$

$$\bar{A}_1(s,t) = \sum_{k=0}^{\infty} t^k \bar{w}_k(s) \quad (101)$$

then we find, as in chapter III, that the leading behavior of the j -th partial wave projection of the $\pi^+\pi^-\rightarrow\pi^+\pi^-$ amplitude near threshold is

$$A_j^{+-}(s) \sim \gamma\{(\lambda+c)\bar{v}_j(s)+d\bar{w}_j(s)+\lambda\bar{v}_{j-1}(s)\}\frac{(j!)^2(s-1)^j}{(2j+1)!} \quad (102)$$

where $\bar{v}_{-1}(s)\equiv 0$. $\text{Im}\bar{w}_k(s)$ has the threshold behavior (54) while, near $s=1$,

$$\text{Im}\bar{w}_k(s) \sim (s-1)^{k-\alpha_1(1)} \ln(s-1) \text{Im}\alpha_1(s) \quad . \quad (103)$$

If $\Psi(s)$ has the behavior (73) for $s\approx 1$ and if $\Psi_1(s)$ has the threshold behavior

$$\Psi_1(s) \equiv \text{Im}\alpha_1(s) \sim (s-1)^{\alpha_1(1)+\frac{1}{2}} [\ln(s-1)]^{-1} \quad , \quad (104)$$

then $\text{Im}A_j^{+-}(s)$ will have the correct power dependence, $(s-1)^{2j+\frac{1}{2}}$ (III.36b), near threshold for all j including $j=0$.

ii) Review of Restrictions. In this section we shall list the restrictions on the functions $\Psi(s)$ and $\Psi_1(s)$ which we have found in this chapter. First, there are restrictions on the positions at which the functions $s^{-1}\Psi(s)$ and $s^{-1}\Psi_1(s)$ can have singularities. The positions of possible singularities are

$$s = \{\infty, 1\pm 2n\pi i\eta, 1-\eta \ln(\frac{1}{2}+iy)\pm 2n\pi i\eta\} \quad (9)$$

where $n=0,1,2,\dots$ and $y^2>3/4$. Second, there are several bounds

on the functions Ψ and Ψ_1 :

$$0 < \Psi(s) < -\pi[\ln(1-e^{(1-s)/\eta})]^{-1} \quad (1 < s < \infty) \quad (8)$$

$$s^{-1}\Psi(s) \rightarrow 0 \quad \text{as } s \rightarrow \infty \quad (6)$$

$$\Psi(s) \rightarrow 0 \quad \text{as } s \rightarrow 1 \quad (7)$$

$$c_1 |s| [\ln|s|]^{-\rho_1 - 1} > |\Psi(s)| > c_2 |s|^{\rho_2} \quad (|s| > W) \quad (10)$$

where $\rho_1, \rho_2 > 0$ and W is a (large) constant. Third, there is a restriction on the strength of the singularities in the second set of (9) which states that these singularities are weaker than

$$[s - 1 \pm 2n\pi i\eta]^{1/(\rho_2 - 1)} \quad (105)$$

where ρ_2 is the constant appearing in (10). Fourth, there are two limits which must be satisfied by $\Psi(s)$ and $\Psi_1(s)$:

$$\bar{\Psi}(s) \sim s(\ln s)^{-\rho_1 - 1} \quad \text{as } s \rightarrow \infty \quad (67)$$

with $\rho_1 > 0$ and

$$\bar{\Psi}(s) \sim -(s-1)^{\bar{\alpha}(1) + \frac{1}{2}} [\ln(s-1)]^{-1} \quad \text{as } s \rightarrow 1 \quad (106)$$

The functions $\bar{\Psi}, \bar{\alpha}$ represent either Ψ, α or Ψ_1, α_1 so that (106) represents (73) and (104). With (67) and (10) we see that ρ_2 can be chosen to be close to 1. Thus (105) does not provide a

significant restriction. Notice that $\bar{A}_1(s,t)$ has a pole when $\alpha_1(s) = 0$. If this pole is to occur for $s > 1$ and therefore represent a resonance and if (7) and (104) are to be satisfied, then we must require

$$-\frac{1}{2} < \alpha_1(1) < 0 \quad . \quad (107)$$

This restriction is one of the motivations for our choosing $b_1 \approx b-1$. Finally, as we shall see in the Appendix, if $\Psi(s)$ behaves (to within logarithmic factors) like s^j as $s \rightarrow \infty$ and like $(s-1)^k$ as $s \rightarrow 1$ where j and k are integers, then the trajectories coming from $\bar{A}(s,t)$ will have unit spacing. The first condition must already be satisfied (67) while the second is satisfied, with (73), if

$$\alpha(1) = \frac{1}{2} \quad . \quad (108)$$

The above relation is very nearly satisfied by the ρ - f^0 trajectory.

VI. Physical Applications

The Veneziano model and the generalizations of it which we have discussed are constructed primarily to describe two particle scattering in the asymptotic (Regge) region and in the resonance region. These two regions are connected by duality and FESR. The Veneziano model, however, has been applied successfully to other regions as well, both physical and unphysical. In this chapter we shall discuss some of these applications for both the Veneziano model and the DT model of chapter V. In addition, we shall discuss methods which can be used to perform calculations in the DT model.

VI.1 Experimental Situation

We start with the experimental facts which we shall try to understand in terms of the Veneziano and DT models. The processes considered are

$$\pi_1 + \pi_2 \rightarrow \pi_3 + \pi_4 \quad (1)$$

and

$$\pi_1 \rightarrow \bar{\pi}_2 + \pi_3 + \pi_4 \quad (2)$$

which are shown in figure VI.1 a and b respectively. They are clearly related by crossing symmetry. Neither of these processes has been studied directly. The second, in fact, can never be directly measured. All experiments performed for this process involve allowing one of the pions, say π_1 , to be

off mass shell, i.e. $M^2(\pi_1) \neq \frac{1}{4} = m_\pi^2$. The results are then either extrapolated to the mass shell or the models which are to be compared with the results are extrapolated off shell.

i) The Process $\bar{p}n \rightarrow \pi^- \pi^- \pi^+$. The initial state in the reaction $\bar{p}n \rightarrow 3\pi$ can be in the 1S_0 , $^3P_{0,1,2}$ and higher orbital angular momentum states. Near threshold, we expect the S-wave to give the dominant contribution. This is the case experimentally (Anninos 1968). The quantum numbers of the initial state near threshold are therefore $I^G(J^P) = 1^-(0^-)$. Since these are the quantum numbers of the pion, we follow Lovelace (1968) and treat the $\bar{p}n$ system as a heavy pion. Comparing figures VI.1b and c, we can see that the process $\bar{p}n \rightarrow \pi^- \pi^- \pi^+$ is the same as $\pi^- \rightarrow \pi^- \pi^- \pi^+$ where the initial pion has a (mass)² of 3.52 GeV^2 . The Dalitz plot for $\bar{p}n \rightarrow \pi^- \pi^- \pi^+$ is shown in figure VI.2 (Anninos 1968). The axes of the plot, s and t, are the (mass)² of the two $\pi^+ \pi^-$ subsystems. The density of points in the Dalitz plot is related to the |amplitude|² for the processes (1) and (2) where π_1 is a heavy pion. We should stress again that, since the amplitude determined in this way is off shell, we shall need to extrapolate the Veneziano and DT models off shell before comparing them with figure VI.2. We shall discuss this procedure in section VI.3.

ii) The Process $\pi N \rightarrow \pi \pi N'$. Most of the information about $\pi\pi$ elastic scattering is obtained from the inelastic πN reaction

$$\pi_2 N \rightarrow \pi_3 \pi_4 N' \quad . \quad (3)$$

In the one pion exchange (OPE) model, the process (3) is related to (1) as is indicated in figure VI.1d. The $(\text{mass})^2$ of π_1 in the process (1) is given by $M^2(\pi_1) = -q^2(NN')$ where $q(NN')$ is the momentum transfer between N and N' . The amplitude for $\pi\pi$ elastic scattering on the mass shell is obtained by extrapolating the off shell amplitude to the point $M^2(\pi_1) = \frac{1}{4} = m_\pi^2$. This (Chew-Low) extrapolation is discussed in numerous texts (for example, Källén 1964, ch. 7).

Most of the data on the $I=0$ S-wave phase shifts for $\pi\pi$ elastic scattering comes from the reaction



The most recent solutions for δ_0^0 are shown in figure VI.3. Below 700 MeV there is a unique solution (Baton 1970). Above 700 MeV, however, there are two solutions, the "down-down" and "down-up" solutions. There are also slight differences depending upon whether δ_0^0 is taken to be elastic or is allowed to be inelastic. The "down-up" solution of Baton (1970) implies an S-wave $\pi\pi$ resonance (ϵ) near the mass of the ρ :

$$M_\epsilon = 736 \text{ MeV}, \quad \Gamma_\epsilon = 181 \text{ MeV} \quad . \quad (5)$$

The "down-down" solution is mildly preferred, however. As is seen in figure VI.3, this solution is in qualitative agreement with the higher energy solutions (Beaupre 1971, Oh 1970). The $I=1$ P-wave phase shift solution is unique. The result for elastic δ_1^1 (Baton 1970) will be shown in figure VI.9 in comparison

with the DT model results.

The S-wave scattering lengths for the process $\pi\pi\rightarrow\pi\pi$ are somewhat more difficult to study. Notice that the phase shift solutions of figure VI.3 extend down to $s=.25\text{GeV}^2$. The threshold for $\pi\pi$ scattering, however, is at $s=.075\text{GeV}^2$. In order to determine scattering lengths we must therefore perform two extrapolations. First, we must perform a Chew-Low extrapolation to the mass shell. Second, we must extrapolate to the elastic threshold for $\pi\pi$ scattering. Two results for the I=0 S-wave scattering length obtained from studies of the process $\pi^-p\rightarrow\pi\pi N$ are

$$\begin{aligned} a_0 &= (.16 \pm .04)m_\pi^{-1} && \text{(Morgan 1970)} \\ a_0 &= (.28 \pm .21)m_\pi^{-1} && \text{(Maung 1970) .} \end{aligned} \tag{6}$$

In addition, the I=2 S-wave scattering length is found to be (Morgan 1970)

$$a_2 = -(.05 \pm .01)m_\pi^{-1} . \tag{7}$$

iii) PCAC Results. The Adler consistency condition, which is derived from the divergence-field identity of PCAC

$$\partial^\mu j_{5\mu}^\alpha(x) = \pi^\alpha(x) , \tag{8}$$

implies (Adler 1965) that the amplitude for the process (1) must vanish when the four-momentum of one of the pions vanishes.

Again, we have an off shell result since one of the pions, say π_1 , has $M^2(\pi_1)=0$. The point at which this result is valid is

$p_1^2=0, s=t=u=p_2^2=p_3^2=p_4^2=m_\pi^2$. This is known as the Adler point.

Notice that the Adler point is not far from the elastic threshold for the process (1). We should therefore be able to obtain information about $\pi\pi$ elastic scattering near threshold by extrapolating PCAC results from the Adler point to the threshold point. This extrapolation is model dependent but the results are consistent. Two such results for the $I=0$ and $I=2$ S-wave scattering lengths are

$$\begin{aligned} a_0 &= .20 m_\pi^{-1} \\ a_2 &= -.06 m_\pi^{-1} \end{aligned} \quad (\text{Weinberg 1966})$$

$$\begin{aligned} a_0 &= (.15 \pm .02) m_\pi^{-1} \\ a_2 &= -(.04 \pm .004) m_\pi^{-1} \end{aligned} \quad (\text{Cronin 1967}) \quad (9)$$

Two other quantities which are often used in discussing scattering lengths are the combinations $L \equiv (2a_0 - 5a_2)/6$ and $R \equiv a_0/a_2$. The a_0 and a_2 in (6), (7) and (9) yield the following results

$L(m_\pi^{-1})$	R	Reference
$.10 \pm .01$	-3.2 ± 1.0	(Morgan 1970)
$.10 \pm .01$	-3.5	(Weinberg 1966)
$.09 \pm .01$	-3.7 ± 0.8	(Cronin 1967)

Table VI.1

VI.2 The DT Model

The DT model of chapter V has a number of desirable properties, including the fact that it reduces to the Veneziano model in the zero width ($\Psi(s) \equiv 0$) limit. This limit is useful because, if the resonances are narrow, the real parts of the DT model amplitudes should be close to the real parts of the Veneziano amplitudes provided that we stay away from the resonance region. For exact calculations, however, the DT model is somewhat more difficult to work with than the Veneziano model. There are at least two reasons for this. First, the Veneziano model is described by a relatively small number of parameters, including coupling constants and slopes and intercepts of the relevant (linear) trajectories. The model of chapter V, and any other model incorporating trajectories which are complex above threshold, has additional parameters characterizing the imaginary parts of those trajectories. Experimental information about these imaginary parts is rather scanty. The second difficulty lies in the mathematical complexity of the model. The Veneziano model is constructed from the well known Beta and Gamma functions. Calculations are easily performed since these functions are tabulated. The model of chapter V cannot be handled with such ease. If we hope to obtain an amplitude with reasonable behavior in the resonance region, then we must be prepared to work with models which are more complicated than the Veneziano model.

The difficulties described above are not serious. In previous chapters we have already obtained some restrictions on the imaginary parts of the trajectories. The second part of

this section will be concerned with the fixing of parameters for a specific form of the DT model. In the first part, we shall examine methods which can be used to calculate the function $A(s,t)$ of chapter V.

i) Analytic Continuations. The function $A(s,t)$ defined in equation (V.2) can be written

$$A(s,t) = D(s,t) + D(t,s) \quad (10)$$

where

$$D(s,t) = \int_0^{\frac{1}{2}} dz z^{-\alpha(s,z)} (1-z)^{-\alpha(t,1-z)} \quad (11)$$

and where $\alpha(s,z)$ is defined in (V.3). If $\text{Re}\alpha(s) < 1$, then $D(s,t)$ can be calculated from (11) with simple numerical integration. If the integrations defining $\alpha(s,z)$ and $\alpha(t,1-z)$ can be performed analytically, then the calculation is simple. If, however, the trajectory functions themselves must be determined by numerical integration, then the procedure is still straightforward but somewhat more costly. Care must be taken if the points $z = e^{(1-t)/\eta}$ and/or $z = 1 - e^{(1-s)/\eta}$ lie on the path of integration of (11) since the trajectory functions are singular at those points. No significant difficulties arise, however, because the singularities are logarithmic.

Suppose we now add and subtract the function $z^{-\alpha(s)}$ from the integrand of (11) and use the function $f(s,z)$ defined in (IV.1) and (V.4). Then we find

$$D(s, t) = \frac{2^{\alpha(s)-1}}{1-\alpha(s)} + \int_0^{\frac{1}{2}} dz z^{-\alpha(s)} \{z^{f(s, z)} (1-z)^{-\alpha(t, 1-z)} - 1\}. \quad (12)$$

This expression can be integrated numerically to give $D(s, t)$ in the region $\text{Re}\alpha(s) < 2$.

In the region $\text{Re}\alpha(s) > 2$, $\text{Im}\alpha(s) > 0$ we can calculate $D(s, t)$ from the integral representation

$$D(s, t) = \int_C dx e^{-x(1-\alpha(s, e^{-x}))} (1-e^{-x})^{-\alpha(t, 1-e^{-x})} \quad (13)$$

where the contour C is shown in figure VI.4. The vertical part of the path is chosen to lie to the right of the points $x=(t-1)/\eta$ and $x=-\ln(1-e^{(1-s)/\eta})$ at which the trajectory functions are singular. With some algebra, we can recast (13) in a form which is slightly better suited to numerical integration:

$$\begin{aligned} D(s, t) = & \int_{\ln 2}^p dx e^{-x(1-\alpha(s, e^{-x}))} (1-e^{-x})^{-\alpha(t, 1-e^{-x})} \\ & + 2\pi i e^{p(\alpha(s)-1)} \sum_{k=0}^{\infty} e^{2\pi i k(\alpha(s)-1)} \int_0^1 dq \{e^{2\pi i q(\alpha(s)-1)} x \\ & x e^{-(p+2\pi i q)f(s, e^{-p-2\pi i(q+k)})} (1-e^{-p-2\pi i q})^{-\alpha(t, 1-e^{-p-2\pi i q})} x \\ & x e^{-2\pi i k f(s, e^{-p-2\pi i(q+k)})} (1-e^{-p-2\pi i q}) \delta_k(t, p+2\pi i q)\} \end{aligned} \quad (14)$$

where $p > \max\{\text{Re}[(t-1)/\eta], \text{Re}[-\ln(1-e^{(1-s)/\eta})], \ln 2\}$ and

$$\delta_k(t, y) = \frac{2\pi i k \eta}{\pi} \int_0^t dr \frac{\Psi(r+1+\eta y)}{(r+1+\eta y)(r+1+\eta y-t)} \quad (15)$$

In order to study the region $\text{Re}\alpha(s) > 2$, $\text{Im}\alpha(s) < 0$ we need only to make the replacement $i \rightarrow -i$ in (14) and (15). Notice that the first factor in the sum appearing in (14) vanishes exponentially with k for $\text{Im}\alpha(s) > 0$. We can therefore truncate the summation after a reasonable number of terms.

With the representations (11), (12) and (14) we can determine $D(s,t)$ and $\rho(s,t)$, with (10), $A(s,t)$ for all finite values of s and t on the first sheets of the s - and t -planes. The function $\rho(s,t)$, which is used in obtaining the subtractive corrections of section V.3, can be found by direct numerical integration of equation (V.14).

ii) A Specific Model. We shall now discuss the reactions (1) and (2), for which the s -channel isospin amplitudes are given by (II.7). We define the function $C(s,t)$ by

$$C(s,t) = \gamma(\lambda s + \lambda t + c)A(s,t) + \gamma d A_1(s,t) \quad (16)$$

where A is given by (V.2) with (V.3) and A_1 by (V.96) with (V.97). We choose the parameter η to be

$$\eta = (2 \ln 2)^{-1} \approx .72 \quad (17)$$

so that the double spectral boundary is the dotted line in figure V.1.

Notice that we have neglected the subtractive corrections discussed in sections V.3 and 4. Although this is done for simplicity, there are two justifications for the approximation.

First, in the narrow resonance approximation mentioned at the beginning of this section, the subtractive corrections enter only in the second order. Thus, if the resonances are narrow, with widths characterized by a parameter ϵ , then the subtractive corrections are $O(\epsilon^2)$. Second, one of the main motivations for introducing these corrections was to adjust the behavior of the partial wave projections near the elastic threshold. For the amplitudes constructed from (16), such corrections are necessary only for $j \geq 2$. The only quantitative study near threshold in this chapter will involve just the $j=0$ and 1 partial waves. Notice also that we have not included a Pomeron contribution in the model. Since we shall be working at low energies in this chapter, we do not expect diffractive effects to be important.

In order to parameterize the ρ - f^0 trajectory, we choose the imaginary part to be of the form

$$\text{Im}\alpha(s) \equiv \psi(s) = \frac{\omega s(s-1)}{[(s-1)^2 + L^2]} \quad (18)$$

where ω is a constant and where

$$L = 2\pi\eta = 4.53 \quad (19)$$

The function (18) has a threshold behavior consistent (to within logarithmic factors) with the requirement (V.73) for a ρ - f^0 trajectory satisfying $\alpha(1) = \frac{1}{2}$. In addition, the function $s^{-1}\psi(s)$ has no inadmissible singularities. Finally, (18) has a constant behavior as $s \rightarrow \infty$. Although this behavior is not strictly admissible, we can always add a small but asymptotically growing

part without altering significantly the results below. The advantage of a form like (18) for $\Psi(s)$ is that the integrals defining $\alpha(s)$ and $\alpha(s,z)$ can be performed analytically. This enables us to perform the numerical integrations of the first part of this section somewhat more easily.

Using (18) we find

$$\text{Re}\alpha(s) = \lambda s + b + \frac{\Psi(s)}{2\pi(s-1)} \left\{ (s-1) \ln \left(\frac{L^2}{(s-1)^2} \right) + L\pi \right\}. \quad (20)$$

If we demand that the ρ - f^0 trajectory pass through the ρ and f and that the ρ have the correct width ($m_\rho \Gamma_\rho = .095 \text{GeV}^2$), then we can use (20) to obtain the parameters λ , b and ω . We have

$$\begin{aligned} \lambda &= .0783 \quad (1.04 \text{ GeV}^{-2}) \\ b &= .37 \\ \omega &= .114 \end{aligned} \quad (21)$$

The real and imaginary parts of the resulting trajectory are shown in figures VI.5 and 6. Notice that, even near threshold, the ρ - f^0 trajectory, $\text{Re}\alpha(s)$, deviates only slightly from linearity. In addition, notice that once a specific form is chosen for $\Psi(s)$ we can fix all of the trajectory parameters. The ρ - f^0 trajectory which we have constructed is acceptable for phenomenological purposes. The small value of $-s$ at which $\alpha(s)=0$ ($s=-.34 \text{GeV}^2$) arises from our particular parameterization and is not a requirement of the model (see chapter VII).

We shall choose the function $\Psi_1(s)$ appearing in (V.97) to have the form

$$\text{Im}\alpha_1(s) \equiv \Psi_1(s) = \frac{\omega_1 s^2}{[(s-1)^2 + L^2]} \quad . \quad (22)$$

This function, like (18), has a constant behavior as $s \rightarrow \infty$. In addition, it has a nonvanishing behavior at $s=1$, which is not satisfactory. Except at $s=1$, however, we expect that (22) will give results close to those arising from a $\Psi_1(s)$ with a $(s-1)^\epsilon$ dependence ($\epsilon \ll 1$) near $s=1$. Notice that the threshold behavior of (22) is consistent (to within logarithmic factors) with the requirement (V.104) for $\alpha_1(1) = -\frac{1}{2}$. Like (18), (22) has the advantage that the integrals for $\alpha_1(s)$ and $\alpha_1(s,z)$ can be done analytically. We find

$$\text{Re}\alpha_1(s) = \lambda s + b_1 + \frac{\Psi_1(s)}{2\pi s} \left\{ s \ln \left(\frac{L^2}{(s-1)^2} \right) + \frac{\pi(L^2+1-s)}{L} \right\} \quad . \quad (23)$$

We shall choose the intercept of $\text{Re}\alpha_1(s)$ to be

$$b_1 = b - 1 = -.63 \quad . \quad (24)$$

With this choice, the trajectory α_1 becomes degenerate with the first daughter of the ρ - f^0 trajectory in the zero width resonance limit.

From the discussion of section V.1.v, we know that $C(s,t)$ has the approximate form

$$C(s,t) \approx \frac{\gamma(\lambda s + \lambda t + c)}{1 - \alpha(s)} - \frac{\gamma d}{\alpha_1(s)} \quad (25)$$

for $\alpha(s) \approx 1 + \alpha_1(s) \approx 1$. In this region there are resonances in the S- and P- waves. A reasonable choice for the parameters

of (16) and (22) is as follows:

$$\omega_1 = .50; \quad \gamma = .50; \quad c = -.334 \quad (26)$$

and

$$d = -.5\lambda - c = .295 \quad (27)$$

(remember that $m_\pi^2 = \frac{1}{4}$ in our units). With these choices, the amplitudes have the following features:

a) There is an $I=J=1$ resonance with mass 765 MeV and width 125 MeV (ρ meson). Furthermore, in the approximation (25), the contribution of this resonance to the $I=J=1$ $\pi\pi$ partial wave projection near $\alpha(s)=1$ is elastic.

b) There is an $I=J=0$ resonance with mass 765 MeV and width 125 MeV (ϵ meson). The partial width of this resonance is adjusted to be small.

c) There is a second pole in the $I=J=0$ partial wave corresponding to $\sqrt{s} \approx 750$ MeV. The width, however, is exceedingly large (≈ 1000 MeV) so that this pole could hardly manifest itself as a conventional resonance but should rather be considered as a phenomenological account of a strong $\pi\pi$ interaction. Such an effect could well be a manifestation of the opening of the $K\bar{K}$ threshold near 1 GeV (see figure VI.3). We shall, however, refer to this pole as the " ϵ_1 " for convenience. As we shall see below (section VI.3.ii), the presence of this pole is very important in providing an S-wave phase shift in fair agreement with the "down-down" solution (Baton 1970).

d) Finally, the choice (27) enables us to approximately satisfy the Adler condition in the zero width resonance limit.

Notice that in this limit (16) becomes

$$C(s,t) = \gamma(\lambda s + \lambda t + c + d)A(s,t) \quad . \quad (28)$$

As discussed by Lovelace (1968), the trajectories cannot change when we take one of the external pions off its mass shell. Thus only γ , c and d (and possibly η) can be changed. If we assume that these parameters do not vary significantly as we move to the Adler point, then we see that the Adler condition is satisfied for (28) provided that (27) is satisfied.

VI.3 Applications of the Veneziano and DT Models

We shall now examine the extent to which the DT model of the last section and the Veneziano model discussed in chapter II can account for the experimental information of section VI.1.

i) Dalitz Plot of $\bar{p}n \rightarrow \pi^- \pi^- \pi^+$. The Veneziano model has been used by Lovelace (1968) to determine the density of points in the Dalitz plot for $\bar{p}n \rightarrow \pi^- \pi^- \pi^+$. As we showed in section VI.1, this process is related to the (off shell) process $\pi^- \pi^+ \rightarrow \pi^- \pi^+$:

$$\bar{p}n \rightarrow \pi^- \pi^- \pi^+ \quad (29a)$$

↓ ($\bar{p}n = \text{heavy } \pi^-$)

$$\pi^- \rightarrow \pi^- \pi^- \pi^+ \quad (29b)$$

↓ (crossing symmetry)

$$\pi^- \pi^+ \rightarrow \pi^- \pi^+ \quad . \quad (29c)$$

We can therefore use the isospin decomposition (II.7) to show that the Dalitz plot density for (29a) is proportional to $|C(s,t)|^2 \times \text{Phase Space}$, where s and t are the $(\text{mass})^2$ of the two $\pi^+\pi^-$ subsystems in the right hand side of (29a).

As we mentioned in the last section, the parameters γ and c of (II.10) and γ , c and d of (16) can change as we take one of the pions off its mass shell. Since the $\bar{p}n$ system in (29a) represents a pion with a $(\text{mass})^2$ of 3.52 GeV^2 , we cannot expect these parameters to remain the same as those for the scattering of on shell pions. Lovelace uses the fact that no ρ is observed in the 3π Dalitz plot (Anninos 1968) to set $\gamma=0$ in (II.8), i.e. γ small and c large in (II.10). The Dalitz plot density for (29a) is therefore proportional to $|A(s,t)|^2 \times \text{Phase Space}$, where $A(s,t)$ is defined in (II.5).

Instead of using the linear form (II.2) for his trajectories, Lovelace uses the form

$$\alpha(s) = .483 + .885s + .281(s-4m_\pi^2)^{\frac{1}{2}} \quad (30)$$

where s is in GeV^2 . With this choice he is able to obtain a good fit to the Dalitz plot shown in figure VI.2 (see Lovelace 1968). The Veneziano model provides an explanation of the three major features of the Dalitz plot: the enhancement near $s=t=m_\rho^2$; the depletion of events near $s=t=1.1 \text{ GeV}^2$ ($\text{Re}\alpha(s) = \text{Re}\alpha(t) \approx 1.5$) and the enhancement at the upper right edge of the plot. This is the only type of model which has been able to obtain this structure. Unfortunately, the rather arbitrary use of nonlinear trajectories leads to the ancestors discussed at

the end of chapter II.

The DT model of the last section can also be used to obtain a qualitative description of the Dalitz plot of figure VI.2. Since the trajectories are already nonlinear, we avoid the arbitrariness of the Lovelace approach and, more important, we do not introduce ancestors. As in the Lovelace model, we eliminate the ρ contribution by taking γ small and c large in (16). For simplicity, we also set $\gamma d=0$. The Dalitz plot distribution is thus proportional to $|A(s,t)|^2 \times \text{Phase Space}$, where $A(s,t)$ is given by (V.2). Using the ρ trajectory of the last section and the continuation (12), we can find $A(s,t)$ for $\text{Re}\alpha(s), \text{Re}\alpha(t) < 2$ by numerical integration. A contour plot of $|A(s,t)|$ is shown in figure VI.7. Notice that, even though we have not covered the entire region of figure VI.2, the majority of the structure is visible. We find an enhancement at $s=t=m_\rho^2$, a depletion near $\text{Re}\alpha(s) \approx \text{Re}\alpha(t) \approx 1.5$ and the beginnings of the enhancement occurring near the upper right edge of the Dalitz plot.

ii) $\pi\pi$ Phase Shifts. An alternative approach for the introduction of finite width resonances into the Veneziano model is the K-matrix method. Once the Veneziano amplitudes have been projected into partial waves, say $R_j^I(s)$, a new amplitude is defined in such a way that it has partial wave projections

$$A_j^I(s) = R_j^I(s) / [1 - i\rho(s)R_j^I(s)] \quad . \quad (31)$$

Near a resonance, $R_j^I(s)$ has the form

$$R_j^I(s) \approx \frac{-M\Gamma}{s-M^2} \quad . \quad (32)$$

Substituting (32) into (31) we have

$$A_j^I(s) \approx \frac{-M\Gamma}{s-M^2+i\rho(s)M\Gamma} \quad (33)$$

which is the form of a resonance with a positive width (if $\rho(s)\Gamma$ is positive). In addition, since R_j^I is real in the Veneziano model, it is easily shown that the elastic unitarity condition

$$\text{Im}A_j^I(s) = \rho(s) |A_j^I(s)|^2 \quad (34)$$

is satisfied, where

$$\rho(s) = [(s-1)/s]^{\frac{1}{2}} \quad . \quad (35)$$

Since the amplitude (31) has well defined real and imaginary parts, the $\pi\pi$ phase shifts are well defined. A slightly more complicated K-matrix method has been used by Lovelace (1969) to fit the "down-up" solution for the phase shift δ_0^0 .

The K-matrix approach to the unitarization of the Veneziano model suffers from a serious drawback: once the partial wave amplitudes have been redefined, it is difficult (if not impossible) to recombine them into a crossing symmetric amplitude.

Such an artificial method as the K-matrix approach is not necessary for the DT model defined in section VI.2.ii. Using the methods of section VI.2.i, we calculate the s-channel isospin amplitudes for $\alpha(1) < \text{Re}\alpha(s) < 2$ with θ_s fixed. From these

fixed angle isospin amplitudes, it is a simple matter to calculate the lowest partial wave projections $A_j^I(s)$. The Argand diagrams for the A_0^0 and A_1^1 partial waves are displayed in figures VI.8 and 9 along with the phase shifts δ_0^0 and δ_1^1 . The phase shifts are compared with the elastic phase shifts of Baton (1970).

The partial wave A_0^0 exceeds the unitarity limit but the deviation is not large below $s \approx 7.5$ ($\approx .56 \text{ GeV}^2$). The agreement with unitarity below the inelastic threshold, in fact, is to within 8% (see figure VI.10). The resulting phase shift δ_0^0 is not too far from the "down-down" solution of Baton (1970). By examining the S-wave phase shift of (25) (dotted line in figure VI.8), we can see that most of the structure is due to pole contributions. The rapid rise of δ_0^0 above threshold is due to the fact that the ϵ_1 , in addition to having a very large total width, has a very large partial width. The dip in the phase shift is due to interference between the ϵ and ϵ_1 . Notice that the behavior is similar to that found by Baton (1970) near the $K\bar{K}$ threshold.

The A_1^1 partial wave is characteristic of the ρ resonance. The elasticity is somewhat low and the ρ mass is shifted slightly upward from the input. The agreement with unitarity below the inelastic threshold is again rather good (see figure VI.11). There is some deviation from unitarity as we approach the elastic threshold, reaching 30% at $s=1.5$.

iii) $\pi\pi$ Scattering lengths. Because of the constant behavior of $\Psi_1(s)$ near threshold, we cannot directly determine the

partial wave amplitudes at $s=1$. We can, however, arrive at an estimate by making a quadratic fit through three points close to threshold ($s=1.5, 2$ and 3 in this case) and then extrapolating to $s=1$. With this method and the relation

$$a_I = \lim_{k \rightarrow 0} \delta_0^I/k = A_0^I(1)m_\pi^{-1} \quad (36)$$

for the S-wave scattering lengths, we find the $I=0$ and $I=2$ values to be

$$a_0 = .201m_\pi^{-1}, \quad a_2 = -.045m_\pi^{-1} \quad (37)$$

We also find

$$R = -4.476. \quad L = .1045m_\pi^{-1} \quad (38)$$

where R and L are defined in section VI.1.iii. The results are in satisfactory agreement with those of section VI.1. A complete table, showing Veneziano model results due to Lovelace as well, is presented below. L, a_0 and a_2 are in units of m_π^{-1} .

Table VI.2

a_0	a_2	L	R	Reference
$.16 \pm .04$	$-.05 \pm .01$	$.10 \pm .01$	-3.2 ± 1.0	(Morgan 1970)
$.28 \pm .21$				(Maung 1970)
$.20$	$-.06$	$.10 \pm .01$	-3.5	(Weinberg 1966)
$.15 \pm .02$	$-.04 \pm .004$	$.09 \pm .01$	-3.7 ± 0.8	(Cronin 1967)
			-3.8	(Lovelace 1968)
$.29$	$-.06$	$.15$	-4.5	(Lovelace 1969)
$.20$	$-.045$	$.10$	-4.5	(This work)

Notice that, except for the Adler condition, all of the parameters of our model were fixed by constraints in the resonance region. Thus, the low energy approximation to unitarity occurs solely as an output of the model. The scattering length results are also consistent with experimental and theoretical results, but this may be a consequence of the Adler condition. The results in the resonance region are not unitary but not unreasonable. It therefore appears likely that, with subtractive corrections, more sophisticated forms for $\Psi(s)$ and $\Psi_1(s)$, adjustment of parameters and the addition of a Pomeron contribution, a model can be constructed which describes $\pi\pi$ scattering in all experimentally observable regions.

VII. Conclusions, Prospects for Future Development

In the last three chapters, we have developed a generalized Veneziano model which can be used to examine low and intermediate energy scattering processes as well as scattering in the asymptotic region. The model is based on the distorted trajectory model discussed in chapter III. By demanding that the amplitudes be well behaved asymptotically, have physically reasonable singularities and a curved double spectral boundary, we have been able to significantly restrict the number of functions under consideration. The results of chapter VI suggest that the model is physically reasonable in the low energy region. In addition, with the continuations of section VI.2.i, we can perform calculations with the model in a straightforward way. The bulk of the work presented here has been concerned with the mathematical structure of the model. There have been no serious attempts to apply the model to the fitting of experimental data, only to the determination of qualitative results. Indeed, it would have been pointless to attempt such fits without first having shown that the model does not lead to violations of asymptotic bounds.

The amount of work remaining to be done with the model is significant. All of the phenomenological work which has been done in connection with the Veneziano model in the limit $s \rightarrow \infty$, $t < 0$ and fixed can be done with this model as well. In addition, we can make numerous low energy calculations. Finally, there are several theoretical problems which should be studied. In this chapter, we shall discuss some of the investigations

which should be undertaken in the near future. These include studies of the two body reaction model from both the mathematical and phenomenological points of view and an examination of a model with finite width resonances for multiparticle processes.

VII.1 Applications to Two Body Reactions

We shall now examine several interesting calculations which can be performed with the DT model.

1) $\pi\pi$ Elastic Scattering. In the last chapter, we performed a crude but encouraging calculation for the process $\pi\pi \rightarrow \pi\pi$. This calculation is inexact for three reasons. First, the amplitude does not have the correct double spectral boundary for the scattering of either scalar or pseudoscalar bosons. In addition, it cannot satisfy the elastic unitarity relation (VI.34) near threshold for $j \geq 2$. These difficulties are due to the fact that we have neglected the subtractive corrections of section V.3. Second, we have not included a Pomeron contribution. Such a term is expected to dominate the asymptotic behavior of any process which can exchange the vacuum quantum numbers in the crossed channel. We also notice that the $I=2$ invariant amplitude defined in equation (II.7) cannot be correct because $C(t,u)$ does not have an imaginary part for $s > 1$ and $t, u < 0$. In several models (see, for example, Moffat 1971 and Curry 1971), it is the Pomeron contribution which provides this imaginary part. In addition, $\pi\pi$ scattering has been observed to be highly diffractive for a dipion mass greater than 1.6 GeV (Oh 1970). Third, the Regge

trajectories which we have used for the calculation do not satisfy all of the conditions which have been discussed. The imaginary parts must grow asymptotically, probably as in equation (V.67). The threshold behavior of $\alpha(s)$ and $\alpha_1(s)$ is constrained by (V.106). A further constraint on the ρ trajectory is that

$$\alpha(-8) \approx 0 \quad . \quad (1)$$

This requirement, which in more conventional units implies $\alpha(t)=0$ for $t \approx -.6 \text{ GeV}^2$, provides the well known explanation of the dip at this value of t in the differential cross sections for $\pi^- p \rightarrow \pi^0 n$ and $\pi^+ p \rightarrow \pi^0 \Delta^{++}$. Relation (1) is not satisfied for the ρ trajectory of chapter VI (see figure VI.5).

Taking the above considerations into account, we can certainly perform a study of $\pi\pi$ elastic scattering similar to those of Lovelace (1969) and Curry (1971). Such a study should probably proceed in the following way. First, choose a set of trajectories satisfying the constraints mentioned above. Second, use the zero width resonance approximation with the Adler condition to estimate c (or d) of (VI.16) in terms of λ , b , b_1 and d (or c). Third, use the requirement of unitarity at the ρ resonance to determine γ . Fourth, use the fact that (VI.25) should give a reasonable approximation for the $I=J=0$ partial wave in the region $3 \leq s \leq 15$ to further restrict the parameter d (or c) and the trajectory parameters. Finally, include subtractive corrections and a Pomeron and perform the calculations of chapter VI. The results of these calculations should be sufficiently reasonable to enable us to improve them

by making minor changes in the parameters. In addition, the Adler condition should be tested. Once reasonable fits have been obtained for the lower partial waves, elastic unitarity can be tested for higher partial waves.

ii) $\pi N \rightarrow \pi N$ and $\gamma N \rightarrow \pi N$. Throughout this work, we have concentrated on the process $\pi\pi \rightarrow \pi\pi$. The advantage of this, at least in the Veneziano model, is that only one type of Regge trajectory is exchanged in all channels. The invariant amplitudes are therefore in a relatively simple form. Two problems with $\pi\pi$ elastic scattering are that the widths of the resonances lying on the ρ - f^0 trajectory are not well known and that the process has been studied only up to a center of mass energy of approximately 1.5 GeV. The first problem makes it difficult to restrict the function $\Psi(s)$ while the second means that we have no high energy data with which to compare the asymptotic form of our model.

Since the processes $\pi N \rightarrow \pi N$ and $\gamma N \rightarrow \pi N$ can be studied directly, there is experimental data at high energies in both forward and backward directions. Furthermore, since a large number of πN resonances have been observed, it should be easier to parameterize the baryon trajectories. The first process has been studied in the context of the Veneziano model by Berger (1969) while the second has been examined by Argyres (1971). The basic procedure in both cases is to write down a simple Veneziano representation for each invariant amplitude and then to fix the parameters in the resonance region. Unobserved resonances are decoupled while observed resonances are required

to have the correct partial widths. These models give definite predictions about the high energy behavior of the above reactions in both forward and backward directions (see figure VII.1). The forward cross sections, which are characteristic of meson exchanges, are satisfactory. The cross sections in the backward direction, which involve baryon trajectories, are incorrect for both processes. If satellite Veneziano terms are used, introducing additional parameters, then the backward results can be correctly accounted for (Argyres 1971).

It is a straightforward exercise to apply the DT model to these processes in place of the Veneziano representation. As was the case for $\pi\pi$ elastic scattering, subtractive corrections should be ignored until all parameters have been fixed. In any case, these terms should not contribute significantly to the asymptotic behavior in either the forward or backward direction. We will, however, need a Pomeron in order to discuss πN elastic scattering at high energies (see figure VII.1).

There are several factors which may change the Veneziano model results as we give widths to the resonances according to the DT prescription. First, if the imaginary parts of the trajectory functions behave like (V.67) for large s , then the most prominent non-leading terms in the asymptotic expansions for large $|s|$ will differ from the leading terms only in powers of $\ln|s|$. These non-leading terms may therefore modify the asymptotic behavior which results from the simple Veneziano approach. Second, the fact that the threshold behavior of the amplitudes can now be described may reduce the arbitrariness involved in the addition of satellite terms. This was the case

in $\pi\pi$ elastic scattering, where the satellite term $A_1(s,t)$ was required by threshold conditions. It will be interesting to see what changes, if any, occur in the description of πN elastic scattering and pion photoproduction as a result of this new representation.

iii) Tests for Duality. Although the Veneziano model is dual, in the sense that the sum of its resonances is equal to the sum of its crossed channel Regge exchanges, the amplitude which we have constructed is not. There are non-resonance contributions in the direct channel and contributions in the crossed channel which do not correspond to Regge pole exchange (see Appendix). Since the DT amplitudes reduce to those of the Veneziano model in the zero width resonance limit, we expect it to have broken duality. We can test the extent to which duality is still satisfied by substituting the resonance contributions of the model into an FESR whose right hand side comes solely from the Regge pole part of the asymptotic behavior. An easier test is to compare the imaginary part of the resonance contribution with the extrapolation to the resonance region of the imaginary part of the leading Regge pole contributions. The Regge contributions should average the resonance contribution.

VII.2 Theoretical Problems in Two Body Reactions

Although we have examined a number of the basic properties of the DT model, there are several interesting areas which remain to be investigated.

i) Subtractive Corrections. As yet, we have not studied the behavior of the subtractive corrections of chapter V in much detail. These terms are expected to play a significant role in the unitarization of the model, especially for higher partial waves.

ii) J-Plane Structure. Some information about the J-plane singularities of the $A_J^I(s)$ for $\pi\pi$ scattering can be obtained from the treatment in the Appendix. However, we have yet to examine this problem in detail. In particular, we have studied neither the J-plane structure of the subtractive corrections nor the possibility of fixed poles at nonsense wrong signature points in the $I=0$ and $I=2$ amplitudes.

iii) Non-Leading Terms. In the Appendix we will develop a technique which enables us to obtain all of the terms in the asymptotic expansion and the singularity expansion of the DT model. In order to study these non-leading terms, we must adopt a specific form for the function $\Psi(s)$. Of particular interest are the branch points which occur for $\alpha(s)=2$ and for higher values of $\alpha(s)$ and which have projections into all partial waves. Since these are weak singularities and, in addition, occur on the second sheet of the s-plane, they would certainly be impossible to detect experimentally. It is interesting to speculate on the possible physical significance of such terms.

iv) Alternative Trajectory Functions. The form of the trajectory function which we introduced in equation (VI.1) is

certainly not the most general. One change which could be introduced would be to write the function $\Psi(s',z)$ in place of $\Psi(s')$ in the definition (IV.1), where

$$\Psi(s,0) = \text{Im}\alpha(s) \quad (1 < s < \infty) \quad . \quad (2)$$

All of the studies of chapters IV and V could be carried out with such a function. A second possibility is the introduction of inelastic thresholds into the models. A form like

$$\alpha(s,z) = \lambda s + b + \frac{s}{\pi} \int_{\phi(z)}^{\infty} ds' \frac{\Psi(s')}{s'(s'-s)} + \frac{s}{\pi} \int_{s_i \phi_i(z)}^{\infty} ds' \frac{\Psi_i(s')}{s'(s'-s)} \quad , \quad (3)$$

where $\phi(0) = \phi_i(0) = 1$ and $\phi(1) = \phi_i(1) = \infty$, would introduce another threshold at $s = s_i$ into the trajectory $\alpha(s)$.

VII.3 Extensions, Applications in Production Processes

One of the most exciting facets of the Veneziano model is its simple generalization to multiparticle processes. The amplitudes for N particle processes ($N = \text{incoming} + \text{outgoing}$) are described by the function (Chan 1970a)

$$B_N = \int_0^1 \left(\prod_{i=2}^{N-2} dx_i \right) (1/J_1) \prod_P u_P^{y_P} \quad (4)$$

where

$$J_1 = \prod_{i=2}^{N-2} \prod_{j=i+1}^{N-1} (u_{ij})^{j-i-1} \quad , \quad (5)$$

$$y_P = y_{ij} = -\alpha_{ij} - 1 \quad , \quad (6)$$

$$\alpha_{ij} = b_{ij} + \lambda s_{ij} \quad , \quad (7)$$

and

$$s_{ij} = [p_i + p_{i+1} + \dots + p_j]^2 \quad . \quad (8)$$

The P in (4) and (6) refers to permutations in which $i < j$, while the λ in (7) is a universal slope. The u_{ij} are defined by

$$u_{ij} = \frac{(1-x_i x_{i+1} \dots x_{j-1})(1-x_{i-1} x_i \dots x_j)}{(1-x_i x_{i+1} \dots x_j)(1-x_{i-1} x_i \dots x_{j-1})} \quad , \quad (9)$$

while the x_i needed in (9) but not included in the set of integration variables are

$$x_0 \equiv \infty, \quad x_1 \equiv x_{N-1} \equiv 0 \quad . \quad (10)$$

We can introduce finite width resonances into the model above by replacing (7) with

$$\alpha_{ij}(s_{ij}, \{x\}) = \lambda s_{ij} + b_{ij} + \frac{s_{ij}}{\pi} \int_{L_{ij}(\{x\})}^{\infty} dq \frac{\psi_{ij}(q)}{q(q-s_{ij})} \quad . \quad (11)$$

The lower limit of integration is given by

$$L_{ij}(\{x\}) = m_{ij}(1-\eta_{ij} \ln(1-u_{ij})) \quad (12)$$

where η_{ij} are constants and $s_{ij} = m_{ij}$ is the elastic threshold for the ij channel. Notice that this is a simple extension of the DT model of section V.1. There are clearly a number of

other possibilities.

Some of the earliest applications of the 5-point function, B_5 , were to the processes $K^- p \rightarrow \pi^+ \pi^- \Lambda$ (Petersson 1969) and $K^+ p \rightarrow K^0 \pi^+ p$ (Chan 1970b) and to reactions related to these by crossing symmetry. Good fits were obtained to many of these reactions with a small number of parameters. In all cases, however, it was necessary to use trajectories which were complex above threshold, leading to the ancestors which we discussed earlier. We are now in a position to perform the same work but with a model whose trajectories have imaginary parts arising in a natural way.

Another area in which it will be of interest to apply the multiparticle DT model is in the study of inclusive reactions. According to Mueller's theorem (Mueller 1970), the amplitude for the production of the particle c in the reaction

$$a + b \rightarrow c + \text{anything} \quad (13)$$

is related to the direct channel discontinuity for the process

$$a + b + \bar{c} \rightarrow a + b + \bar{c} \quad (14)$$

where there is to be no momentum transfer in this last reaction. The reaction (14), however, can be described by the function B_6 . We can therefore apply our generalization to the study of (14) and therefore to (13). This application should follow the methods of Olesen (1971) or Virasoro (1971). The work of Olesen, in fact, was performed with two generalizations which

incorporated finite width resonances. Neither of his generalizations, however, was based on a four point model with Regge behavior as $s \rightarrow +\infty$ for all physically attainable values of the crossed channel variable. We have now overcome this difficulty.

Appendix. Non-Leading Terms

As we mentioned in chapter VI, one of the most useful properties of the DT models and of the Suzuki model of chapter III is that they reduce to the Veneziano model in the zero width resonance limit, i.e. as

$$\Psi(s) \rightarrow 0 \quad (\text{for all } s) \quad . \quad (1)$$

We have already used this property to obtain approximations to the DT model in various regions. Another use of the property lies in the fact that a parameter characterizing the size of the resonance widths is a natural one in which to expand the amplitudes.

The singularities mentioned in section V.1.v remain essentially unchanged in the limit (1). The only difference is that they are shifted to the real, positive s -axis. The function $A(s,t)$ has additional singularities which we have not discussed and which vanish in the limit (1). In this Appendix, we shall introduce methods which enable us to study, at least in a qualitative manner, these non-leading singularities. In addition, we shall use similar techniques to examine in detail the asymptotic expansion of $A(s,t)$ in the large $|s|$, fixed t limit.

1) The Singularity Expansion. The s -channel singularities of $A(s,t)$ arise from the divergence of (V.2) at the lower endpoint of integration. We therefore make a separation similar

to (II.19):

$$\begin{aligned}
 A(s,t) &= \int_0^{\nu} \int_{\nu}^1 dz z^{-\alpha(s)} (1-z)^{-\lambda t - b} z^{\nu} f(s,z) (1-z)^{-g(t, 1-z)} \\
 &\equiv I_{0\nu}(s,t) + I_{\nu 1}(s,t) \quad .
 \end{aligned}
 \tag{2}$$

In order to examine the s -channel singularities of $A(s,t)$, we need only to study $I_{0\nu}(s,t)$.

In chapter II we obtained the singularity expansion by integrating $I_{0\nu}$ explicitly in the region $\text{Re}\alpha(s) < 1$. The result of the integration provided us with an analytic continuation into the region $\text{Re}\alpha(s) > 1$. The function $I_{0\nu}(s,t)$ defined in equation (2) is not so easily integrated because the integrand is a complicated function of z . We can, however, simplify the z dependence of the integrand by making use of the Laplace transform and its inverse transform (Carrier 1965, ch. 7).

We write $f(s,z)$ in the form

$$f(s,z) = z \int_0^{\infty} dp z^p F(s,p) \tag{3}$$

where

$$F(s,p) = \frac{1}{2\pi i} \int_{\beta-i\infty}^{\beta+i\infty} dx e^{x(p+1)} f(s, e^{-x}) \tag{4}$$

and where the path $\text{Re}x = \beta$ lies to the right of all singularities in the integrand of (4). The representation (3) converges for $|z| < \min\{1, |1 - e^{(1-s)/\eta}|\}$ so that by taking ν sufficiently small in (2) we can use (3) for $f(s,z)$. With some algebra, we obtain

the expansion

$$z^f(s, z) = \int_0^{\infty} dp F(s, p; d/dp) z^p \quad (5)$$

where

$$F(s, p; d/dp) = \delta(p) + \sum_{n=1}^{\infty} \frac{1}{n!} \int_0^{\infty} dp_1 \dots dp_n F(s, p_1) \dots F(s, p_n) \delta(p_1 + \dots + p_n - p) (d/dp)^n . \quad (6)$$

Similarly, we write $g(t, 1-z)$ in the form

$$g(t, 1-z) = \int_0^{\infty} dq z^q G(t, q) \quad (7)$$

where

$$G(t, q) = \frac{1}{2\pi i} \int_{\beta-i\infty}^{\beta+i\infty} dx e^{qx} g(t, 1-e^{-x}) \quad (8)$$

and where the representation (7) converges for $|z| < \min\{1, |e^{(1-t)/\eta}|\}$. Again, with v sufficiently small, we can use equation (7) for $g(t, 1-z)$ in (2). We have

$$(1-z)^{-g(t, 1-z)} = \int_0^{\infty} dq G(t, q; d/dw) z^q (1-z)^{-w} \Big|_{w=0} \quad (9)$$

where

$$G(t, q; d/dw) = \delta(q) + \sum_{m=1}^{\infty} \frac{1}{m!} \int_0^{\infty} dq_1 \dots dq_m G(t, q_1) \dots G(t, q_m) \delta(q_1 + \dots + q_m - q) (d/dw)^m . \quad (10)$$

We now substitute (5) and (9) into (2) and perform the z integration to obtain, for $I_{0\nu}$,

$$I_{0\nu}(s,t) = \int_0^{\infty} dpdq \{ F(s,p;d/dp) G(t,q;d/dw) \times \\ \times B_{\nu}(1+p+q-\alpha(s), 1-\lambda t-b-w) \} \Big|_{w=0}. \quad (11)$$

The incomplete Beta function, B_{ν} , has poles at $\alpha(s)=p+q+1+j$ ($j=0,1,2,\dots$) whose residues are polynomials of degree j in $(\lambda t+w)$. The function $I_{0\nu}(s,t)$, then, will have singularities at

$$\alpha(s) = p' + q' + 1 + j \quad (j=0,1,2,\dots) \quad (12)$$

where p' is either zero or a singular point of F while q' is either zero or a singular point of G .

If ϵ is a parameter characterizing the size of the resonance widths (i.e. the size of $\Psi(s)$), then the j -th terms in the expansions (6) and (10) are $O(\epsilon^j)$. Thus the contribution to (11) coming from the j -th term in (6) and the k -th term in (10) is of order $j+k$ in the narrow resonance expansion. The leading term in this expansion, found by using the first terms of (6) and (10) in (11), simply gives the singularities discussed in section V.1.v.

Let us now keep all of the terms in (6) but only the first term in (10) and, further, let us suppose that the function $s^{-1}\Psi(s)$ has the expansion, for $s \approx 1$,

$$s^{-1}\Psi(s) = \sum_{m=0}^{\infty} \sum_{n=0}^{\infty} c_{mn} (s-1)^{\rho_0+m} [-\ln(s-1)]^{-n} \quad (13)$$

It is then an easy matter to show that I_{0V} has singularities at

$$\alpha(s) = j(\rho_0+1) + k + 1 \quad (k=0,1,2,\dots) \quad (14)$$

which have a polynomial t dependence of degree k . The nature of these singularities is as follows:

- a) Simple poles for $j=0,1,2,\dots$;
- b) Branch points for $j=1,2,\dots$;
- c) Multiple poles of maximum multiplicity $j+1$ for $j=1,2,\dots$.

The singularities c) occur only if $c_{m0} \neq 0$ in (13). Thus, if $c_{m0} \equiv 0$ in (13) then $A(s,t)$ will have no multiple poles. Such a threshold behavior for $s^{-1}\psi(s)$ is consistent with (V.73).

Except for the threshold branch point discussed in chapter V, the singularities a) and b) [and c) if $c_{m0} \neq 0$] are the only ones occurring in the neutralized model of section V.2.

Finally, if higher order terms in the expansion (10) are used, we can show that $A(s,t)$ has singularities at

$$\alpha(s) = j(\rho_0+1) + k + 2 \quad (j,k=0,1,2,\dots) \quad (15)$$

whose t dependence is not polynomial. These singularities will therefore appear in all partial wave projections, unlike those of (14). If the c_{m0} vanish for all m then the singularities at the points (15) are branch points. The nature of these branch points depends upon the behavior of the function $s^{-1}\psi(s)$ for large $|s|$.

ii) The Asymptotic Expansion. With the change of variables $z = (1-e^{-x})$, equation (V.43) becomes

$$A(s, t) \sim \int_0^{\bar{v}(\phi_s)} dz z^{-\alpha(t)} (1-z)^{-\lambda s - b} z^f(t, z) (1-z)^{-g(s, 1-z)} \quad (16)$$

where, for small v ,

$$\bar{v}(\phi_s) \equiv [1 - \exp(-v e^{-i\phi_s})] \approx v e^{-i\phi_s} \quad . \quad (17)$$

The representation (5) can be used for $z^f(t, z)$ in (16). Similarly, we use the representation (9) for $(1-z)^{g(s, 1-z)}$. We must be careful in working with the latter term since (7) converges only for $|z| \lesssim e^{-\text{Res}/\eta}$ when $\text{Res} > 0$. This problem can be overcome, without effecting the asymptotic expansion, by defining $G(s, q)$ as

$$G(s, q) = \frac{1}{2\pi i} \int_{\beta-i\infty}^{\beta+i\infty} dx e^{qx} \tilde{g}(s, 1-e^{-x}) \quad . \quad (18)$$

The function \tilde{g} is the asymptotic expansion of g :

$$\tilde{g}(s, 1-e^{-x}) = g(s, 0) + \frac{s}{\pi} \sum_{k=0}^{\infty} (s-1)^{-k-1} \int_1^{1+\eta x} ds' \frac{\Psi(s')(s'-1)^k}{s'} \quad . \quad (19)$$

With the above substitutions we find

$$A(s, t) \sim \int_0^{\infty} dp dq \{ F(t, p; d/dp) G(s, q; d/dw) \times \\ \times B_{\bar{v}(\phi_s)}^{-1}(1+p+q-\alpha(t), 1-\lambda s-b-w) \} \Big|_{w=0} \quad (20)$$

as $|s| \rightarrow \infty$ with $-\pi \leq \arg(1-\alpha(s)) \equiv \phi_s \leq \pi$ for t fixed and such that $\text{Re} t < 1$.

The leading asymptotic behavior of (20) is just (V.46). Thus the amplitudes constructed from $A(s,t)$ will have asymptotic behavior characteristic of the exchange of the ρ - f^0 trajectory. The positions and natures of the non-leading trajectories will depend upon the behavior of $\Psi(s)$ near $s=1$ and $s=\infty$. Suppose that $\Psi(s)$ has the behavior (13) near threshold and behaves, to within logarithmic factors, like $s^{1-\xi}$ for large s . We can then show, with (20), that the amplitudes constructed from $A(s,t)$ have terms in their asymptotic expansions which are characteristic of the exchange of trajectories lying $j(\rho_0+1)+k\xi+n$ units of angular momentum below the ρ - f^0 trajectory ($j,k,n=0,1,2,\dots$). Notice that if $\Psi(s)$ has the behavior (V.67) for large s then $\xi=0$. If, furthermore, ρ_0 is an integer then $j(\rho_0+1)$ is also an integer. All trajectories will then lie an integral distance below the ρ - f^0 trajectory.

If only the first term in the expansion (10) for G is used in (20), then only the $k=0$ trajectories appear. It can easily be shown that these are the trajectories on which lie the resonances and branch points of (14) and the following discussion. These are the only terms appearing in the asymptotic expansion of the neutralized model of section V.2. The trajectories resulting from higher terms in the expansion of G evidently do not "surface" at physical J . We therefore have the situation shown in figure A.1.

References

- S.L. Adler: Phys. Rev. 137B, 1022 (1965)
- V. Alessandrini, D. Amati, M. Le Bellac and D. Olive: Phys. Reports 1C, 269 (1971)
- P. Anninos, L. Gray, P. Hagerty, T. Kalogeropoulos, S. Zenone, R. Bizzarri, G. Ciapeti, M. Gaspero, I. Laakso, S. Lichtman and G.C. Moneti: Phys. Rev. Letters 20, 402 (1968)
- E. Argyres, A.P. Contogouris, C.S. Lam and S. Ray: Nuovo Cim. 4A, 156 (1971)
- D. Atkinson, A.P. Contogouris and R. Gaskell: Bonn preprint (1972) and to be published (Phys. Rev.).
- J.P. Baton, G. Laurens and J. Reignier: Phys. Lett. 33B, 525 and 528 (1970)
- J.V. Beaupre, M. Deutschmann, H. Graessler, P. Schmitz, R. Speth, H. Boettcher, J. Kaltwasser, H. Kaufmann, S. Nowak, A. Angelopoulos, K.W.J. Barnham, J.R. Campbell, V.T. Cocconi, P.F. Dalpiaz, J.D. Hansen, G. Kellner, W. Kittel and D.R.O. Morrison: Nud. Phys. (Netherlands) B28, 77 (1971)
- E. Berger and G. Fox: Phys. Rev. 188, 2120 (1969)
- A. Bugrij, L. Jenkovsky and N. Kobylinsky: Lett. Nuovo Cim. 1, 923 (1971)
- G.F. Carrier, M. Krook and C.E. Pearson: Functions of a Complex Variable (McGraw-Hill, 1965)
- Chan Hong-Mo: Proc. Roy. Soc. Lond. A318, 379 (1970)a
- Chan Hong-Mo, R.O. Raitio, G.H. Thomas and N.A. Törnqvist: Nucl. Phys. B19, 173 (1970)b
- G. Cohen-Tannoudji, F. Henyey, G. Kane and W. Zakrzewski: Phys. Rev. Letters 26, 112 (1971)
- J.A. Cronin: Phys. Rev. 161, 1483 (1967)
- P. Curry, I.O. Moen, J.W. Moffat and V. Snell: Phys. Rev. D3, 1233 (1971)
- R.J. Eden: High Energy Collisions of Elementary Particles (Cambridge, 1967)
- S. Frautschi: Regge Poles and S-Matrix Theory (Benjamin, 1963)

- M.H. Friedman, P. Nath and Y.N. Srivastava: Phys. Rev. Letters 24, 1317 (1970)
- S. Fubini and G. Veneziano: Nuovo Cim. 64A, 811 (1969)a
- S. Fubini, D. Gordon and G. Veneziano: Phys. Lett. 29B, 679 (1969)b
- R. Gaskell and A.P. Contogouris: Lett. Nuovo Cim. 3, 231 (1972)
- I. S. Gradshteyn and I.M. Ryzhik: Table of Integrals, Series and Products (Academic Press, 1965)
- J.D. Jackson: Rev. Mod. Phys. 42, 12 (1970)
- G. Källén: Elementary Particle Physics (Addison-Wesley, 1964)
- K. Kikkawa, B. Sakita and M.A. Virasoro: Phys. Rev. 184, 1701 (1969)
- C. Lovelace: Phys. Lett. 28B, 264 (1968)
- C. Lovelace: Proceedings of the ANL Conference on $\pi\pi$ and $K\pi$ Interactions, 562 (1969) (Unpublished)
- A. Martin: Phys. Lett. 29B, 431 (1969)
- T. Maung, G.E. Masek, E. Miller, H. Ruderman, W. Vernon, K.M. Crowe and N.T. Dairiki: Phys. Lett. 33B, 521 (1970)
- L. Gonzales Mestres: Lett. Nuovo Cim. 2, 251 (1971)
- J.W. Moffat: Phys. Rev. D3, 1222 (1971)
- D. Morgan and G. Shaw: Phys. Rev. D2, 520 (1970)
- A.H. Mueller: Phys. Rev. D2, 2963 (1970)
- B.Y. Oh, A.F. Garfinkel, R. Morse, W.D. Walker, J.D. Prentice, E.C. West and T.S. Yoon: Phys. Rev. D1, 2494 (1970)
- P. Olesen: CERN preprint TH 1322 (1971)
- B. Petersson and N.A. Törnqvist: Nucl. Phys. B13, 629 (1969)
- R. Ramachandran and M.O. Taha: Phys. Rev. (to be published), (1971)
- R. Roskies: Phys. Rev. Letters 21, 1851 (1968)
- M. Schmidt: Lett. Nuovo Cim. 1, 1017 (1971)
- D. Sivers and J. Yellin: Rev. Mod. Phys. 43, 125 (1971)

- M. Suzuki: Phys. Rev. Letters 23, 205 (1969)
- G. Veneziano: Nuovo Cim. 57A, 190 (1968)
- M.A. Virasoro: Phys. Rev. D3, 2834 (1971)
- S. Weinberg: Phys. Rev. Letters 17, 616 (1966)

Figure Captions

Chapter I

1. Definition of the Mandelstam variables s , t and u .

Chapter II

1. Reaction channels for the process $1+2 \rightarrow 3+4$.
2. The reactions a) $\omega + \pi_1 \rightarrow \pi_2 + \pi_3$ and b) $\omega + \bar{\pi}_2 \rightarrow \bar{\pi}_1 + \pi_3$.
3. The reactions a) $\pi_1 + \pi_2 \rightarrow \pi_3 + \pi_4$ and b) $\pi_1 + \bar{\pi}_3 \rightarrow \bar{\pi}_2 + \pi_4$.
4. Definition of the s-channel center of mass scattering angle for the process $1+2 \rightarrow 3+4$.
5. Trajectories and particles in the Veneziano model for $\pi\pi$ scattering. Numbers are elastic partial widths in MeV normalized to $\Gamma_\rho = 112$ MeV. From (Jackson 1970).
6. Paths of integration for (II.28).
7. Paths of integration for (II.34).
8. Paths of integration for (II.36) showing singularities at $x = \pm 2n\pi i$.
9. Saturation of the FESR (II.39) with zero width resonances. Solid lines are values from (II.39). Dashed lines are values from (II.40). Cutoffs: $\lambda_N = 2, 4$.
10. Path of integration for examining $A(s, t)$ as $|s| \rightarrow \infty$, u fixed, $\phi - \pi < \arg(1 - \alpha(s)) < -\frac{1}{2}\pi$. Singularities at $x = \pm(2n+1)\pi i$ are shown.
11. Paths of integration for examining $A(s, t)$ as $|s| \rightarrow \infty$, χ_s fixed, $\phi - \pi < \arg(1 - \alpha(s)) < -\frac{1}{2}\pi$. Singularities at $x = (1 - \chi_s) \ln(1 - \chi_s) + \chi_s \ln \chi_s \pm (2n+1)\chi_s \pi i$ are shown.

Chapter III

1. Double spectral boundaries for the Suzuki, DT and CHKZ models. Dashed line is the ϕ^3 boundary.

2. Contour of integration for (III.27) used to find $\text{Re}v_j(s)$ in all models and $\text{Im}v_j(s)$ in Suzuki model.
3. Contour of integration for (III.27) used to find $\text{Im}v_j(s)$ in CHKZ and DT models.
4. Contour deformation of (III.42) providing analytic continuation into right half s-plane. Singularities (III.43) and (III.44) are indicated.
5. Contour deformation of (III.45) providing analytic continuation into right half s-plane. Singularities at $y=y_n$ are indicated.

Chapter IV

1. Regions of analyticity required in the z-plane for $\phi(z)$ and $\Psi(\phi(z))/\phi(z)$ for several χ_s .

Chapter V

1. Double spectral region (V.15) with $\eta \approx .72$ and ϕ^3 double spectral region.
2. Integration contour for (V.31).
3. Contour used in deriving (V.50).
4. Contour C' used in determining fixed angle asymptotic behavior.
5. Double spectral region (V.15) with $\eta \approx .72$ and ϕ^4 double spectral region.

Chapter VI

1. Diagrams of pion reactions studied.
2. Dalitz plot for the reaction $\bar{p}n \rightarrow \pi^- \pi^- \pi^+$ near threshold. (Anninos 1968)

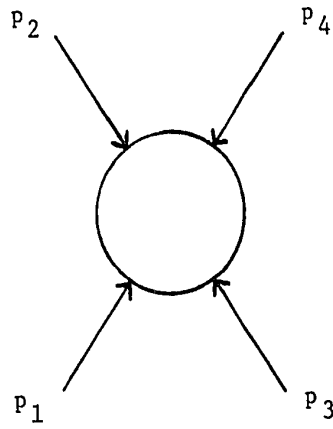
3. $I=0$ S-wave phase shifts for $\pi\pi$ scattering.
 - a) Beaupre (1971)
 - b) Oh (1970)
 - c) Elastic "down-down" ($c-c_d$) and "down-up" ($c-c_u$) solutions of Baton (1970)
 - d) Inelastic "down-down" ($d-d_d$) and "down-up" ($d-d_u$) solutions of Baton (1970).
4. Path of integration for (VI.13). Points marked (o) indicate singularities in $\alpha(s, e^{-x})$ or $\alpha(t, 1-e^{-x})$.
5. Real parts of the trajectories $\alpha(s)$ and $\alpha_1(s)$.
6. Imaginary parts of the trajectories $\alpha(s)$ and $\alpha_1(s)$.
7. a) $|A(s, t)|$ in the region $1 < s, t < 20$. b) Cross section of figure VI.7a along diagonal $s=t$. Small numbers on vertical axis of b) correspond to numbers in a).
8. a) Phase shifts and b) Argand diagram for $I=J=0$ $\pi\pi$ partial wave. Dashed phase shift: elastic solution of Baton (1970). Solid phase shift: this model. Dotted phase shift: contribution from ϵ and " ϵ_1 " (VI.25).
9. a) Phase shifts and b) Argand diagram for $I=J=1$ $\pi\pi$ partial wave. Dashed phase shift: elastic solution of Baton (1970). Solid phase shift: this model.
10. Satisfaction of elastic unitarity for $I=J=0$ $\pi\pi$ partial wave.
11. Satisfaction of elastic unitarity for $I=J=1$ $\pi\pi$ partial wave.

Chapter VII

1. Regge trajectories dominating asymptotic behavior of πN elastic scattering in a) forward direction and b) backward direction.

Appendix

1. Typical Regge trajectories resulting from using the first term of expansion (A.10) in (A.20) (solid lines) and from using remaining terms (dashed line). Physical J singularities lying on trajectories marked (o).



$$s = (p_1 + p_2)^2 = (p_3 + p_4)^2$$

$$t = (p_1 + p_3)^2 = (p_2 + p_4)^2$$

$$u = (p_1 + p_4)^2 = (p_2 + p_3)^2$$

Figure I.1

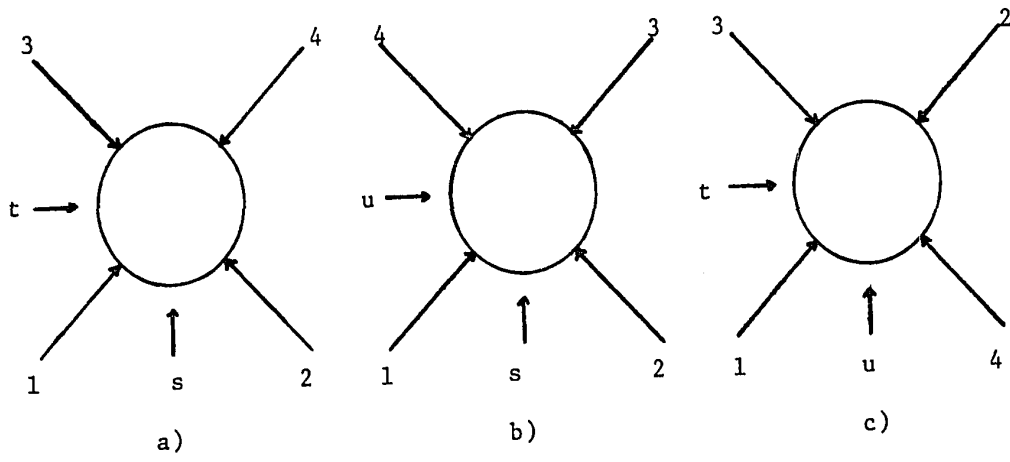


Figure II.1

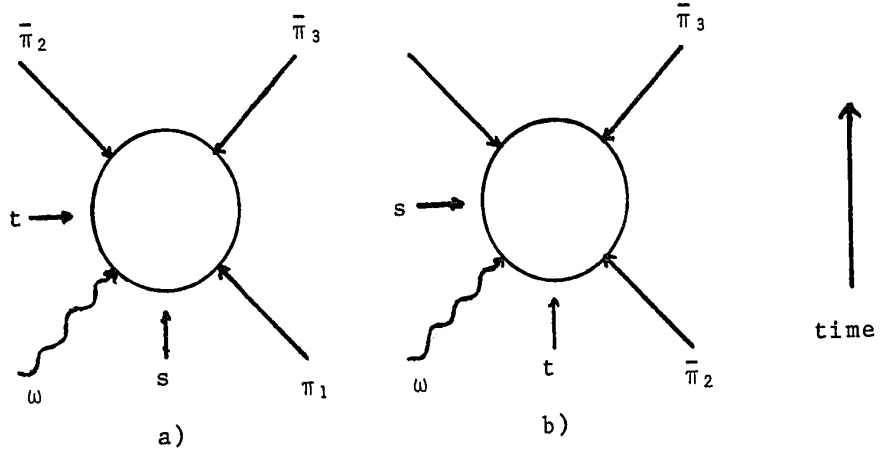


Figure II.2

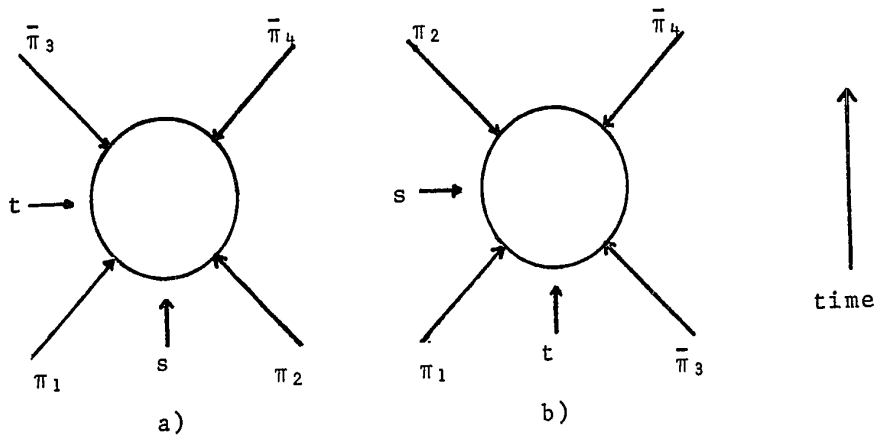


Figure II.3

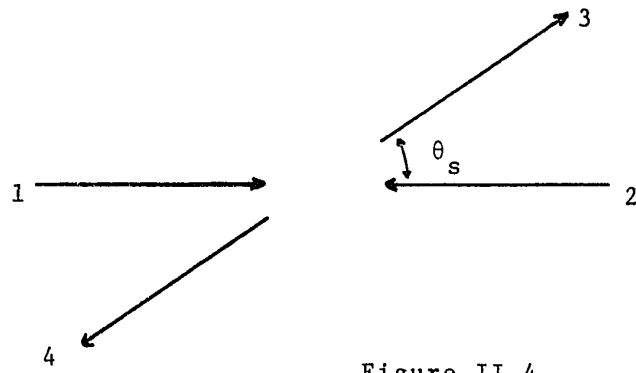
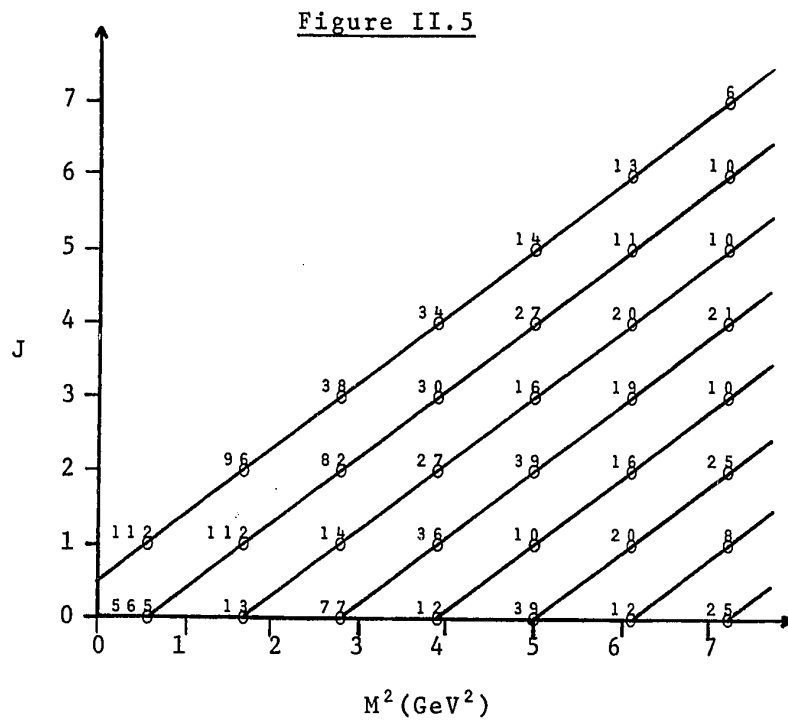


Figure II.4



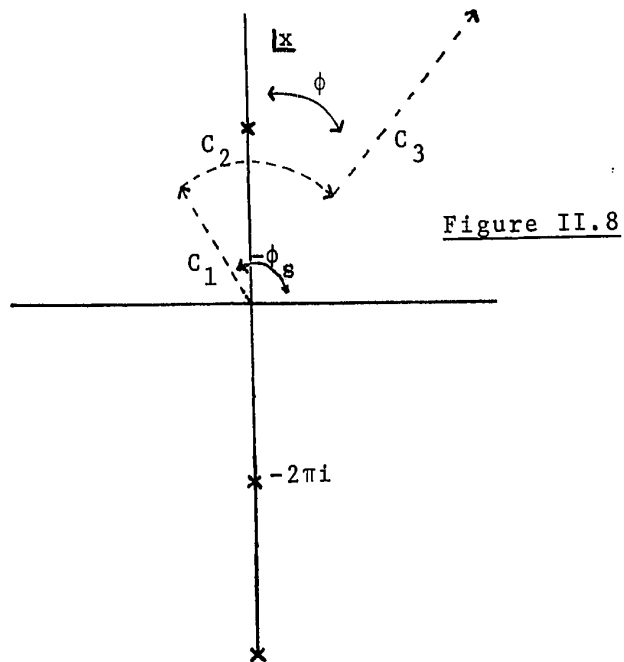
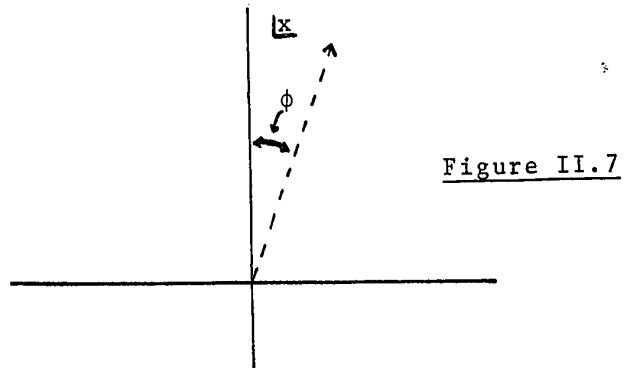
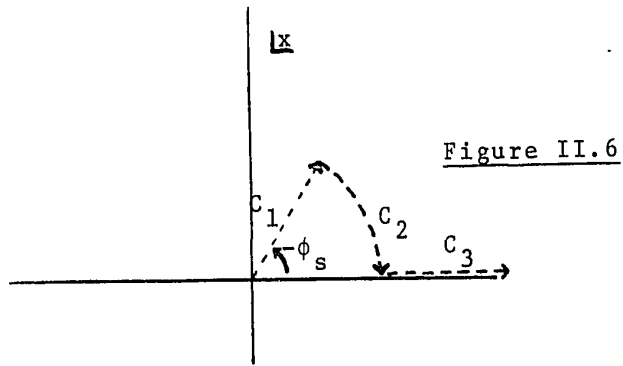
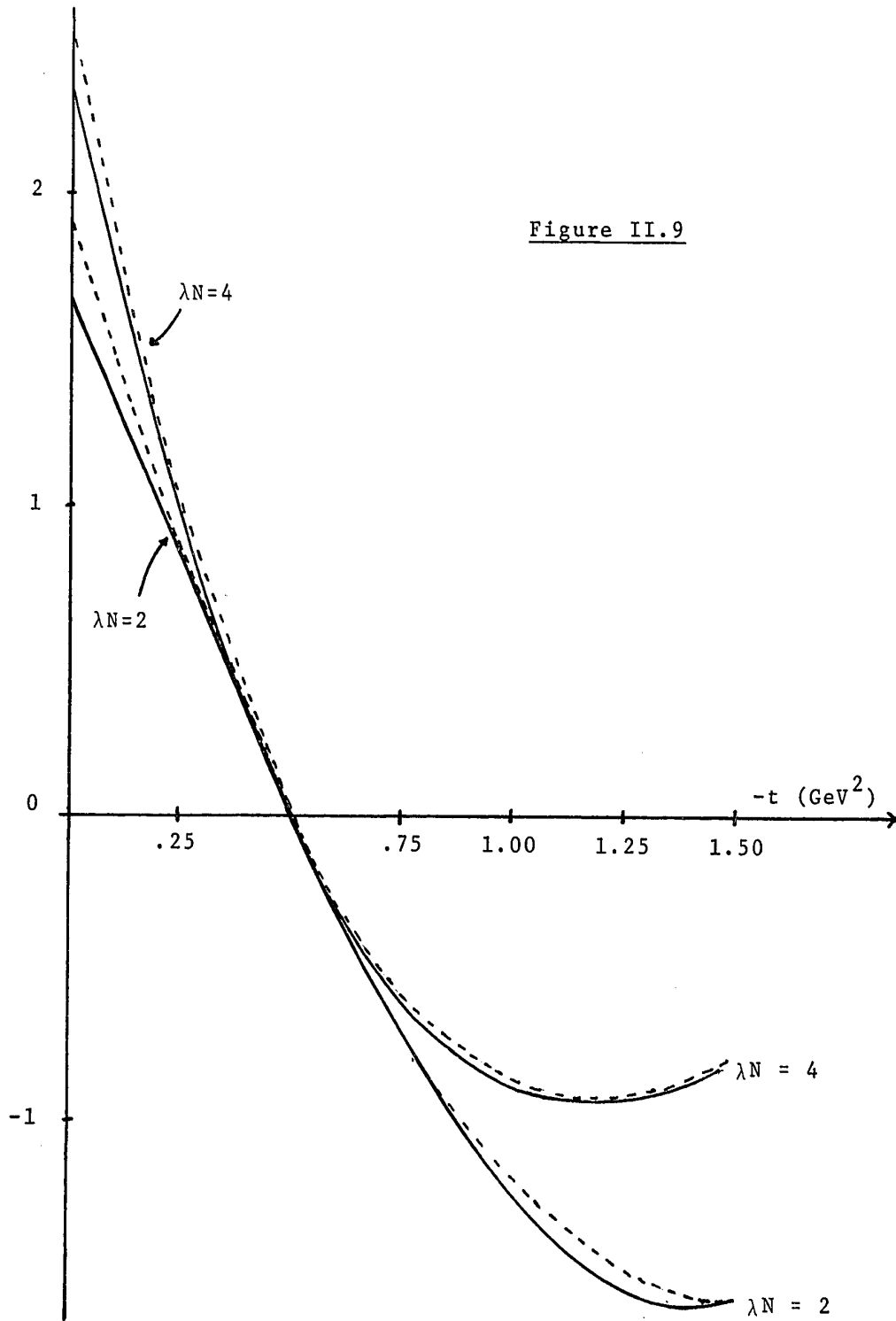


Figure II.9



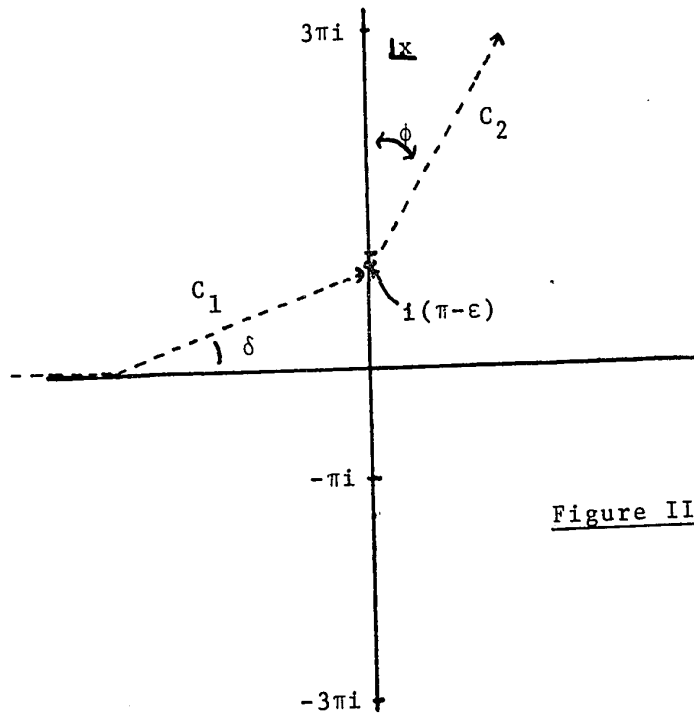


Figure II.10

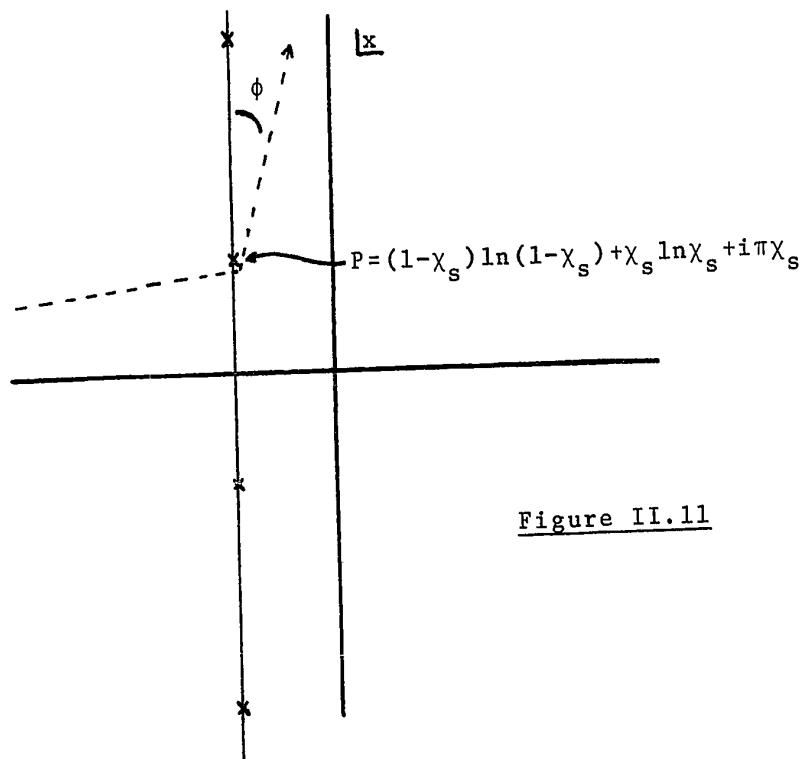
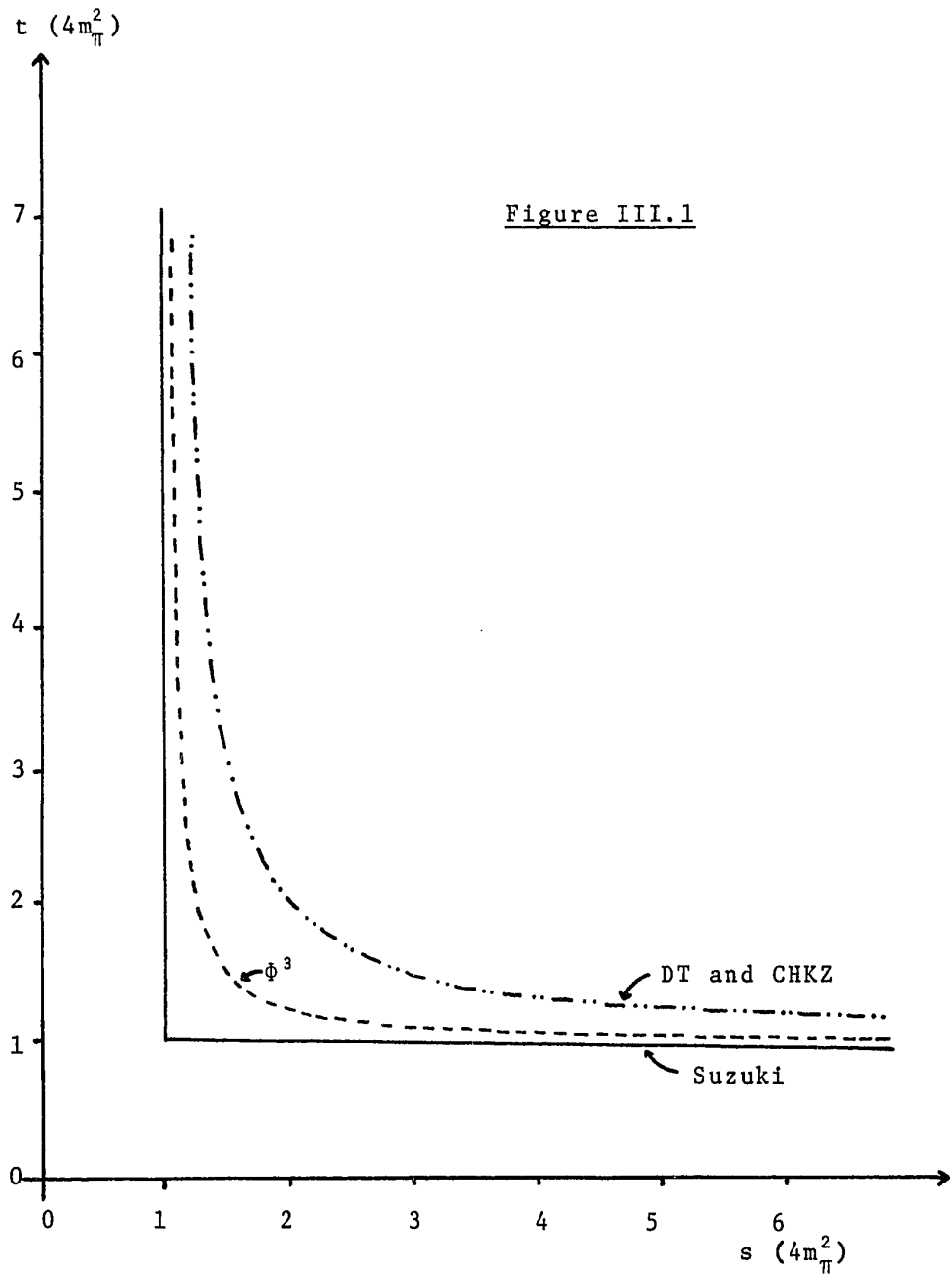


Figure II.11



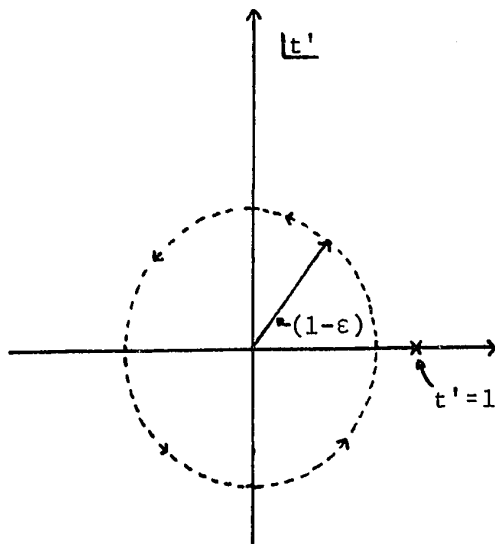


Figure III.2

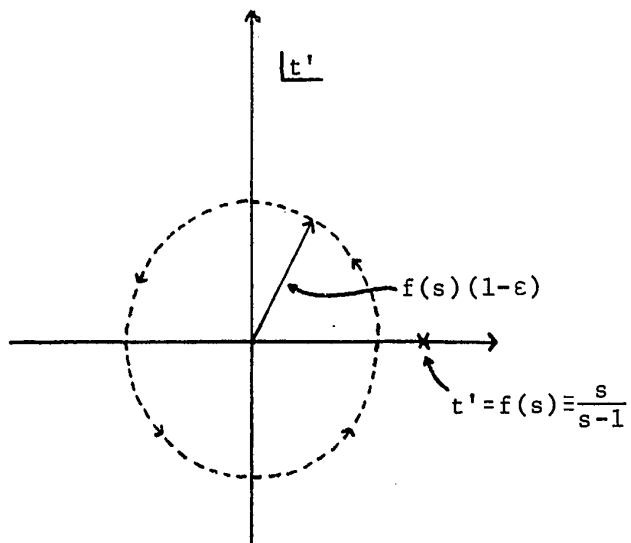


Figure III.3

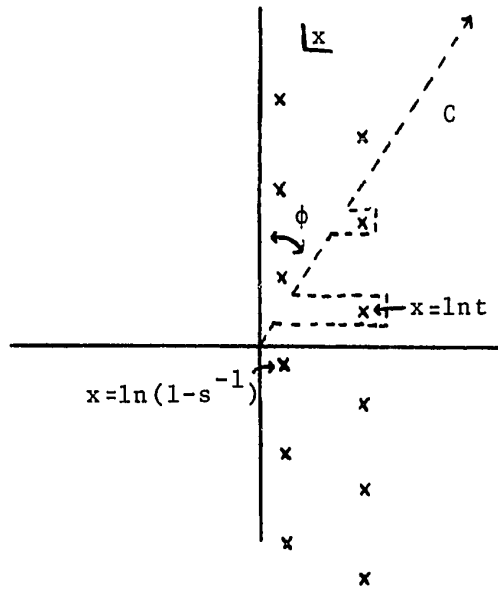


Figure III.4

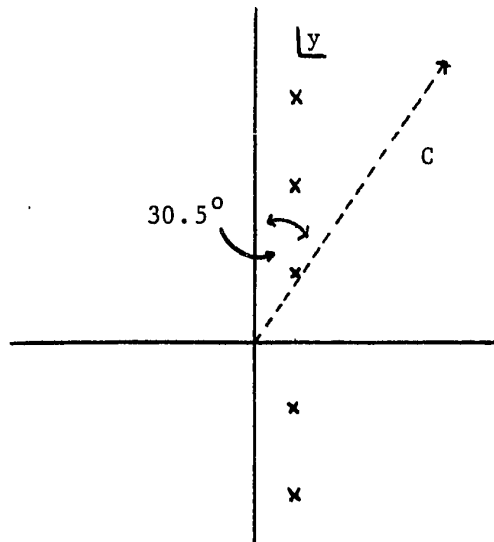


Figure III.5

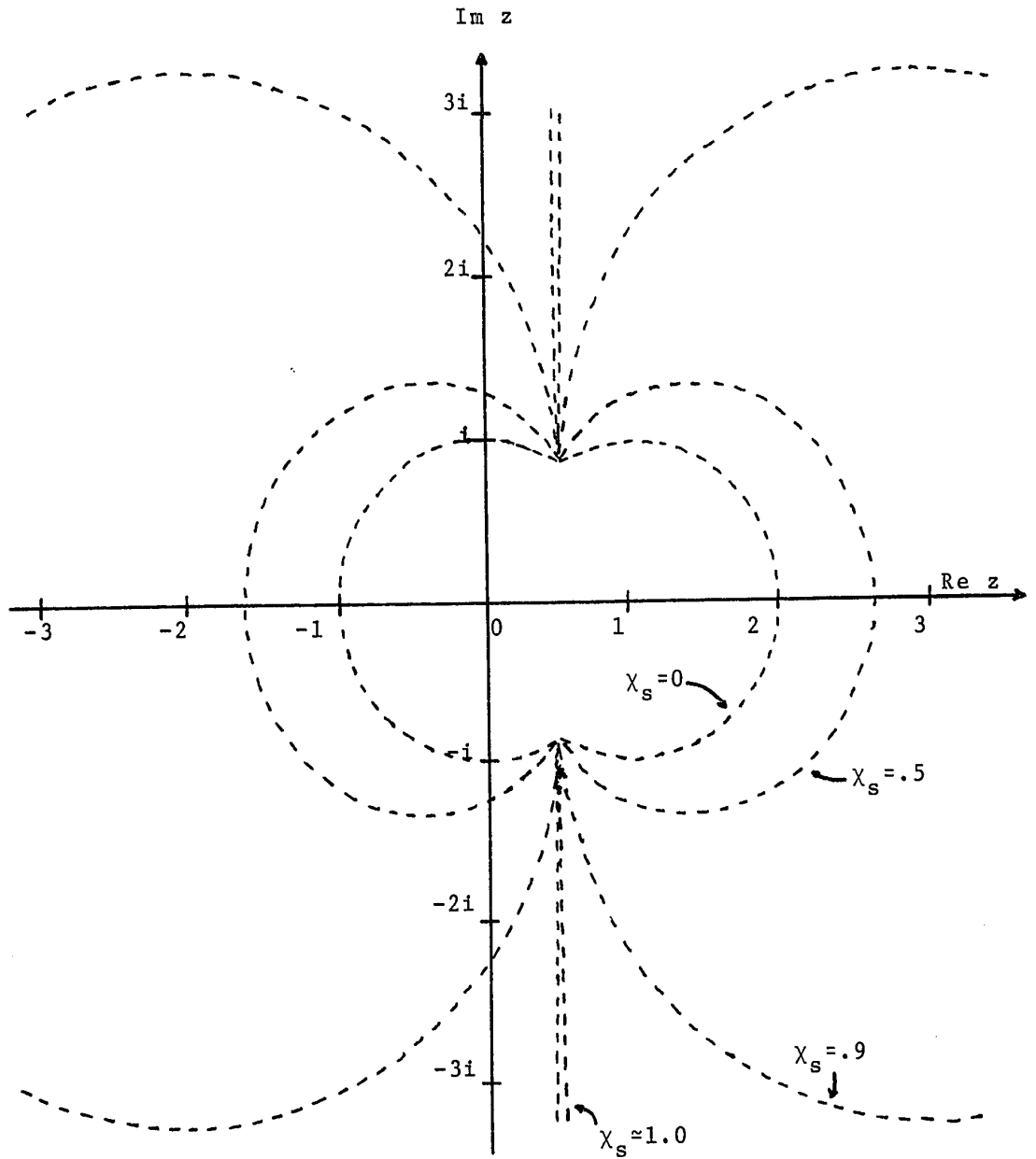
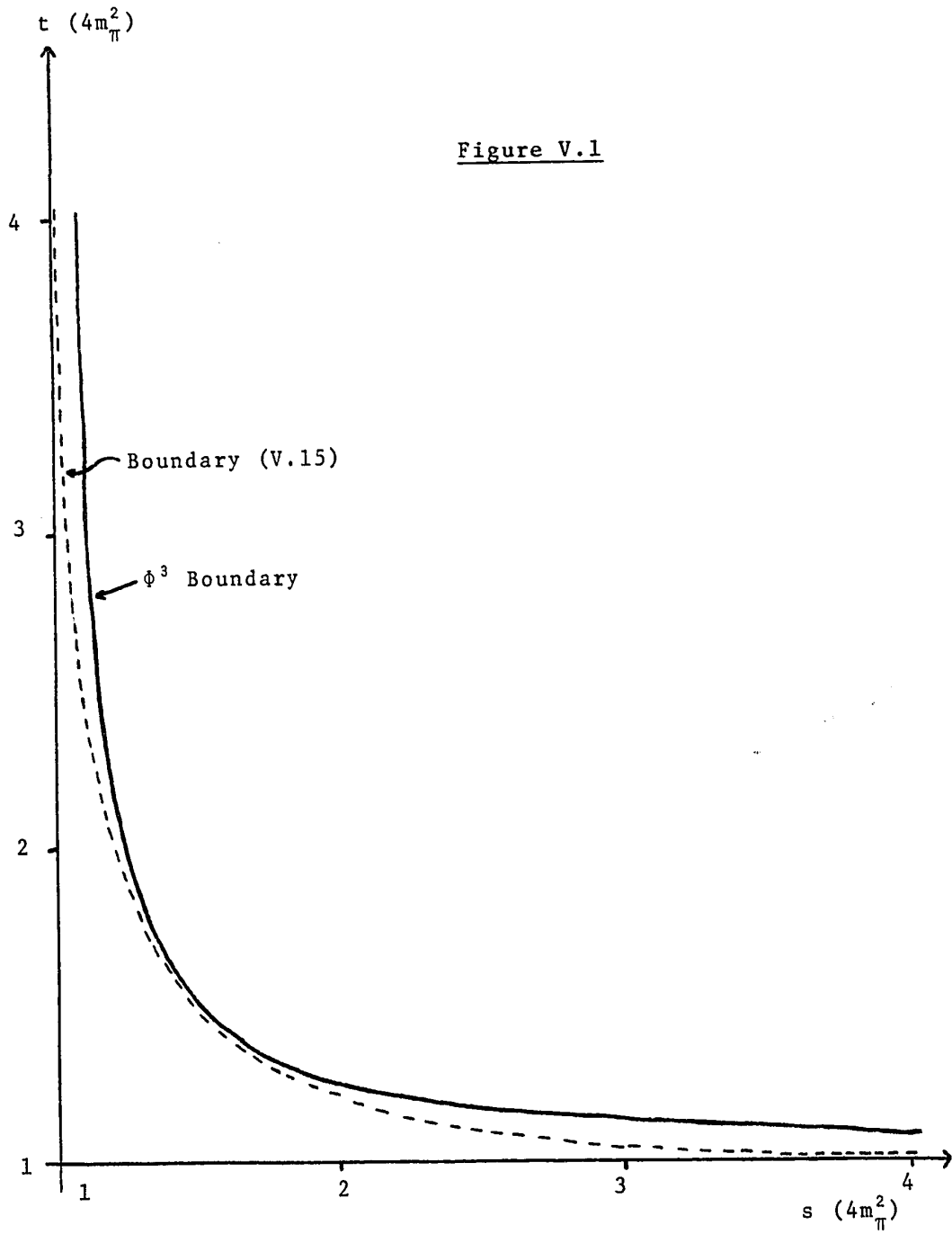
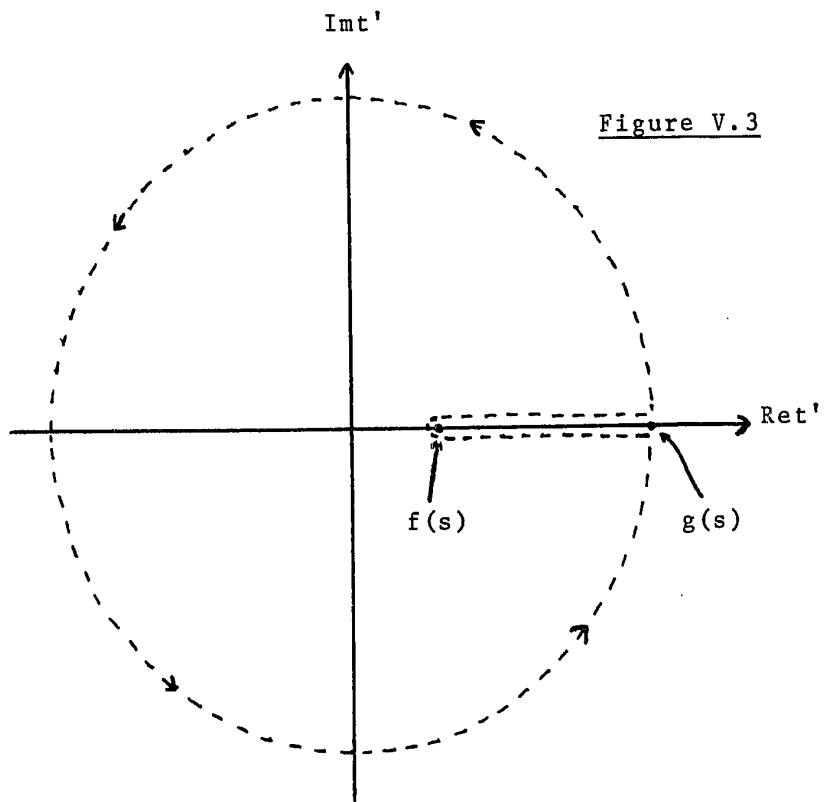
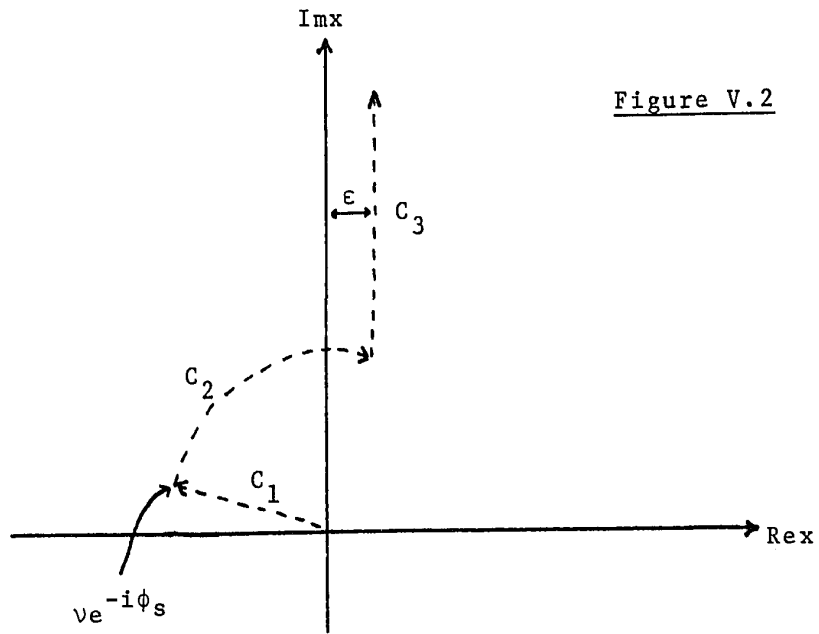


Figure IV.1

Figure V.1





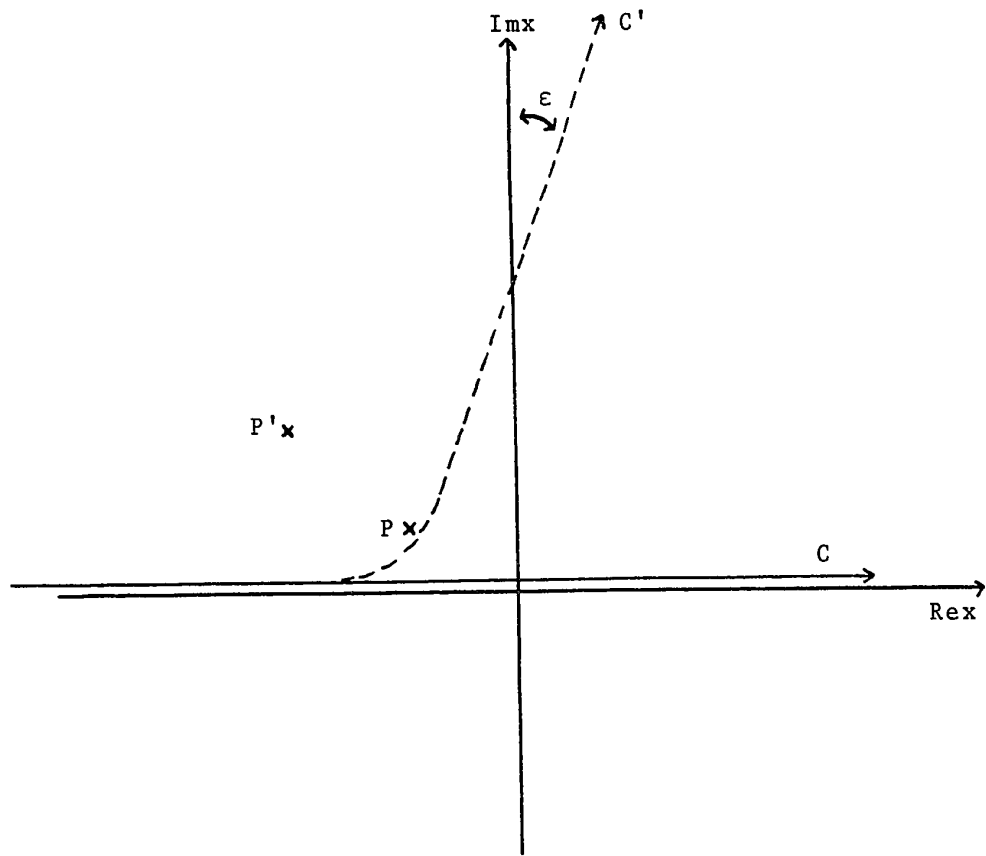


Figure V.4

Figure V.5

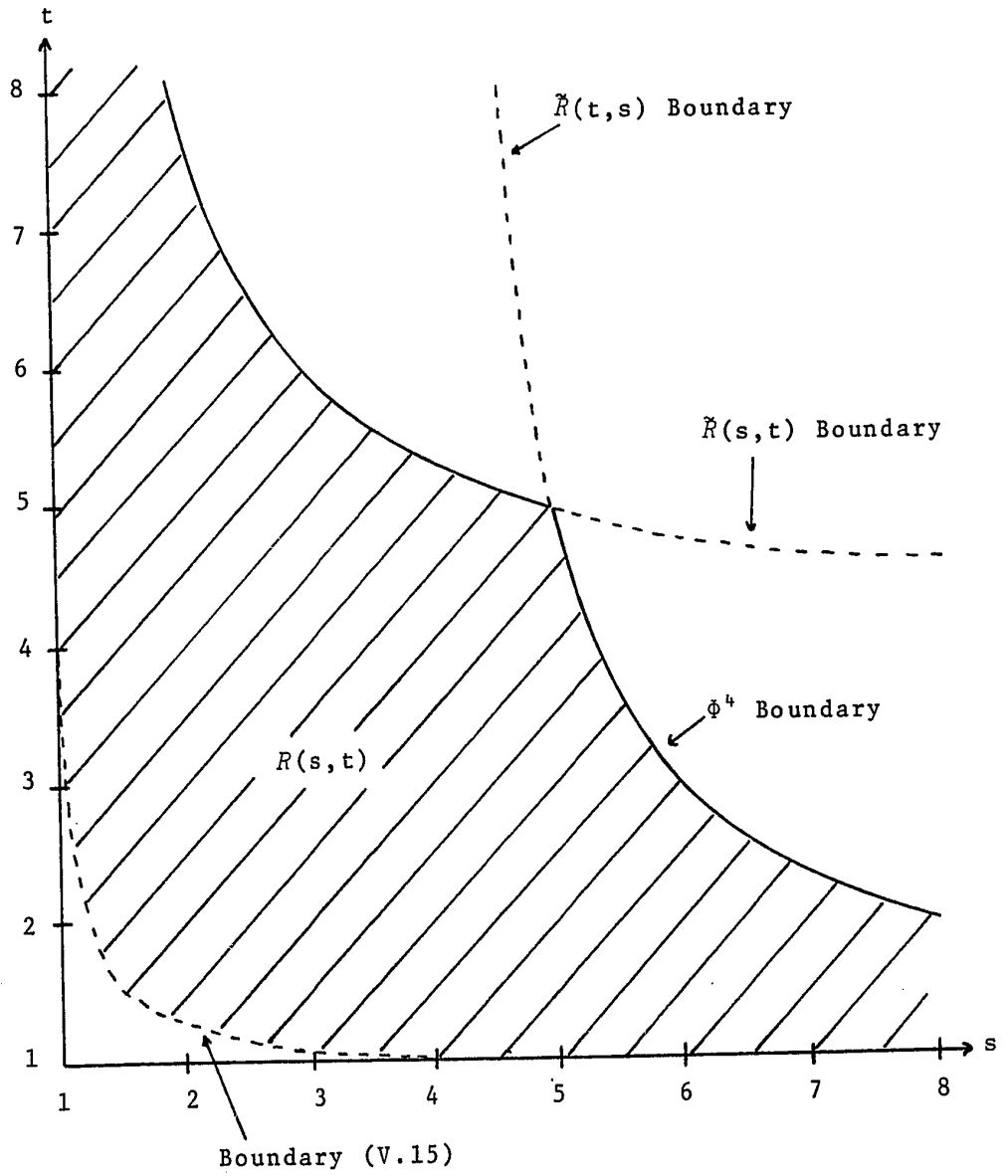
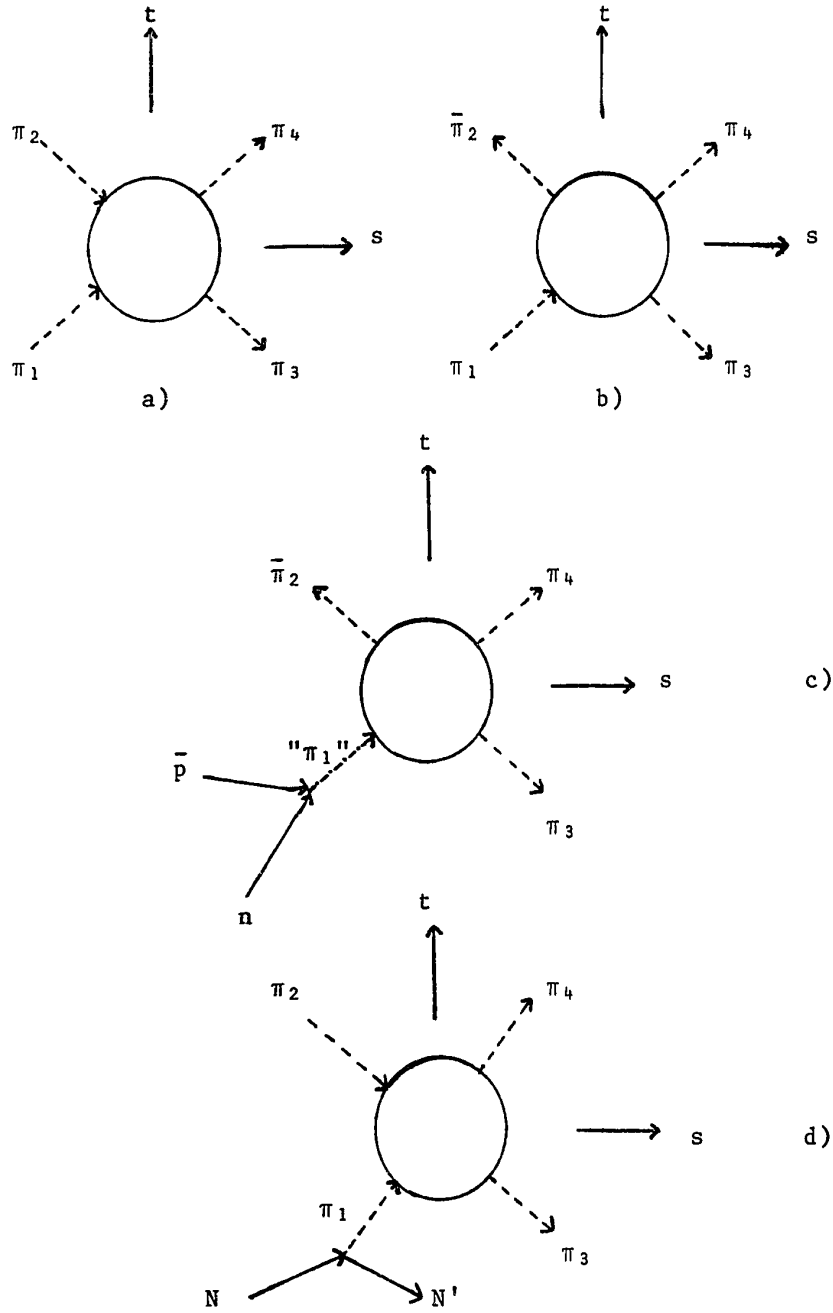


Figure VI.1



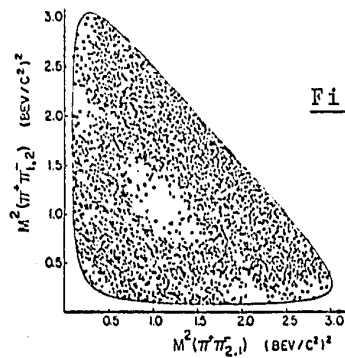
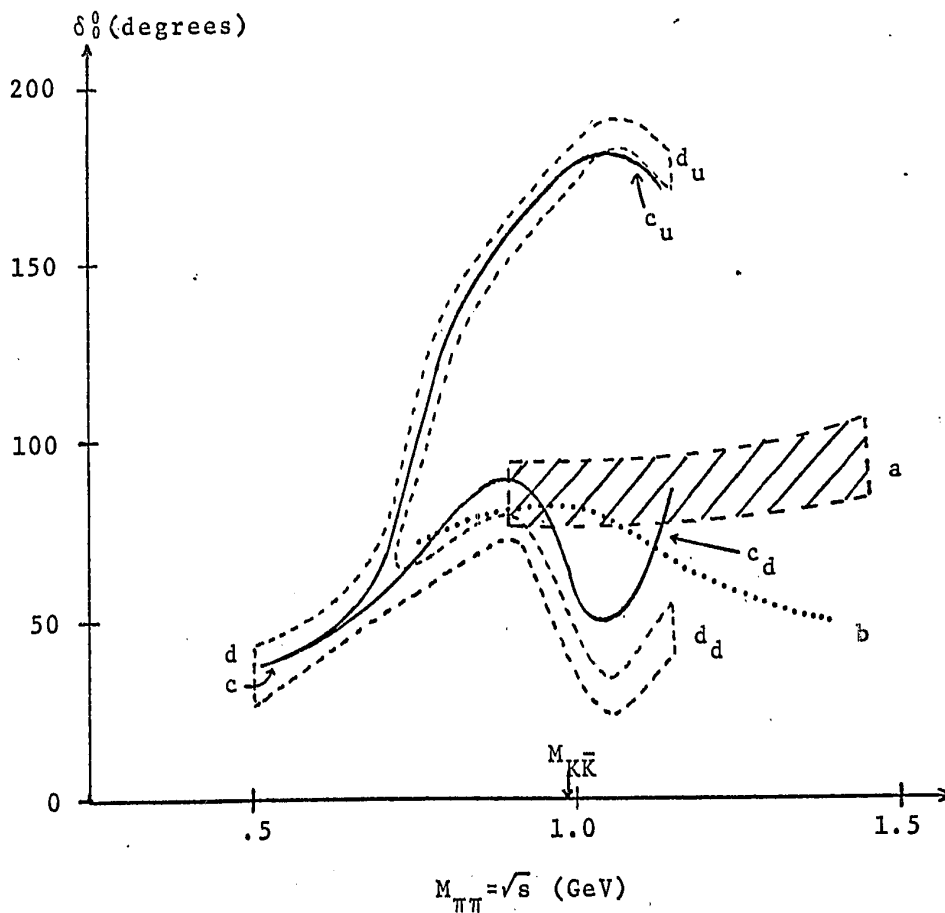


Figure VI.2

Figure VI.3



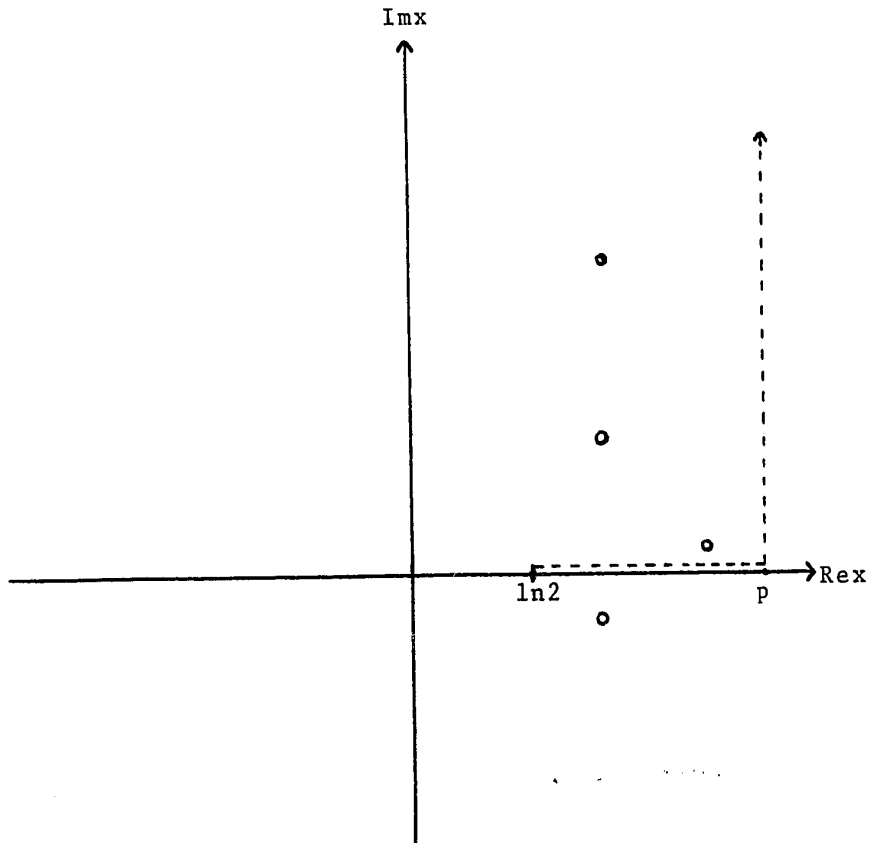


Figure VI.4

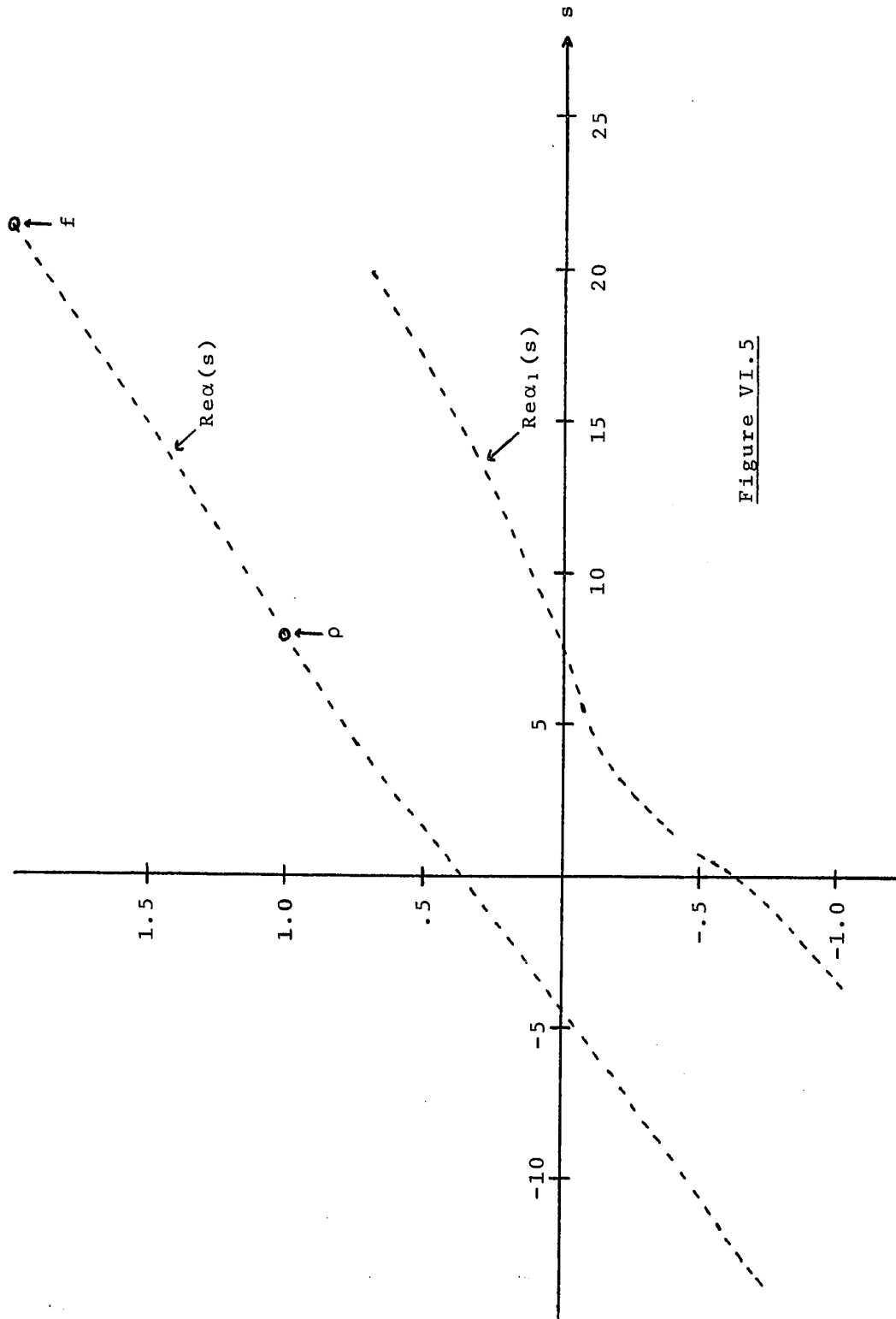


Figure VI.5

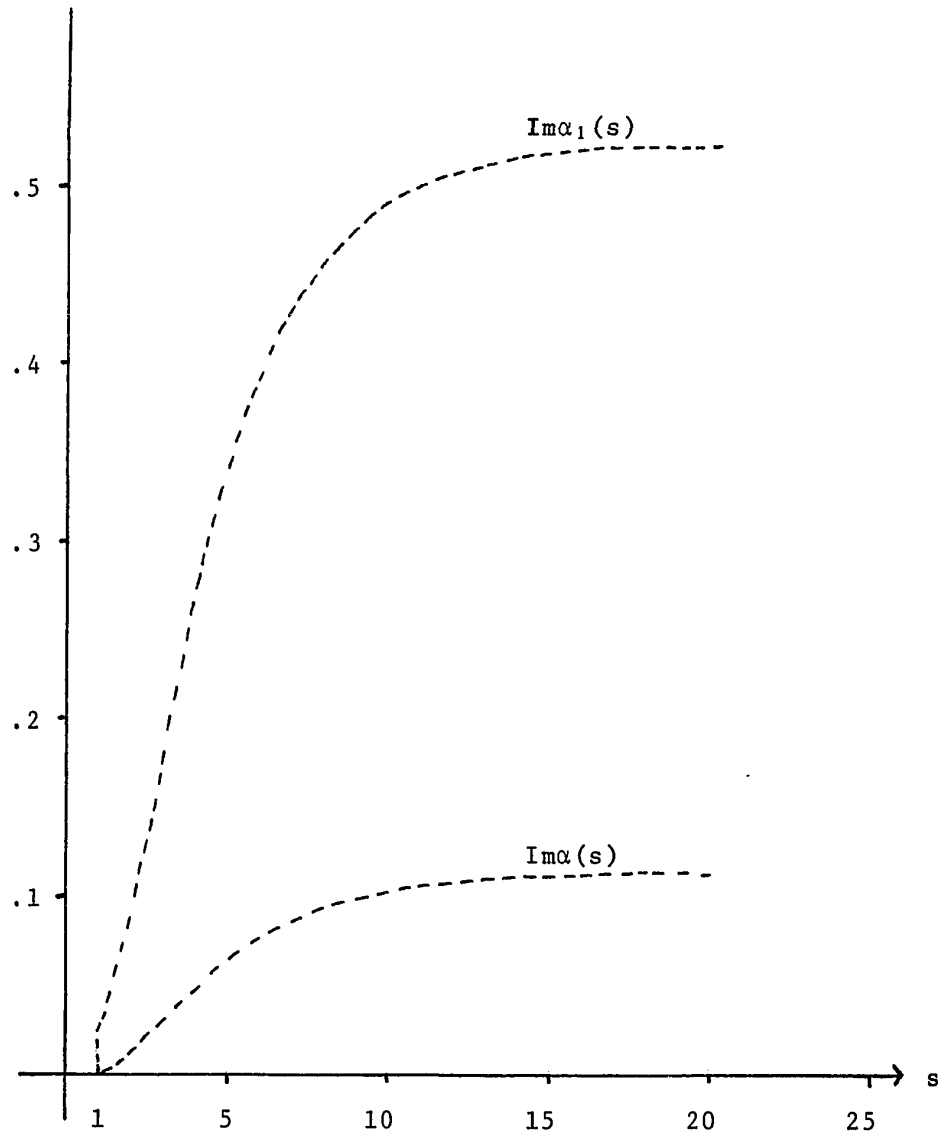
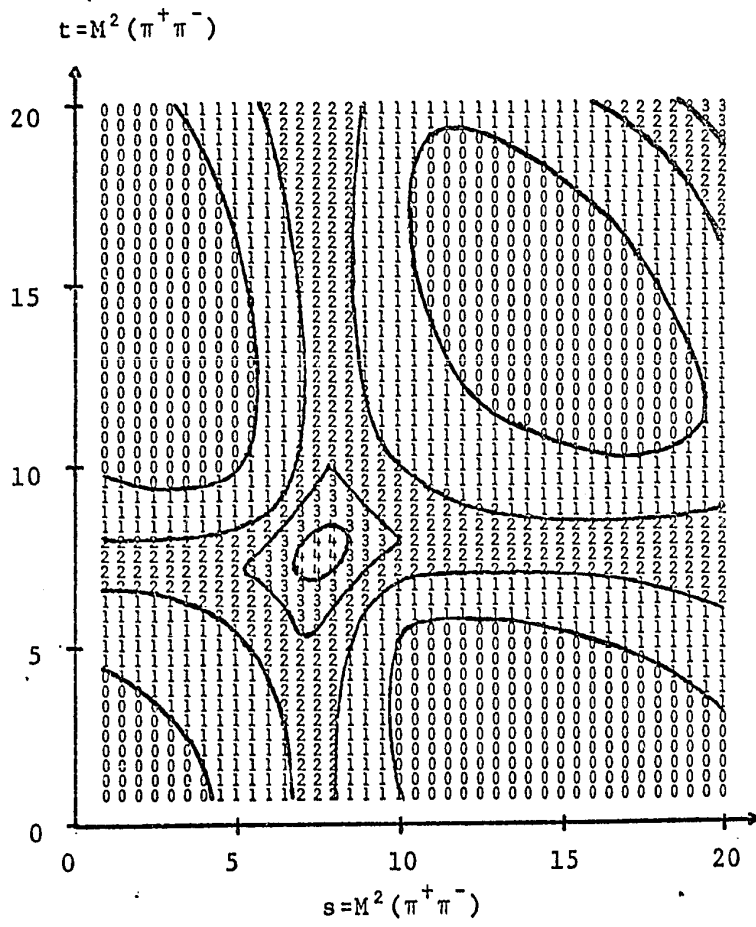
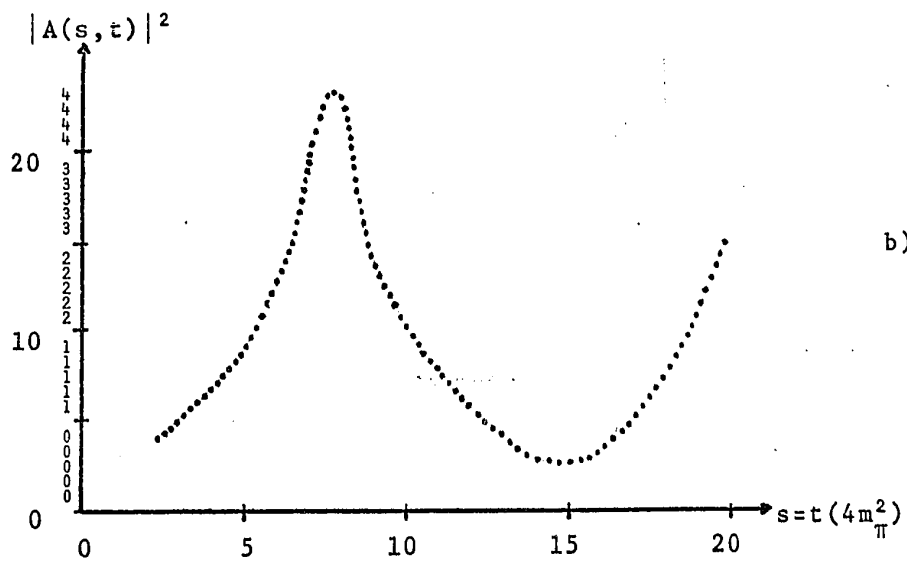


Figure VI.6

Figure VI.7



a)



b)

Figure VI.8

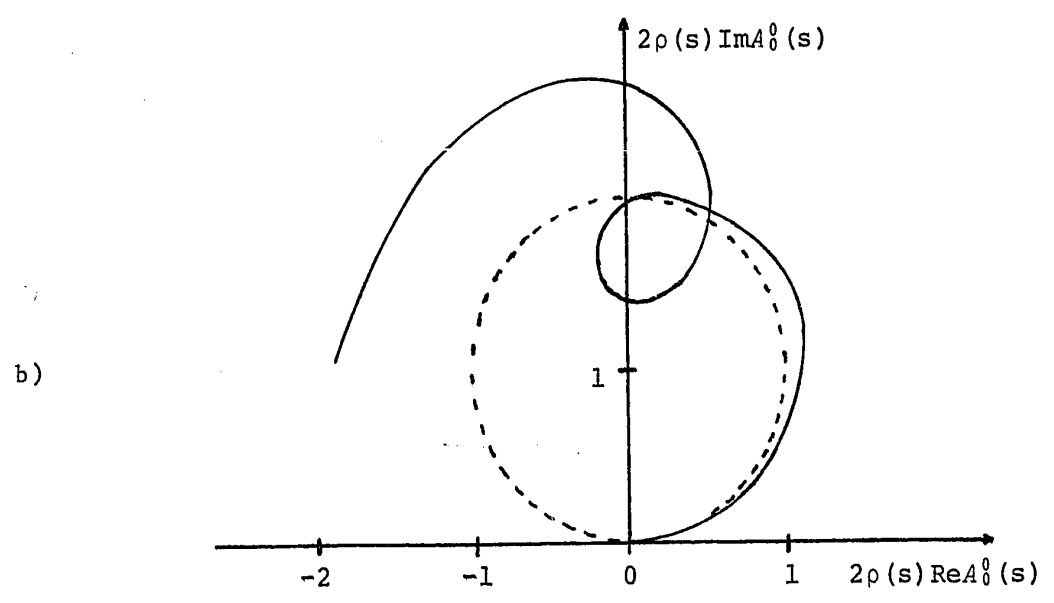
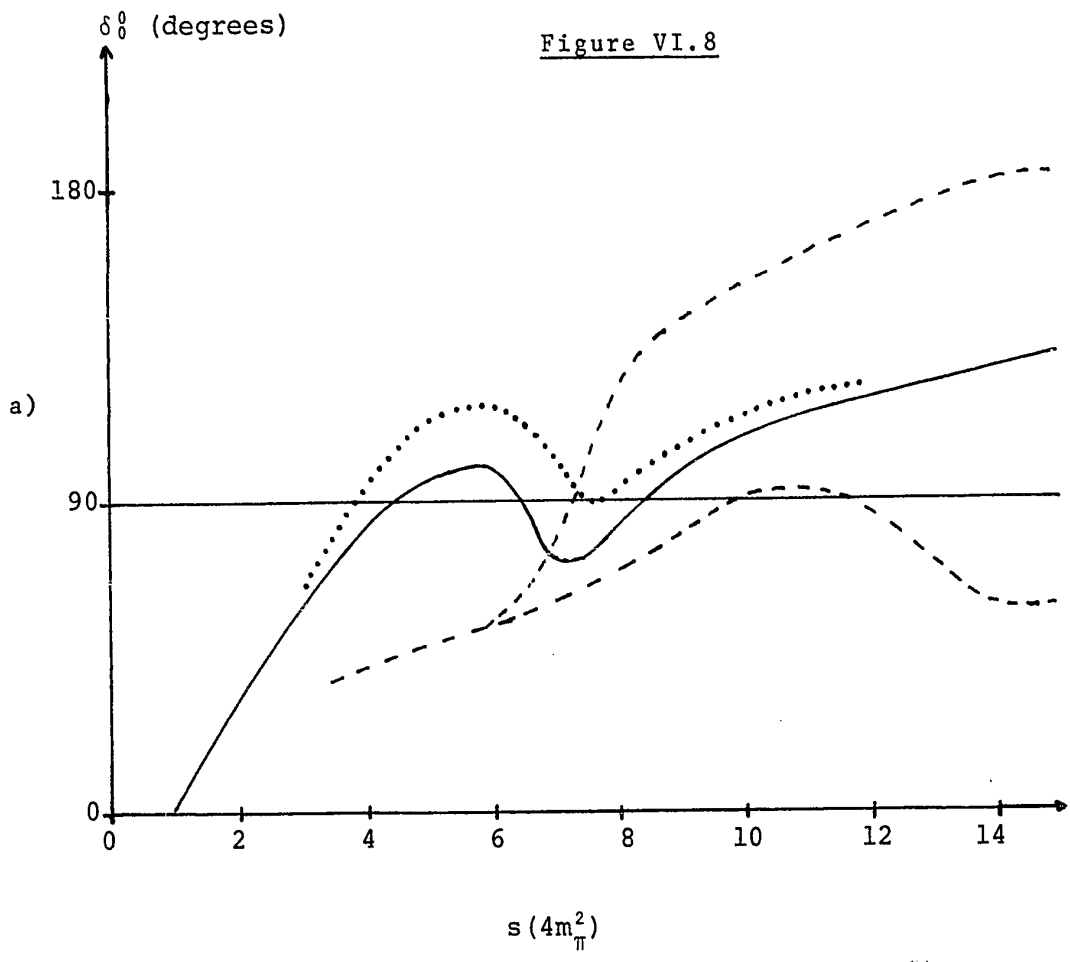


Figure VI.9

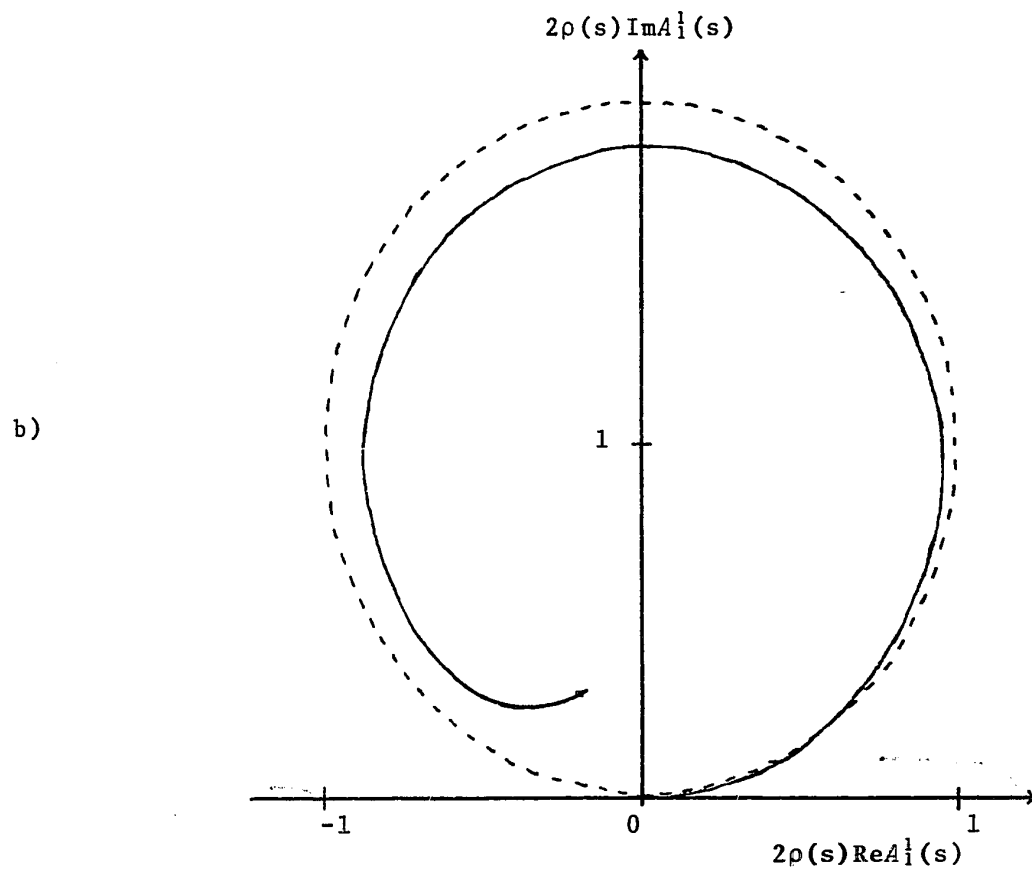
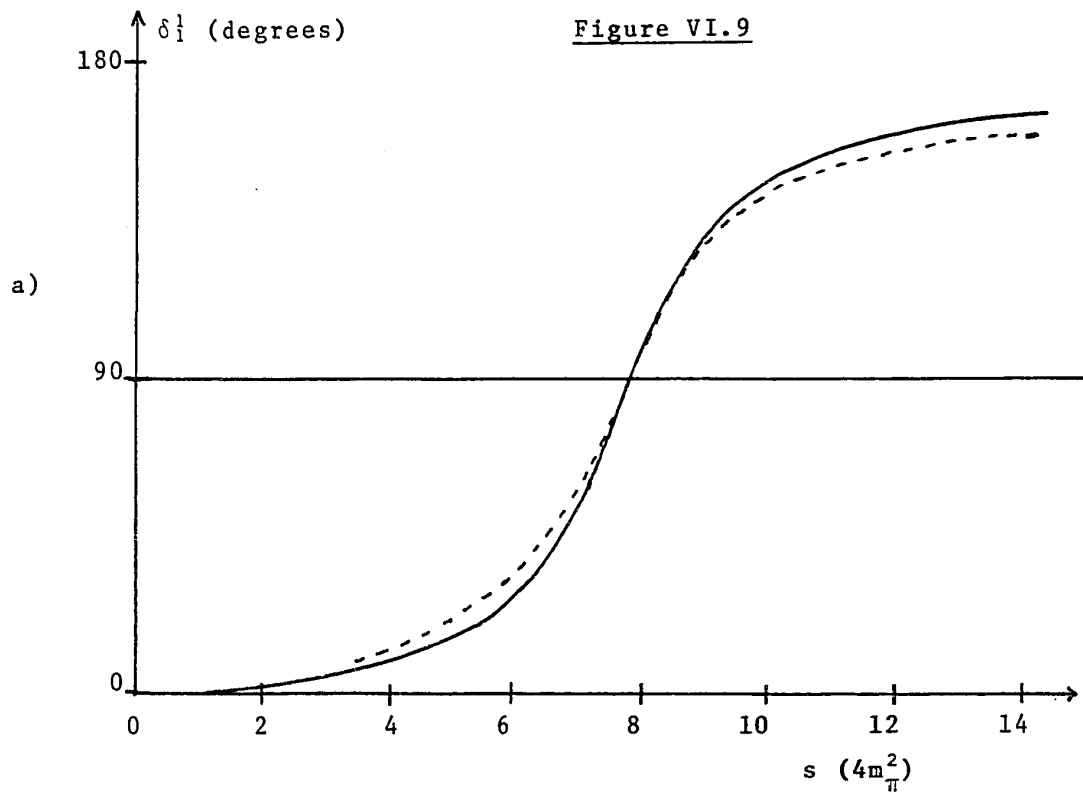


Figure VI.10

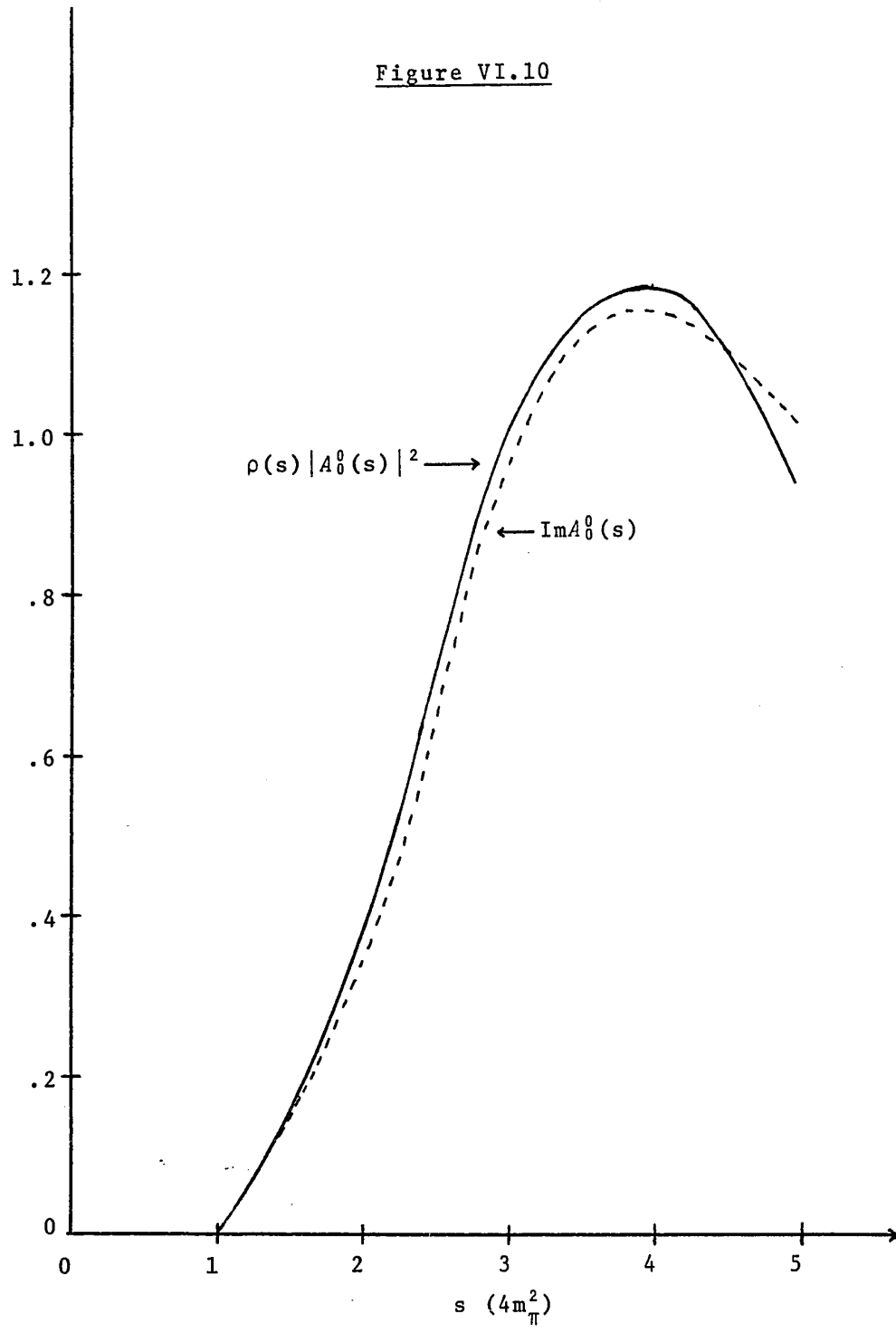


Figure VI.11

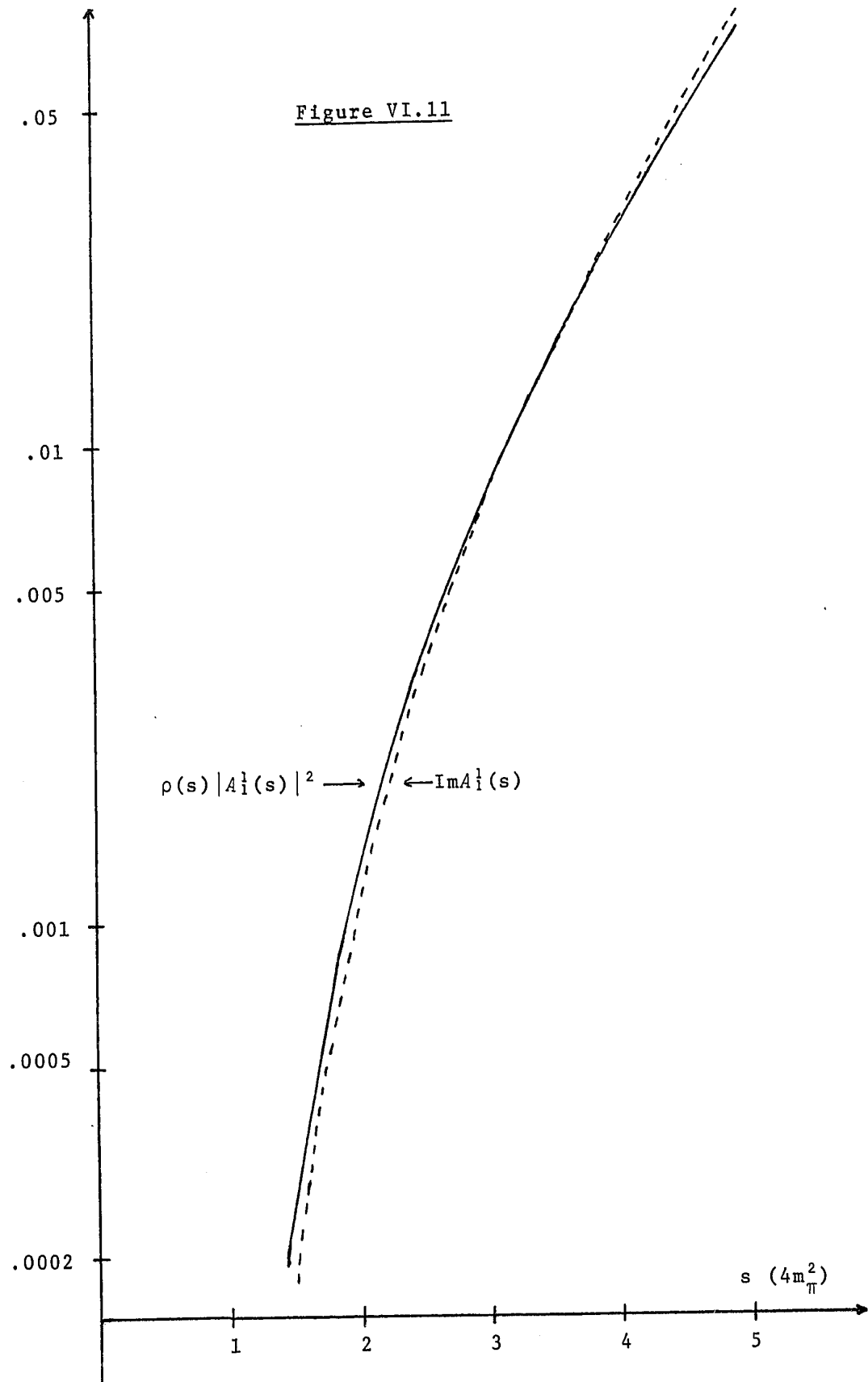


Figure VII.1

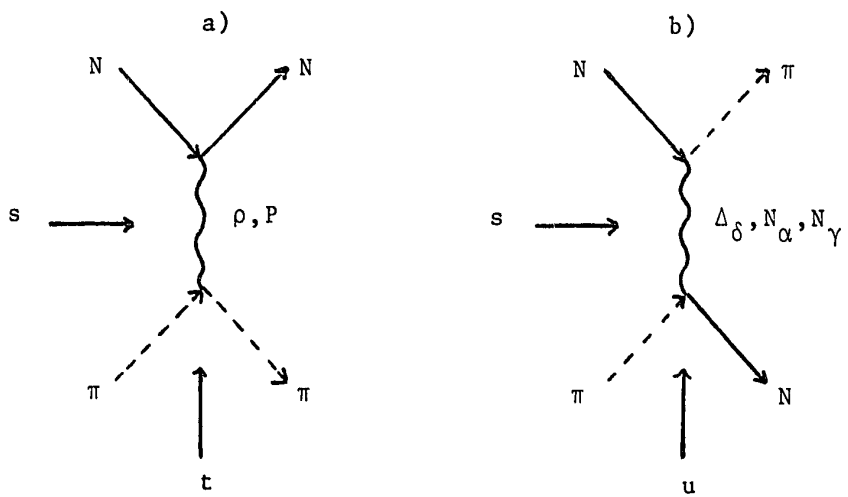


Figure A.1

